School of Pharmacy

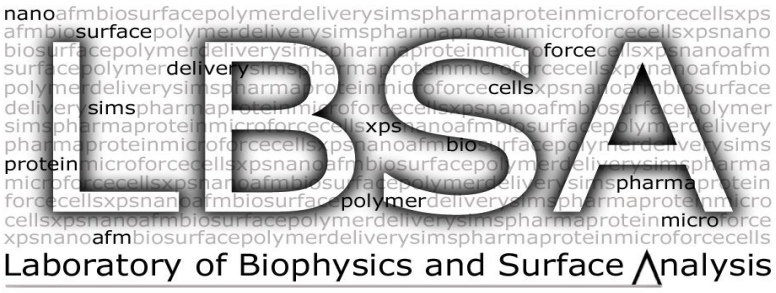

Investigation of the Temperature Dependence of Single Molecule Biomolecular Interactions

By

Mudasir Lone [BSc, ADCA]

Thesis submitted to
The University of Nottingham for the degree Master of Research in Nanotechnology

October 2008

CONTENTS

Abbreviations

OT	**Optical Tweezers**
MT	**Biomembrane Force probe**
BFP	**Optical Tweezers**
SPR	**Surface Plasmon Resonance**
APDES	**Amino-Propyl Dimethyl Ethoxy Silane**
IgG	**Immunoglobulin G**
PA	**poly(amines)**
PAMAM	**poly(amidoamide)**
TFM	**Thermal Fluctuation Method**
SAMs	**Self Assembled Monolayers**
SND	**Sader–Neumeister and Ducker Method**
NHS-PEG	**National Health Service – (poly-ethylene glycol)**
DH_2O	**Deionised water**
PBS	**Phosphate Buffered Saline**
LR	**Loading Rate**
DFS	**Dynamic Force Spectroscopy**
INVOLS	**Inverse Optical Lever Sensitivity**
WLC	**Worm Like Chain**
RNA	**Ribonucleic Acid**
DNA	**De-oxy Ribonucleic Acid**
OT	**Optical Tweezers**
PN	**Pico Newton**

Abstract

Weak non-covalent interactions such as hydrogen bonds, van der Waals forces and hydrophobic interactions form the basis of biomolecular interactions, and hence govern the function of many biological processes such as ligand-receptor interactions (cell adhesion), DNA replication and transcription. Measurement of such forces is important as it enables an understanding of the physio-biochemical properties of biological macromolecules. Single molecule forces and interactions can be measured with the help of ultra high sensitive force measurement devices such as the atomic force microscope (AFM), magnetic tweezers (MT), optical tweezers (OT) and the bio-membrane force probe (BFP). In this study, AFM has been employed over a range of temperatures to study the forced unbinding of streptavidin-biotin and complementary DNA oligonucleotides (30mer). With regards to the DNA based experiments, recently developed dendron immobilization chemistry was employed with the aim of improving sample immobilization and hence force spectroscopy data. At room temperature, the dynamic force spectroscopic measurements of the streptavidin-biotin complex showed two regimes of strength, consistent with previous studies. The unbinding strength of complementary DNA oligonucleotides immobilized via the dendron approach was also investigated at room temperature and found to be consistent with previous studies.

Several factors such as load, temperature and attachment chemistry have the potential to influence unbinding forces in single molecule measurements. Most single molecule force spectroscopic studies within the literature have investigated bonding strength on the basis of loading rate (which can be varied through measurement rate and the mechanical properties of the immobilization chemistry). Few studies have taken into account the critical effect of an increase in temperature. In this work, the temperature dependence of single molecule force spectroscopy measurements has been explored. It was observed that the unbinding forces of both streptavidin-biotin and complementary DNA oligonucleotides decrease with

temperature. The decrease in the unbinding force of both molecular species was attributed to the increase in the thermal energy of the system, which tilts the energy binding energy landscape in the direction of applied force besides decreasing the thermal force scale. Moreover increase in thermal energy decreases thermal off rate exponentially. The combined effect of all these factors reduces the unbinding forces of both the studied systems. However, for DNA, temperature increases are also known to decrease the average fraction of bonded pairs in hybridised DNA duplexes, which in these experiments would result in an additional reduction in force.

The presented data hence provide new insight into the effect of temperature on single molecule force spectroscopy data and the opportunities presented by a novel dendron based immobilization strategy.

Chapter 1. Introduction to Bio-molecular forces and their measurement

1.1 - Bio-molecular Interactions

All biological processes are governed by complex interplay of molecular interactions whether single or multi-molecular. The interaction may be either involve strong covalent or a weak non-covalent bonds. Strong covalent bonds establish static connections and can withstand thermal agitation; their formation and dissociation generally requires enzymatic action [1]. In contrast, weak non-covalent bonds (hydrogen bonds and van der Waals interactions) make up temporary connections, which dissociate spontaneously at room temperature [2]. The lifetime of a single non-covalent interaction is negligible when compared to the lifetime of a covalent bond, but when many non-covalent interactions combine, they can nevertheless build up ordered structures such as a DNA duplex or a folded protein [3]. Non covalent interactions therefore, govern molecular structure and function [4]. The different types of weak inter-molecular interactions are discussed in the following sections.

1.1.1- Hydrogen bonds

When a hydrogen atom is covalently bonded to an electronegative atom, particularly an oxygen or nitrogen atom, the single pair of shared electrons is greatly displaced towards the nucleus of the electronegative atom, leaving the hydrogen atom with a partial positive charge. As a result, the bare, positively charged nucleus of the hydrogen atom can approach near enough to an unshared pair of outer electrons of a second electronegative atom to form an attractive interaction. This weak attractive interaction is called hydrogen bond (see Figure 1.1).

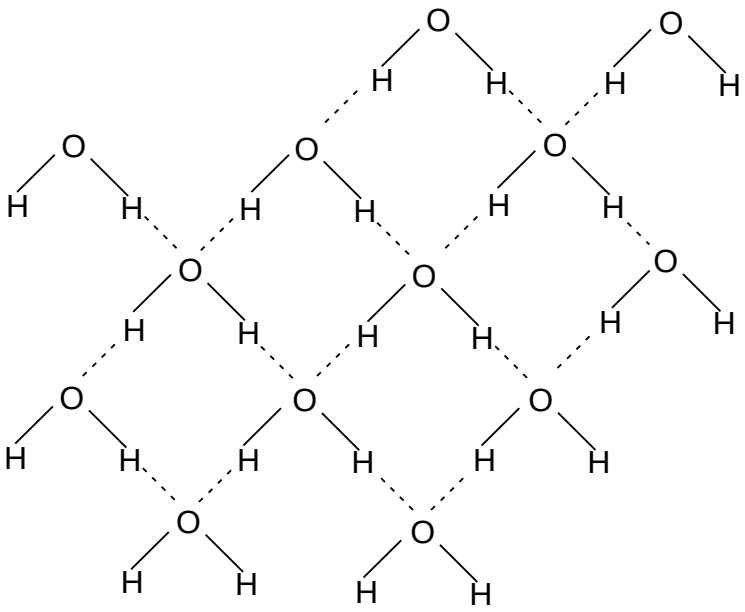

Figure 1.1: Hydrogen bonding between neighbouring water molecules (Adapted from [5]).

The hydrogen bond is a relatively strong fixed dipole-dipole force, but is weaker than covalent, ionic and metallic bonds. The hydrogen bond is somewhere between a covalent bond and an electrostatic intermolecular attraction and can be regarded as an intermediate interaction between a positively charged hydrogen atom and an electronegative acceptor atom. However, the main difference is that hydrogen bonds are highly directional. This is due to the fact that hydrogen bonding depends on the propensity and orientation of lone pair of electrons on the electronegative acceptor atom. Hydrogen bonds (about 0.18 nm in length) are typically about twice as long as the much stronger covalent bonds. The average strength of hydrogen bond ranges from 2-5kcal/mol [6]. Hydrogen bonding is of two types:

(a) Intermolecular hydrogen bonding (between two molecules whether same/different (Figure 1.1)). Intermolecular hydrogen bonding is responsible for the high boiling point of water. Hydrogen bonds are particularly important in determining the structure and properties of water. Each molecule of water can form hydrogen bonds with as many as four

other water molecules, producing a highly interconnected network of molecules. Each hydrogen bond is formed when the partially positive charged atom of one water molecule becomes aligned next to a partially negative-charged oxygen atom of other water molecule. Because of their extensive hydrogen bonding, water molecules have an unusually strong tendency to adhere to one another. This feature is most evident in the physical properties of water. For example, when water is heated, most of the thermal energy is consumed in disrupting hydrogen bonds rather than contributing to molecular motion. Similarly evaporation from liquid to the gaseous state requires that water molecules break the hydrogen bonds holding them to their neighbours, which is why it takes so much energy to convert water to steam [7]. Water molecules form hydrogen bonds with organic molecules that contain polar groups such as amino-acids and sugars, as well as the large macromolecules within the cell (Figure 1.2).

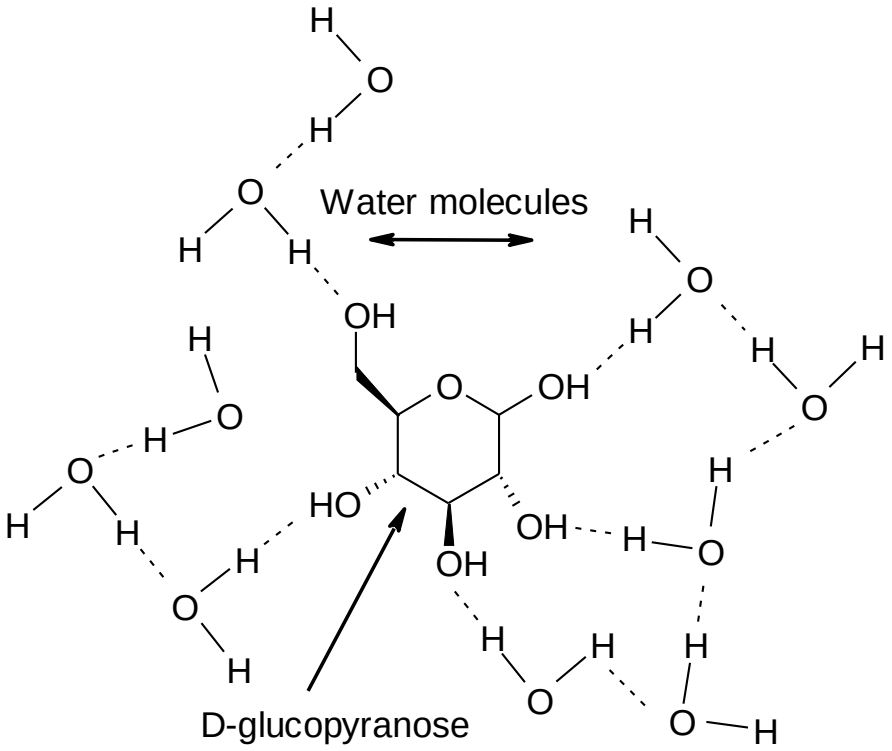

Figure 1.2: Schematic view of the hydrogen bonds that can form between a sugar molecule and the water it is dissolved in. Broken lines show the hydrogen bonds. The sugar molecule D-glucopyranose, in the middle (shown by black lines) is linked to water molecules via inter-molecular hydrogen bonding (Adapted from [8]).

(b) Intra-molecular hydrogen bonding takes place between the different groups within the same molecule. Intra-molecular hydrogen bonding plays an important role in determining the three-dimensional structures of proteins (secondary, tertiary and quaternary structures of proteins) and the duplex structure of DNA (Figure 1.3). In these macromolecules, bonding between parts of the same macromolecule causes it to fold into a specific shape, which helps determine the molecule's physiological or biochemical role [9]. The double helical structure of DNA, for example, is largely due to the hydrogen bonding between the base pairs, which link one complementary strand to the other [10].

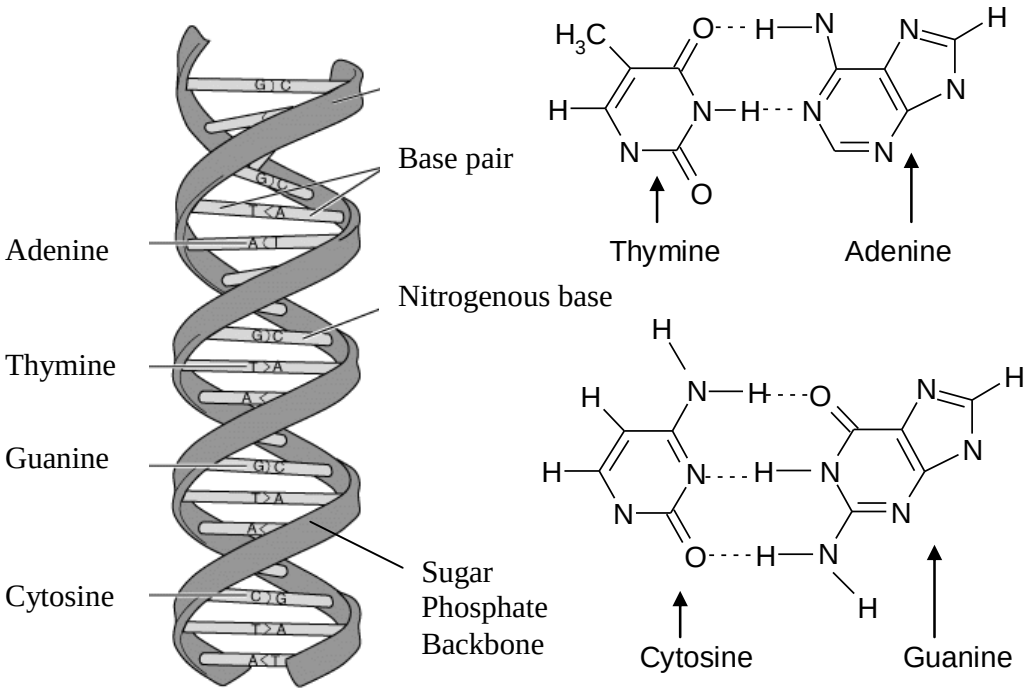

Figure 1.3: The double-helical structure of DNA proposed by Watson and Crick. The two polynucleotide strands are held together by hydrogen bonding between the complementary base pairs. Adenine pairs with thymine by two and guanine pairs with cytosine by three hydrogen bonds respectively [11].

1.1.2 – Hydrophobic Interactions and Van der Waals Forces

Polar molecules such as sugars and amino-acids have the ability to interact with water and are said to be hydrophilic (water loving). Non-polar molecules, such as steroid or fat molecules, are essentially insoluble in water because they lack the charged regions that would attract them to the poles of water molecules. Therefore, when they (non-polar molecules) are mixed with water, they are forced to form aggregates, which minimises their exposure to the polar surroundings [12]. This association of non-polar molecules is termed a hydrophobic interaction (Figure 1.4).

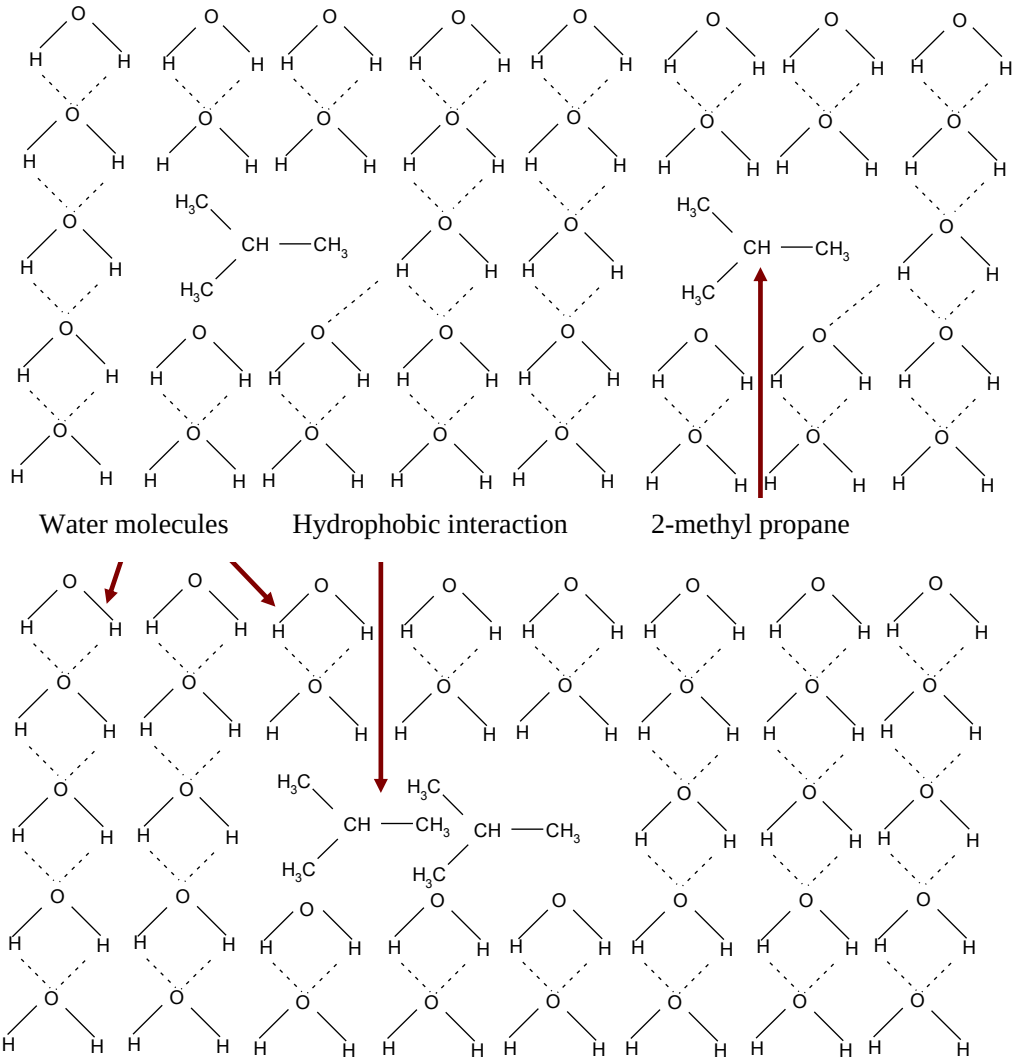

Figure 1.4: The hydrophobic effect: The aggregation of non polar groups in water leads to an increase in entropy owing to the release of water molecules into bulk water (Adapted from [13]).

In everyday life this is why droplets of fat molecules rapidly reappear on the surface of beef or chicken soup even after the liquid is stirred with a spoon. This is also the reason why non-polar groups tend to localise within the interior of most soluble proteins, so that they are away from the surrounding water molecules. Hydrophobic interactions of this type are not classified as true bonds because they do not result from an attraction between hydrophobic molecules. In addition, to this type of interaction, hydrophobic groups can form weak bonds with one another based on electrostatic attractions. Polar molecules associate because they contain permanent asymmetric charge distributions within their structure. Closer examination of the covalent bonds that make up a non-polar molecule (such as H_2 and CH_4) reveals that electron distributions are not always asymmetric. The distribution of electrons around an atom at any given instant is a statistical matter and, therefore, varies from one instant to the next. Consequently, at any given time, the electron density may happen to be greater on one side of an atom, even though the atom shares the electrons equally with some other atom. These transient asymmetries in electron distribution result in momentary separations of charge (dipoles) within the molecule. If two molecules with transitory dipoles are very close to one another and oriented in an appropriate manner, they experience a weak attractive force, called the ***van der Waals force***, which bonds them together. Moreover, the formation of a temporary separation in one molecule can induce a similar separation in an adjacent molecule. Therefore, ***van der Waals force***s are induced dipole-dipole attractions. The dipole is only temporary and is created by vibrations of the nucleus within the negative electron cloud. In this way, additional attractive forces can be generated between non-polar molecules [6]. A single van der Waals force is very weak (0.1 to 0.3 kcal/mol) and very sensitive to the distance that separates the two atoms (Figure 1.5).

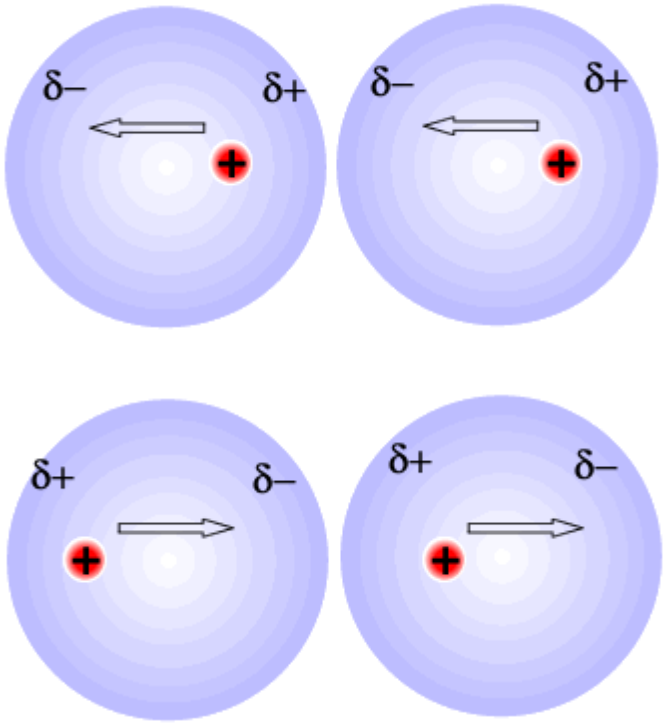

Figure 1.5: As two atoms approach each other; they experience a weak attractive force that increases up to a specific distance, typically about 4 Å. As the two atoms approach each other, vibrations of the nucleus within the electron charge cloud of one creates a temporary dipole shown as δ^+ and δ^-. This induces similar vibrations in the nucleus of neighbouring atom so that positive and negative charges become arranged in an opposite manner to those in the first atom. The atoms approach more closely by an attraction force called ***van der Waals force****. Although individual van der Waals forces are very weak, large numbers of such attractive forces can be formed if two macro-molecules have a complementary surface, as is indicated schematically* [14].

This weak intermolecular force of attraction between the two molecules of finite size is calculated from the van der Waals gas equation given below:

$$(P + av^2)(v-b) = RT \qquad (1)$$

where P is pressure, v is volume of fluid per molecule, a is a measure of attraction of the molecules for each other (van der Waals forces), b is the volume occupied by a single molecule, R is gas constant, and T is the absolute temperature.

Only at conditions of high pressure and/or low temperature are molecules able to participate in van der Waals forces *noticeably*. Nevertheless these weak molecular forces play a significant role in building interactions between two suitable molecules [15,16]. The measurement of such biomolecular forces provides a detailed insight into the biochemical properties of biological macromolecules, besides allowing an exploration of their mechanical properties [17]. This has led to the emergence of field of single-molecule force spectroscopy as detailed in the following text.

1.2 – Measurement of Biomolecular Forces

The advent of single-molecule studies has allowed unprecedented insight into the dynamic behaviour of biological macromolecules and their complexes [17]. Indeed some single-molecule approaches allow us to study the behaviour of biological macromolecules under applied load (single molecule force spectroscopy), therefore enabling us to understand how the mechanical properties of these molecules are related to their biological function [18]. Force probe techniques can directly measure the force required to rupture single molecules (ligand-receptor bonds). Such forces are related to the energy landscape of the weak, non covalent biological interactions (hydrogen bonds, van der Waals interactions). While these methodologies offer high sensitivity in measuring bio-molecular interactions, these measurements can be sometimes challenging, because the underlying chemistry may occupy an important binding site or cause steric hindrance, resulting in crude information regarding bio-molecular interactions. Despite these limitations however, such measurements have stimulated interest in developing techniques for monitoring and screening bio-molecular interactions including nucleic acid hybridizations and protein-protein interactions. Various tools have been used to investigate bio-molecular forces such as the bio-membrane force probe (BFP) [19], optical tweezers (OT) [20], magnetic tweezers (MT) [21], and atomic force microscopy (AFM) [22]. These four classes of techniques allow the detection of the

rupture of ultra-weak bonds with pico-Newton force sensitivity. The basic principle underlying these techniques is given below:

1.2.1 – Bio-membrane Force Probe (BFP)

The Bio-membrane Force Probe was pioneered by E. Evans, and its basic principle is similar to AFM [23]. The BFP is a sensitive force transducer capable of measuring minuscule displacements and forces at biological interfaces. The advantage of this technique is that the stiffness of the force transducer (i.e. the tension) can be set at will, allowing for the measurement of a very large range of forces. The dynamical time range of this technique is $\geq$ 1ms. Typical applications include determination of the strength of membrane anchors, and receptor-ligand pairs. In this technique, a red blood cell is generally used as force transducer (pressurised spring) and the force constant (stiffness) is provided by the membrane tension which is regulated by micro-pipette suction. A glass micro-bead (1-2µm in diameter) glued to the red cell membrane acts as the BFP tip. The functionalised BFP tip is kept stationary, and another glass micro-bead surface functionalised with a molecule of interest is then allowed to interact with the BFP tip to measure the adhesion forces. The BFP measures the adhesion forces in the range of 0.5-1000 pN [23]. The BFP has been employed to determine the dynamic force (or spectra of mechanical strength) of streptavidin-biotin bonds [17] and has been also used to monitor the force required to break bonds between pairs of nectin and cadherin [24].

1.2.2 – Magnetic Tweezers (MT)

This is a special kind of force probe technique which measures the unbinding forces between bio-molecules using a magnetic field gradient. The main applications include single-molecule force measurement and studies of force regulated processes such as DNA

hybridisation [25]. They have the ability to exert large forces up to (0.01-100pN). The dynamical time range of this technique is ≥ 1ms. MT provides precise and reproducible control of distance and time over which molecules and cells interact. Magnetic tweezers offer some advantages over other force spectroscopy techniques. They do not suffer from the problems of sample heating and photo damage that can plague OT. Magnetic manipulation is exquisitely selective for the magnetic beads used as probes, and is generally insensitive to the sample and microscope chamber preparation, which would be difficult or impossible to achieve with other single-molecule force spectroscopy techniques. MT have been employed for the DFS measurements of DNA (Figure 1.6)

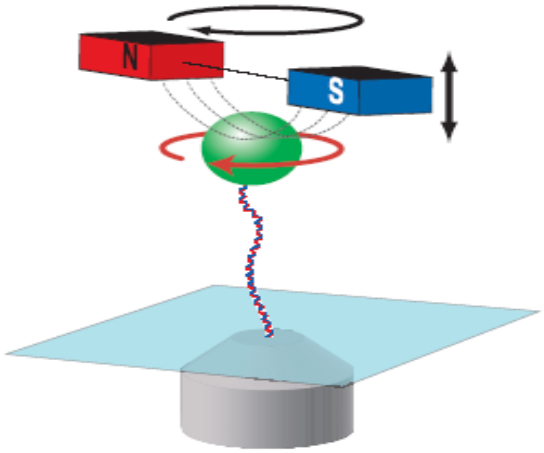

Figure 1.6: Depicting the layout of magnetic tweezers, super-paramagnetic bead (green) is attached to the surface of the trapping chamber by a single molecule of DNA. A pair of small permanent magnets (red and blue) above the trapping chamber produces a magnetic field gradient (dashed lines), which results in a force on the bead directed up toward the magnets. The force is controlled by moving the magnets in the axial direction (bidirectional arrow) [26].

1.2.3 – Optical Tweezers (OT)

OT are very sensitive instruments and have been used to spatially trap viruses, bacteria, living cells, organelles, small metal particles, and even strands of DNA in 3D. OT use a focused laser beam to trap small molecules. They can be used to exert forces of less than 150pN on particles ranging in size from nanometres to micrometers, while simultaneously measuring the three-dimensional displacement of the trapped particle with sub-nanometer accuracy and sub-millisecond time resolution. The dynamic time range of this technique is $\geq$ 10ms. These properties make OT extremely well suited for the measurement of force and motion.

The basic principle behind OT is the momentum transfer associated with bending of light. Light carries momentum that is proportional to its energy and in the direction of propagation. Any change in the direction of light, by reflection or refraction, will result in a change of the momentum of the light. If an object bends the light, (changing its momentum), the conservation of momentum requires that the object must undergo an equal and opposite momentum change. This gives rise to a force acting on the object [27]. The versatility and precision afforded by OT is accompanied by important limitations and drawbacks. There are difficulties associated with using light to generate force. As trap stiffness depends on the gradient of the optical field, optical perturbations that affect the intensity or the intensity distribution will degrade the performance of the OT. High-resolution optical trapping is therefore limited to optically homogeneous preparations and highly purified samples. OT also lack selectivity and exclusivity. When OT are used, local overheating of the biological samples remains a recurrent concern, even in the less damaging infrared spectrum.

Applications include confinement and organization (e.g. for cell sorting), tracking of movement (e.g. of bacteria), application and measurement of small forces (single molecule force measurement), and altering of larger structures (such as cell membranes). Two of the main uses for optical traps have been the study of molecular motors and the physical properties of DNA. Figure 1.7 provides an overview of a typical OT for the measurement of transcription forces.

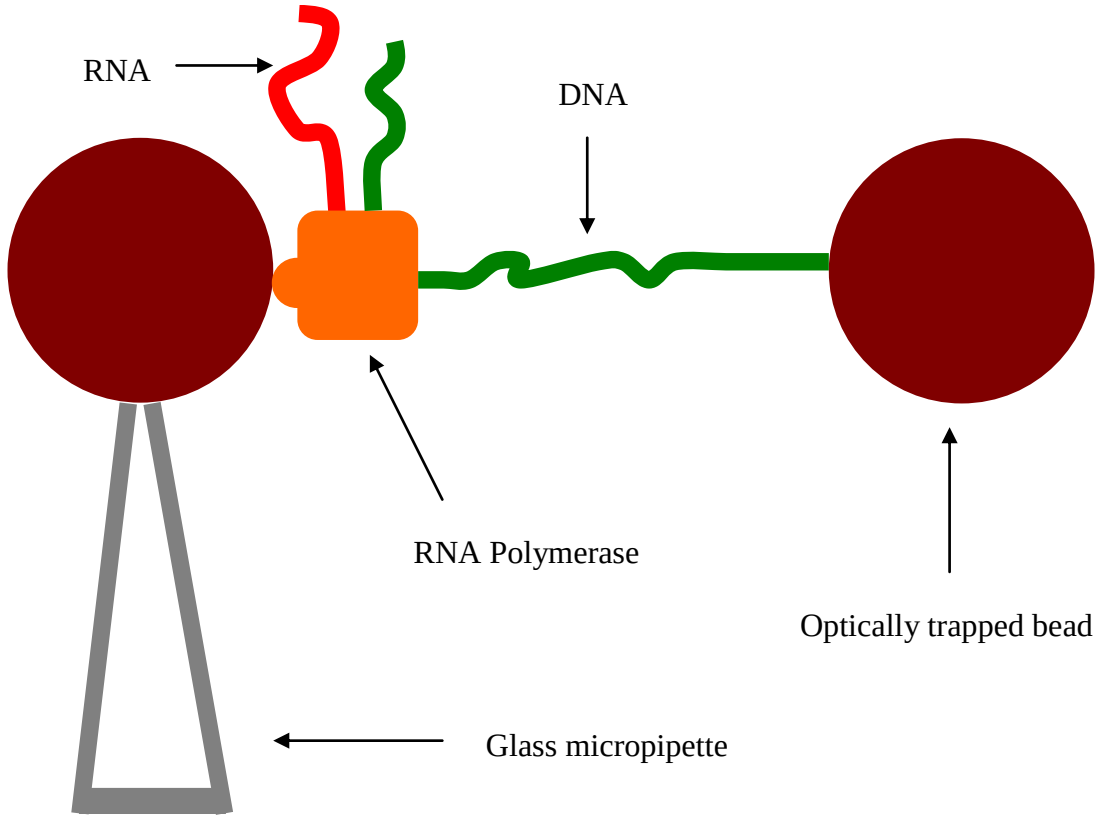

Figure 1.7: Schematic of an OT set up used for measuring transcription forces generated by RNA polymerase (molecular motors).RNA polymerase is itself attached to polystyrene bead, which is then moved to stretch the DNA that is tethered between optically trapped bead and the polystyrene bead held on the end of glass micropipette. The DNA molecule is stretched by applying a force opposing transcription by moving glass micropipette into a specific direction until a specific force on the bead in the optical trap is observed (Adapted from [28]).

1.2.4 - Atomic Force Microscopy (AFM)

AFM was invented by the Binnig, Quate and Gerber in 1986 [1] and it provides probably the most popular force spectroscopic technique due to its commercial availability and relatively low cost. This technique allows mapping of surface characteristics at sub-nanometer resolution. The AFM was initially developed to overcome limitations of the scanning tunnelling microscope in imaging nonconductive samples. However, the possibility of modifying the surface, manipulating individual molecules, and single molecule force measurement has made AFM an ideal tool for biological applications. One important advantage of the technique is the often simple and rapid sample preparation. Another important feature of AFM is the ability to conduct measurements of biological samples under near-physiological conditions. Although the AFM is primarily an imaging tool, it also allows measurement of inter- and intra-molecular interaction forces with pico-Newton resolution. When used for one-dimensional force measurements the cantilever is moved only in the vertical direction, perpendicular to the specimen plane.

The force resolution of AFM is a consequence of the small spring constants of the cantilevers used. However, the ability to measure the ultra low forces is hampered by the fluctuations induced by thermal excitation of these very soft levers. These fluctuations and changes in the intensity distribution in the laser beam are the main contributors of noise in force data.

A schematic of the general layout of an AFM is shown in Figure 1.8. AFM uses a sharp tip mounted at the end of a flexible cantilever to probe a number of properties such as surface the characteristics and mechanical properties of the sample of interest. The cantilever is typically made of silicon or silicon nitride with a tip of radius of lass than 10 nm. The vertical and lateral motion of the sample with respect to cantilever is achieved by a

piezoceramic stage holding the sample. The vertical motion of the cantilever is controlled by piezoelectric actuators affording sub-nanometer resolution. AFM operates in two basic modes to record a force interaction data; the static mode in which an AFM tip is allowed to contact the surface, interacts with the surface and then is retracted by the piezo stage with the lever at equilibrium position throughout. However, in dynamic mode, the cantilever oscillates during the force cycle. Increase in the interaction of the tip and the surface result in a reduction in the amplitude of oscillation [18].

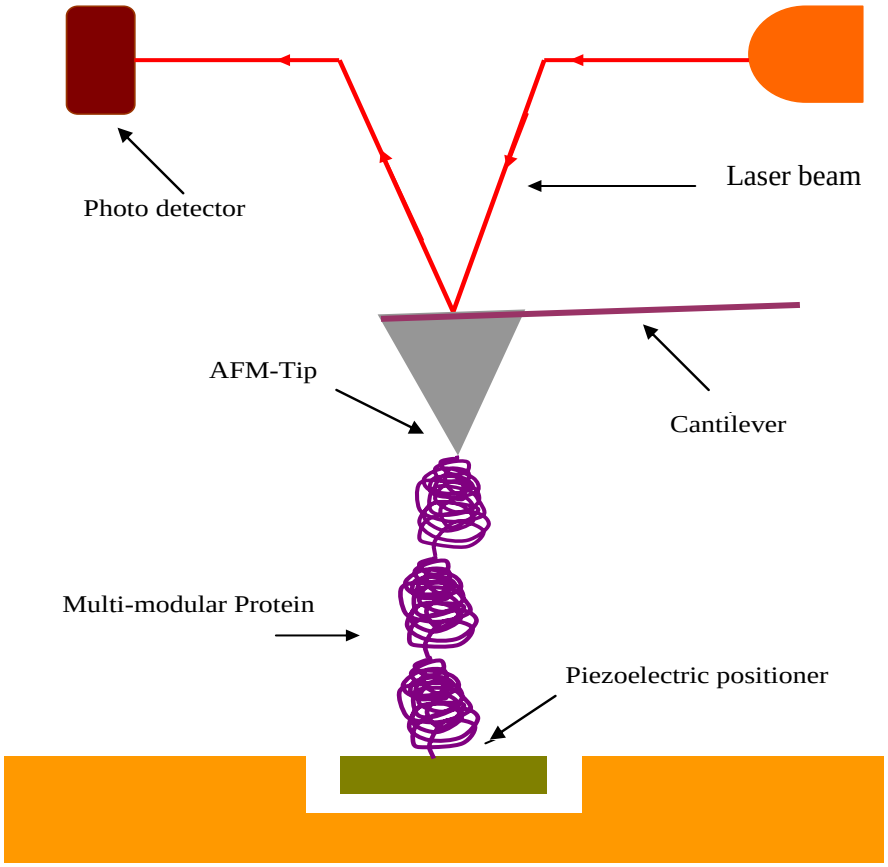

Figure 1.8: Shematic overview of the workings of AFM showing the pulling of a single protein molecule. Retraction of the piezoelectric positioner results in the deflection of the cantilever (*Adapted from* [29]).

1.2.4.1 – Measurements with AFM

AFM has been widely used to obtain single-molecule force-extension measurements which are obtained by mechanically distorting a bio-molecular complex or the structure of a molecule. The resultant force-extension curves provide valuable information on the structure, the folding and unfolding/dissociation processes and even the activity of the molecule [30, 32].

As long as the AFM cantilever is at a distance from the sample surface, no interaction facilitates between the tip and the surface, but when the tip is in close proximity with the surface, forces between atoms of the two surfaces if attractive (van der Waals and electrostatic) result in the bending of lever towards the sample surface and if repulsive (electrostatic) away from the surface. The cantilever bends up to certain limit (elastic limit) and then restores back to its initial position (away from the surface). The jump to contact is observed in the approach trace. The contact region of a force curve gives information about the mechanical properties of the experimental sample. The tip-sample distance is the difference between the piezo-Z displacement and the deflection of the cantilever. After a preset value of load is reached, the direction of the motion is reversed and the probe moves away from the surface. When the probe retracts, the adhesion force is estimated from the deflection of the cantilever right before the jump-off contact. It is important to mention here that the jump-off contact occurs only when the adhesive forces are conquered by the spring constant of the cantilever [18].

The forces acting between the surface and the probe cause deflection of the cantilever that is registered by a laser beam reflected off the back of the cantilever. The deflection is measured using a laser spot reflected from the top of the cantilever onto an array of

photodiodes. The force experienced by the cantilever on deflection is given by Hooke's Law:

$$F = - kx \qquad (1.1)$$

where k is the spring constant of cantilever,

x is deflection produced in the cantilever in the direction of applied force.

The cantilever stiffness k depends on the material properties and shape of the cantilever. There is often a spread in the values of spring constant and therefore it is usually experimentally calibrated by the thermal fluctuation method [33]. Other methods include Sader–Neumeister and Ducker method (SND) [34]. Figure 1.9 shows an example plot of the cantilever deflection versus the separation between the probe and the sample surface, otherwise known as a force curve.

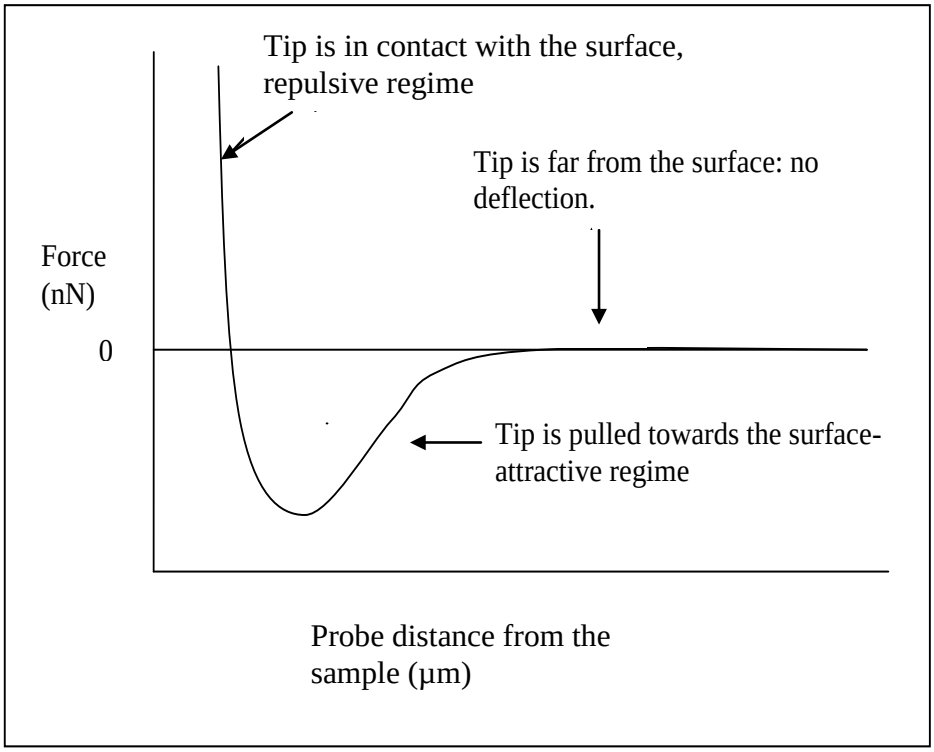

Figure 1.9: Example of force displacement curve generated by AFM showing the deflection produced in the cantilever during its approach and retraction from the sample surface.

1.2.4.2 – Biomolecular Force Measurements measured with AFM

AFM involves direct measurement of strength when an AFM cantilever and the surface functionalised with the molecules of interest are allowed to interact with each other. Numerous types of biomolecular force measurements have been performed using AFM, such as the measurement of individual ligand receptor interactions (strept(avidin)-biotin) [35], interactions between complementary strands of DNA [36], intra-molecular interactions (unfolding of multi-domain proteins [31], polysaccharides [30], etc). Table 1 provides an overview of the some of the bio-molecular force measurements that have been performed with AFM.

TABLE 1 – An Overview of Systems Previously Investigated by Single Molecule Force Studies

1. Biotin-streptavidin

Lee *et al*. (1994) *Langmuir* 10:354
Moy *et al*. (1994) *Science* 266:257
Chilkoti *et al*. (1995) *Biophysical Journal* 69:2125
Florin *et al*. (1994) *Science* 264:415
Allen *et al*. (1996) *FEBS Letters* 390:161
Evans *et al*. (1997) *Biophysical Journal* 72:1541
Wong *et al*. (1998) *Nature* 394:52
Wong *et al*. (1999) *Biomolecular Engineering* 16:45
Merkel *et al*. (1999) *Nature* 397: 51
Evans (1999) *Biophysical Chemistry* 83:97
Moy *et al*. (2000) *Biochemistry* 39:10219-10223.
Marzena *et al*. (2006) *Acta Biochemica Polonica* 53:93

2. Protein-Protein Interactions

Ferritin/anti-ferritin antibody-antigen interactions	Allen *et al*. (1997) *Biochemistry* 36:7457
Integrin-Fibronectin Interaction	Feiya *et al*. (2003) *Biophysical Journa*. 84:1252
Nectin-Cadherin	Tsukasaki *et al*. (2007) *Journal of Molecular Biology* 367:996

3. Intra-molecular Interactions

Unfolding of Protein Titin	Rief *et al*. (1997) *Biophysical Journal* 75:3008 Kellermayer *et al*. (1997) *Science* 276:1112
Polysaccharide (Dextran)	Rief *et al*. (1997) *Science* 276:1295

4. Dissociation of Nucleic Acids

Lee *et al*. (1994) *Science* 266:771
Boland *et al*. (1995) *Proceedings of the National Academy of Science* 92: 5297
Noy *et al*.(1997) *Chemical Biology* 4:143
Strunz *et al*. (1999) *Proceedings of the National Academy of Science* 96:11277
Davenport *et al*. (2000) *Science* 287:2497
Hauke *et al*. (2000) *Current Opinion in Chemical biology* 4:524
Strunz *et al*. (2001) *Single Molecules* 2:75
Strunz *et al*. (2002) *Biophysical Journal* 82: 517
Williams *et al*. (2001) *Biophysical Journal* 80:1932
Williams *et al*. (2002) *Current Opinion in Structural Biology* 12:330
Oh *et al*. (2002) *Langmuir* 18:1764
Kraubtbauer *et al*. (2003) *Nanoletters* 3:493
Green *et al*. (2004) *Biophysical Journal* 86:3811
Hong *et al*. (2005) *Langmuir* 21:4257
Jung *et al*. (2007) *Journal of American Chemical Society* 129:9349

The first studies using AFM in this area were first carried out in 1994, when the biotin-strept(avidin) system was chosen to demonstrate the capability of AFM to measure rupture forces [35,37]. This system was chosen, because it is one of the strongest non-covalent linkages in nature. Streptavidin-biotin force measurements with AFM were also performed by Wong and his co workers in 1998 [38], amongst others. A schematic of their experimental set up is shown in Figure 1.10. More recently, several groups have

investigated the dependence of the rupture forces of biotin-strept(avidin) on the applied loading rate at which the two molecules are pulled apart, and confirmed that the dynamic force spectra possesses two or three regimes of bond strength. A more detailed insight about these studies is described in Chapter 2.

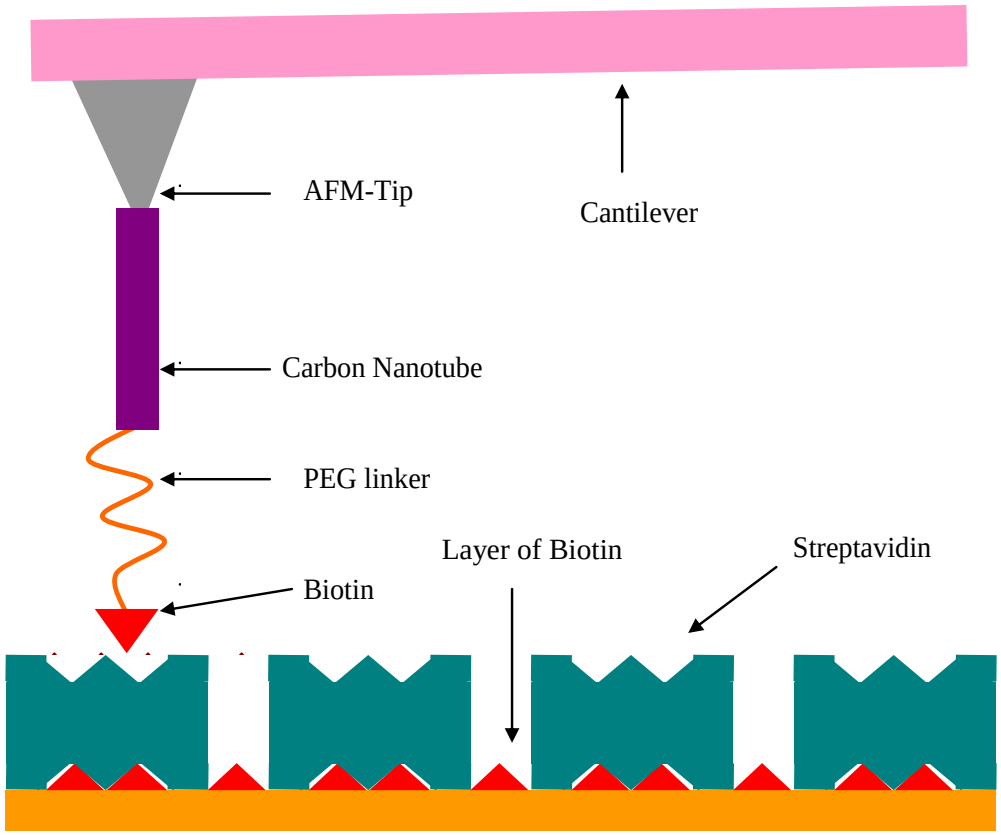

Figure 1.10: Schematic representation of the AFM tip-sample interaction, where the AFM tip and the surface are functionalised with biotin and strept(avidin) molecules respectively. In this case a nanotube has been glued to the AFM tip and the end of the tube is covalently modified with biotin molecule via a PEG linker (*Adapted from* [38]).

Besides strept(avidin)-biotin interactions, several other biological interactions such as antibody-antigen (protein-protein) interactions have been investigated with the AFM. A proper understanding of protein-protein interactions provides an insight into various biological processes such as signal transduction. For example, signals from the exterior of the cell are mediated to the inside of that cell by protein-protein interactions between the

signalling molecules. Various groups have therefore investigated antibody-antigen (protein-protein) interactions such as ferritin/antiferritin antigen-antibody interactions [32], DNA-RNA stretching [39] and dissociation of GroEl proteins [40]. A schematic view of single polymer chain showing stretching and pulling on an antibody-antigen complex with AFM is depicted in Figure 1.11.

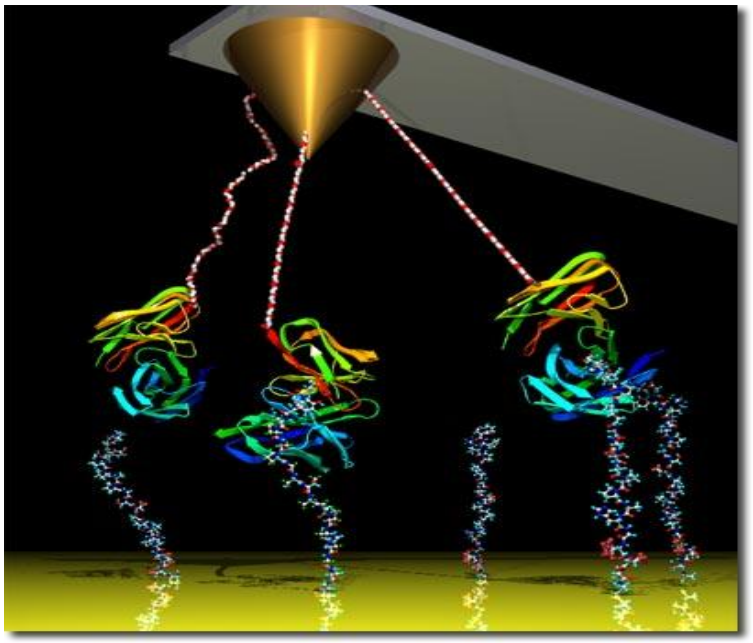

Figure 1.11: Schematic representation of AFM tip with three tethered single chain antibody that mimics the architecture of an anticancer drug [41].

The unbinding kinetics of DNA using AFM was explored by Lee and his co workers in 1994 [42]. They measured the unbinding forces between two complementary oligo-nucleotide strands (20mer), attached covalently to the tip and the surface. The measured rupture force was ~70pN per base pair. A similar experiment was performed by Noy and his co workers using different surface attachment chemistry [43]. They employed self assembled monolayers (SAMs) to immobilize two 14mer complementary oligonucleotides to a gold coated AFM tip and surface. The unbinding forces reported were in the range of 120 ± (50) pN.

Single molecule investigation demands surfaces with desired characteristics such as enough spacing between the immobilized molecules for unhindered interactions, and an optimum density of the surface functional groups. The presently employed bio-molecular immobilization methods such as the silanization approach [44], alkyl thiols [45], self assembled monolayers (SAM) [46], etc. are found to have some shortcomings for effective single bio-molecular screening, because of their ineffectiveness in controlling steric hindrance, nonspecific attachments and the formation of multiple adhesion events. Silanization often yields steric hindrance, because it does not provide sufficient spacing between the immobilized molecules. Even if precise control over the density of surface functional groups was produced by mixed SAMs, the disorder associated with their distribution makes them poor candidates for biomolecular immobilization. The optimum spacing between the immobilized molecules and the probe molecules is very much significant in enhancing specific and unhindered interactions (without steric hindrance) between the probe and the immobilized molecules. This has raised the demand for the development of efficient biomolecular immobilization methods. Recently, dendrons have been employed for bio-molecular immobilization [47] and found to provide sufficient spacing between the immobilized molecules thereby minimising steric hindrance and reducing non-specific adhesion events (see Chapter 4).

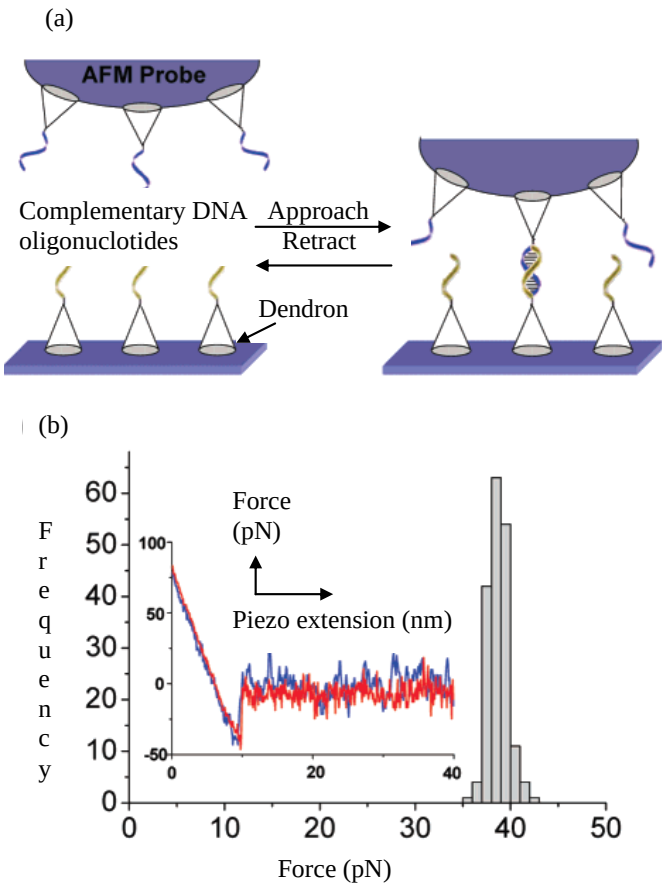

Figure 1.12: (a) Schematic overview of the experimental setup employed for the detection of Hybridisation events between complementary DNA oligonucleotides immobilised on dendron modified AFM tip and the surfaces. (b) An example of AFM generated force extension curve when an AFM cantilever interacts and retracts from the dendron modified surface [47].

Researchers have employed dendron modified surfaces to immobilize different lengths of DNA oligonucleotides (20mer, 30mer, and 40mer) on a dendron modified AFM tip and substrate surface. The unbinding forces were found to increase with increasing loading rate for each sequence and more importantly, they found that the unbinding forces increased with increases in the number of complementary base pairs. For instance, the unbinding force for 40mer sequences at a speed of 1µm/s was around 60pN and for 50mer was around 65pN. Figure 1.12 shows the schematic overview of the experimental set up employed by

Jung and co workers for the detection of DNA hybridisation events and measurement of unbinding forces using an AFM.

AFM has been employed through this approach to study the internal structure of various macromolecules such as polysaccharides [30], and multi-domain proteins [31], and has allowed the reproducible detection of structural transitions that result due to changes in length. By careful handling, a single molecule can be held between the tip and the surface for a long period of time, allowing repeated measurements to study the reproducibility or dynamics of the unfolding or refolding processes in a single molecule. A typical example of the unfolding of a multi-domain protein is shown in Figure 1.13.

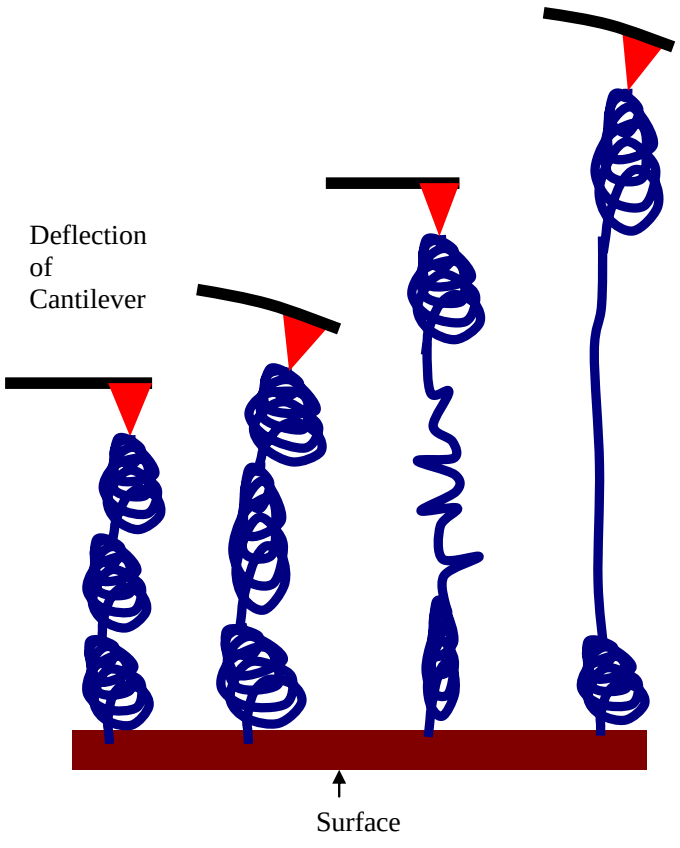

Figure 1.13: Structural transitions in a multi-domain protein (Titin), the extent of unfolding of the protein increases with increase in the externally applied mechanical force (*Adapted from* [31]).

1.2.4.3 – Theory Dynamic Force Spectroscopy (DFS)

Bio-molecular force measurements are performed by recording forces between AFM tips and surfaces functionalised with the molecules of interest. When the tip and the surface functionalised with molecules of interest are allowed to interact with each other (approach and retract), a force-displacement curve is generated. The measured adhesion force (see Figure 1.9) can correspond to the rupture of a single molecule event, if the numbers of interacting molecules, contact force etc. are carefully controlled. The bond rupture depends on the loading rate. The rate with which an AFM cantilever interacts with the surface is called loading rate (change in force with time, dF/dt). Loading rate (r_f) is also given by the product of the spring constant (k_c) of the cantilever and the cantilever retraction velocity (V_c). This concept of loading rate is valid only when force is generated by cantilever alone. However, if linkers such as PEG are used to transmit force, then we need to calculate spring constant of the system (k_s) which changes the loading rate (Chapter 2).

The force with which an AFM cantilever approaches and retracts from a surface can be regulated to achieve the different combinations of loading rates. Measurement of rupture forces of single-molecules at a range of loading rates is known as dynamic force spectroscopy (DFS) [48]. Several hundred force-extension curves are recorded at each loading rate to obtain a dynamic spectrum of bond strength (Figure 1.14).

The measurements of a rupture force of a single-molecule interaction do not form a single value, but a distribution. Therefore, the rupture force values recorded at each loading rate are collected and plotted in a histogram to obtain the most probable value of the unbinding force (mode or f*). All modal forces recorded are plotted against the loading rate to obtain the dynamic spectra of rupture forces. The dynamic spectrum of the bond strength provides

an image of the prominent barriers traversed in the dissociation energy landscape. Each barrier governs the adhesion strength of the single-molecule interaction made when the probe and sample are brought into contact as mentioned earlier. Theory predicts that the rupture force of any single-molecule interactions depends on the external mechanical load. It has been reported that the unbinding strength is governed by the most prominent energy barrier traversed in the energy binding energy landscape along the unbinding pathway [48].

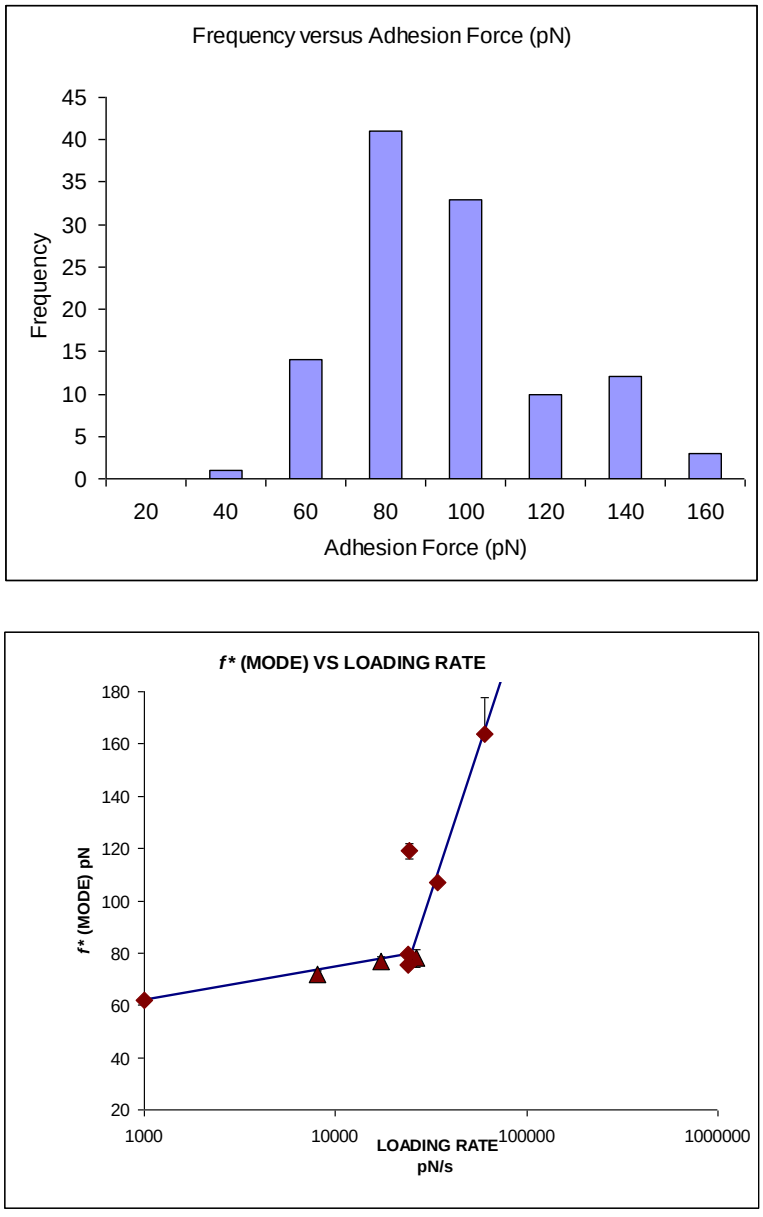

Figure 1.14: An example of a force distribution and a DFS plot obtained when an AFM cantilever functionalised with biotin is allowed to interact with a silicon surface functionalised with streptavidin.

1.3 – Aims of Thesis

Over the past couple of decades researchers have employed DFS to investigate the unbinding kinetics of different single molecules such as strept(avidin)-biotin interaction [35], DNA oligonucleotides hybridisation [49] and the unfolding of proteins [31]. It has been found that the rupture force of the single-molecules increases with increases in loading rate. The unbinding forces of single-molecules are not dependent on loading rate only, but can be influenced by various factors such as temperature, the physics of the cantilevers, noise, drift and underlying attachment chemistry. The majority of biomolecular force measurements performed with AFM have investigated the dependence of rupture forces on the applied load, and very little work has been done on the temperature dependence of the unbinding forces of DNA strands. In this work we observe and discuss the effect of temperature on the unbinding process. In addition, the advantage of employing recently developed dendron immobilization chemistry for force spectroscopy experiments was investigated.

The first objective of this work was to develop a proper understanding of single-molecule force measurements using AFM and to gain experience of performing force spectroscopy measurements by using the previously studied streptavidin-biotin system [19]. However, the primary objective was then to investigate the effect of temperature on the unbinding force measurements of streptavidin-biotin system and DNA oligo-nucleotide hybridisation.

CHAPTER -2:

DYNAMIC FORCE MEASUREMENTS OF STREPTAVIDIN-BIOTIN INTERACTIONS AT ROOM TEMPERATURE

Chapter-2: Dynamic Force Measurements of Streptavidin-Biotin Interactions at Room Temperature

2.1 - Introduction

Molecular interactions are fundamental to biology. The nature of the interaction is non-covalent (e.g. electrostatic or van der Waals interactions). Several weak non-covalent interactions can lead to highly specific and stable intermolecular connections between large molecules to build up a new molecular complex [10]. It is important to understand such weak non-covalent interactions between large molecules as they play a significant and vital role in governing the structure of various bio-molecules such as proteins, lipids, carbohydrates and nucleic acids, besides mediating many biological functions and processes such as protein folding [31], DNA/RNA hybridisation, ligand-receptor interactions, adhesion, transcription, replication and enzyme action [25]. Therefore, it becomes essential to probe these forces at the molecular level.

At the nanometer scale of a molecular system, the detected forces are in the range of few picoNewtons to several nanoNewtons [50]. The life time of single molecule interactions are considerably reduced under the application of an external mechanical load, as already discussed in Chapter 1. There are several experimental techniques available to measure the strength of these weak non-covalent interactions at the nanoscale level such as atomic force microscopy (AFM) [51], optical tweezers (OT) [52], and the MT [53], and the BFP [54].

Weak non-covalent interactions have limited life times and dissociate under any level of force. In this connection, the finite life time of a molecular interaction was considered and how this finite life time influences the rupture force measurement [50]. These observations lead to the emergence of the field of dynamic force spectroscopy. The measurement of the rupture forces of the bonds formed at a range of loading rates when an AFM probe

functionalised with ligand interacts with the surface coated with receptor is called dynamic force spectroscopy [55].

The dynamic force spectroscopy method allows measuring the strength of the molecular binding forces between a small number of various ligand and receptor molecules immobilized on the AFM cantilever and on the surface of substrate. The adhesion is probed with force-distance traces. All the rupture forces recorded at each loading rate are cumulated to obtain the mode (f^*). Plot of modal rupture force values against range of loading rates (r_f) produces the dynamic force spectra of the unbinding forces.

The dynamic spectrum of bond strength obtained gives an image of the prominent energy barriers traversed in the energy landscape along the force driven dissociation pathway when the most frequent value of the unbinding force (modal rupture force) is plotted against log of loading rate [48].

Each barrier governs strength on a different time scale and the attachment of receptors to the substrate surface plays a significant role in governing adhesion strength. When the bond is loaded with an external force, the unbinding force at which it breaks is not a single value but a distribution. Unbinding forces are a continuous spectrum of bond strengths, because theory predicts that the forces will depend on the rate at which the load is applied. The measured strength is governed by the most prominent barrier traversed in the energy landscape along the force-driven bond-dissociation pathway [48].

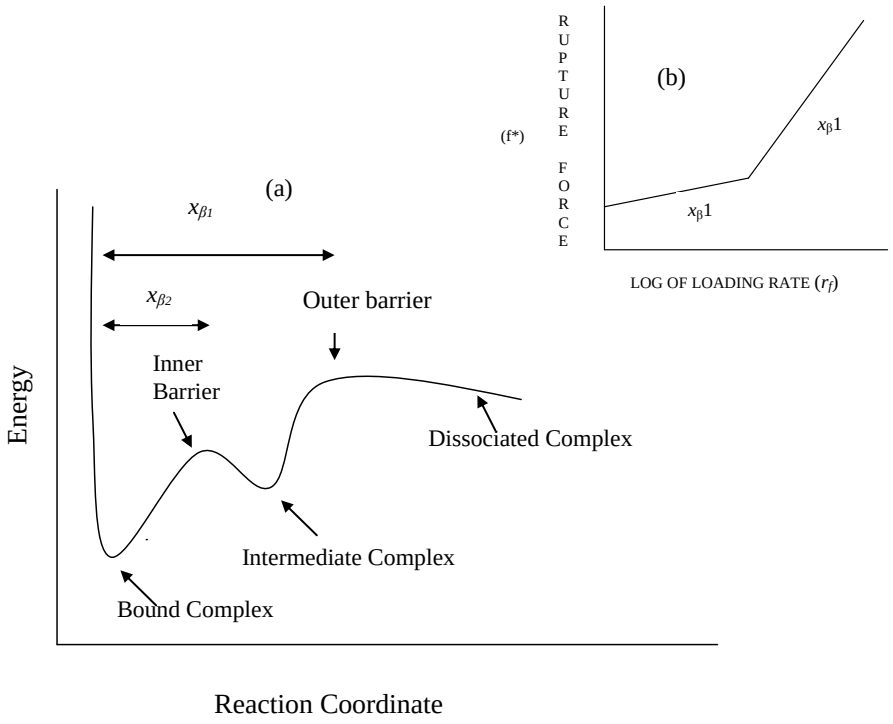

Figure 2.2: (a) Conceptual energy landscapes of the streptavidin-biotin complex. (b) Shows modal rupture force increases with an increase in loading rate, ($x_{\beta 1}$) *and* ($x_{\beta 2}$) *respectively represents the slopes of first and second regimes of unbinding forces (Adapted from* [56]).

It has been reported that the dynamic force spectra for strept(avidin)-biotin complex shows a linear relationship between the mode *(f*)* and logarithm of the loading rate and is given by the following expression [48].

$$f^* = \frac{k_B T}{x_\beta} \ln \frac{(r_f . x_\beta)}{k_B \upsilon} \qquad (2.1)$$

where v is the thermal off-rate, r_f is the loading rate, k_B is Boltzmann's constant, and x_β is the distance between the bound state and transition state along the direction of applied force. The thermal off-rate (thermal dissociation) is given by the following equation:

$$\upsilon = \exp \frac{-[E_b - f . x_\beta]}{k_B T} \qquad (2.2)$$

where E_b is the barrier energy.

f^* versus the log of loading rate is a straight line in each regime of the spectrum with a slope (f_β),

$$f_\beta = \frac{k_B T}{x_\beta} \qquad (2.3)$$

where f_β is the thermal force scale.

It can be observed from Figure 2.2 that modal rupture forces increase with increasing loading rate and at a certain stage with an increase in loading rate, the slope of unbinding forces increases suddenly. This sudden increase in slope from one regime to the next demonstrates the suppression of an outer energy barrier by external force and dominance of an inner barrier to the dissociation of the ligand-receptor complex. This observed change in the slope of mode (f^*) versus log of loading rate (r_f) can be attributed to the suppression of an outer energy barrier of the energy landscape [48].

The distance between the energy state and the transition state (x_β) for a given regime of applied external forces can be estimated from the slope of the fitted line [19]. The force measurements can be used to obtain an estimate of the change in the outer and inner activation energy barriers of the streptavidin-biotin complex.

The rupture (unbinding) force, being a measure of the interaction between the ligand and the receptor, is detected upon withdrawal of the cantilever from the surface, as discussed in Chapter1. Dynamic force spectroscopy then allows these measurements to provide a measure of the transition state displacement and an estimation of the force free dissociation rate of the molecular bond. Examples of DFS measurements that have already been reported include DNA-protein interactions [57], RNA dissociation [58], interactions

between antigens and antibodies [32], intra-molecular forces within polymers [30], and forces in protein folding [31].

Initially single molecule force measurement studies were conducted with strept(avidin)-biotin and these studies confirmed that the strength of this interaction stems from its specificity and high affinity. It was also reported that the strength of the unbinding force was influenced by the molecular determinants which contribute to the enthalpic activation barrier. The increase in the strength of the rupture forces with increasing loading rate was also confirmed [19]. It was reported that the lifetime of an interaction sustained by a non-covalent interaction reduced under the application of external force because of thermal activation, thereby lowering the activation energy of the barriers, consequently decreasing the bond life time and promoting the dissociation process [19,59]. All these findings have contributed to our understanding of the dissociation of different complexes under force.

Recently researchers have investigated bond formation over six orders of magnitude in loading rate and confirmed that the strength of streptavidin-biotin bonds depends on loading rate [23]. Moreover, the DFS measurements showed two regimes of bond strength in the streptavidin-biotin force spectrum, revealing the presence of two activation barriers (transition states) in the unbinding process. They described the activation barriers derived from strength spectra to the shape of the energy landscape derived from simulations of the strept(avidin)-biotin complex. It was also reported that even though strept(avidin)-biotin bonds can break under very small forces, the location of the outer barrier at ~3nm leads to a significant difference in loading rate intercepts of the low and high intermediate strength regimes [23].

The strept(avidin)-biotin system has attracted the focus of many researchers, because of its large binding free energy ΔG [44]. The high specificity and affinity of the streptavidin-biotin interaction became the basis of choosing it as model system. The streptavidin-biotin complex is stabilized by an elaborate network of hydrogen bonds and van der Waals interactions. Streptavidin has molecular weight of 53,000 daltons and is a tetrameric protein with each of the four identical subunits capable of binding one biotin molecule [44]. Due to its tetrameric structure the chances of the binding event in a force measurement is increased, due to an increase in the number of receptor sites. The crystal structure of the streptavidin-biotin complex revealed that each subunit is formed by a single polypeptide chain arranged in an eight-stranded anti-parallel beta-barrel structure to which biotin binds [60]. The complexes are also extremely stable over a wide range of temperatures and pH conditions. The three dimensional structure of the strept(avidin)-biotin complex, and the chemical structure of the biotin is given in Figure 2.2 and Figure 2.3 respectively.

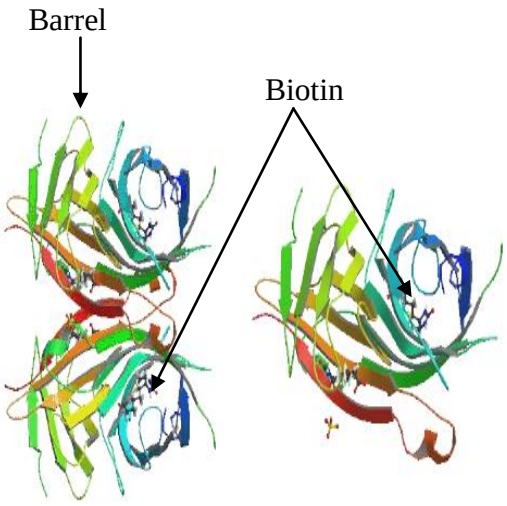

(a). Dimer (b). Monomer

Figure 2.2: The three dimensional structure of streptavidin-biotin complex (Resolution =1.36 Å) (a) A dimer: two biotin molecules bound to two subunits of streptavidin (b) A monomer: a single biotin molecule bound to single subunit of streptavidin [61].

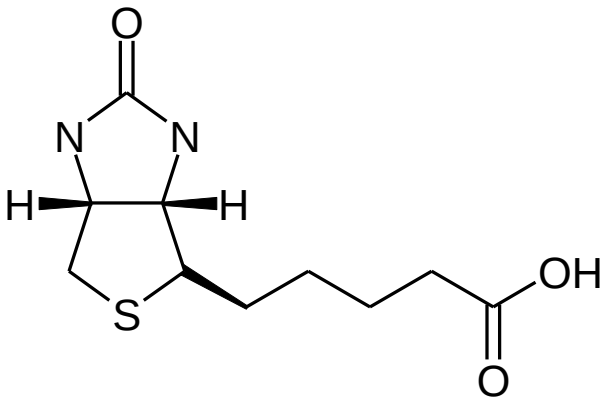

Figure 2.3: The chemical structure of Biotin.

2.2 - Aims

These experiments were carried out to gain some experience of performing force spectroscopy measurements by using a previously studied streptavidin-biotin system model system [48]. As already discussed, the streptavidin-biotin interaction has been studied on numerous occasions and exciting results from previous research can be directly compared with those collected in these studies. A second objective of the work was to provide a reference, or benchmark for the investigation of the effect of temperature on streptavidin-biotin force measurements as presented in Chapter 3.

2. 3 - Materials and Methods

All the chemicals used were obtained from Sigma Aldrich. Extensive care was adopted to prevent the contamination of the silane (APDES) and its exposure to moisture. Deionised water of 18MΩcm resistivity was used through out the entire sample preparation process including the preparation of PBS buffer which was used as a medium for conducting force

measurements. PBS solution was filtered through sterile 0.2µm Ministart filters before use. Nitrile gloves were worn at all times.

2.4 - Functionalisation of AFM Cantilevers and Silicon substrates

Two types of silicon nitride AFM cantilever (Nanoprobes) were used –'NP' and 'MLCT', both were obtained from Veeco (Santa Barbara). Cantilevers were oxygen plasma etched (10 W, 0.2 mbar O_2 for 30 seconds) to remove impurities and oxidise the surface of the cantilevers. Silicon surfaces were cleaned in Piranha solution (1:3 ratio of hydrogen peroxide (30%) and sulphuric acid) for half an hour. Amine groups were established on oxidised AFM cantilevers and silicon surfaces by incubating them in amino-propyl dimethyl ethoxy silane (APDES) solution for an hour (100 µL of APDES in 10 ml anhydrous toluene). The substrates were then rinsed with anhydrous toluene followed by methanol or ethanol and dried under a nitrogen stream. Dried silicon chips were then incubated in an oven for 45 minutes followed by rinsing with toluene and then methanol/ethanol and dried with nitrogen again. Amine reactive polyethylene glycol (PEG) polymers with biotin end groups were covalently linked to dried silanized surfaces of silicon chips and AFM cantilevers by incubating them for at least 3 hours in a PBS solution of 1 mM α-biotin-ω-carboxysuccinimidyl ester poly (ethylene glycol) with a PEG molecular weight of 3400 Daltons (NHS-PEG3400-biotin, Huntsville, AL). After completion of the incubation period both AFM cantilevers and silicon surfaces were first rinsed with PBS and then with de-ionised water followed by drying with nitrogen. The biotinylated silicon surfaces were exposed to a 1 mg/ml streptavidin solution in PBS for half an hour before rinsing with PBS. Biotinylated AFM cantilevers were left in PBS, and rinsed with de-ionised water and dried before use. Figure 2.4 shows the sequence of the reactions involved in the functionalization process.

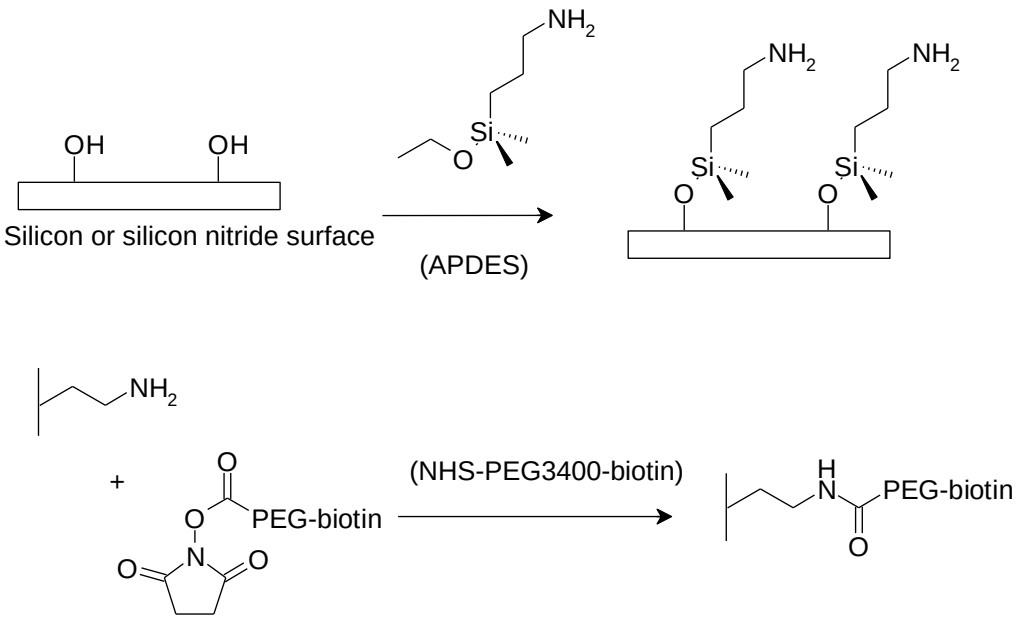

Figure 2.4: Schematic overview of the chemistry and chemical reactions employed in the preparation of the streptavidin-functionalised silicon substrates and PEG (biotinylated) functionalised AFM tips both silanized with APDES (3-aminopropyldimethylethoxysilane)

2.5 - AFM Force Measurement

Force measurements were performed using a 1D Molecular Force Probe (MFP-1D) (Asylum Research) and a Pico-force adaption to a Multimode AFM (Veeco). Force-distance curves were recorded between substrate surfaces coated with streptavidin and tips functionalised with biotin as shown in Figure 2.5.

Mechanical noise was minimised by placing the force apparatus on an air table. The spring constants of each cantilever were individually calibrated using the thermal fluctuation method [33]. Although these spring constant values did not vary significantly from the nominal values given by the manufacturer and were in the range of 23pN/nm to 85pN/nm.

The Inverse Optical Lever Sensitivity (INVOLS) was calibrated from the slope of the contact region of the force curve recorded on reference glass slide surface.

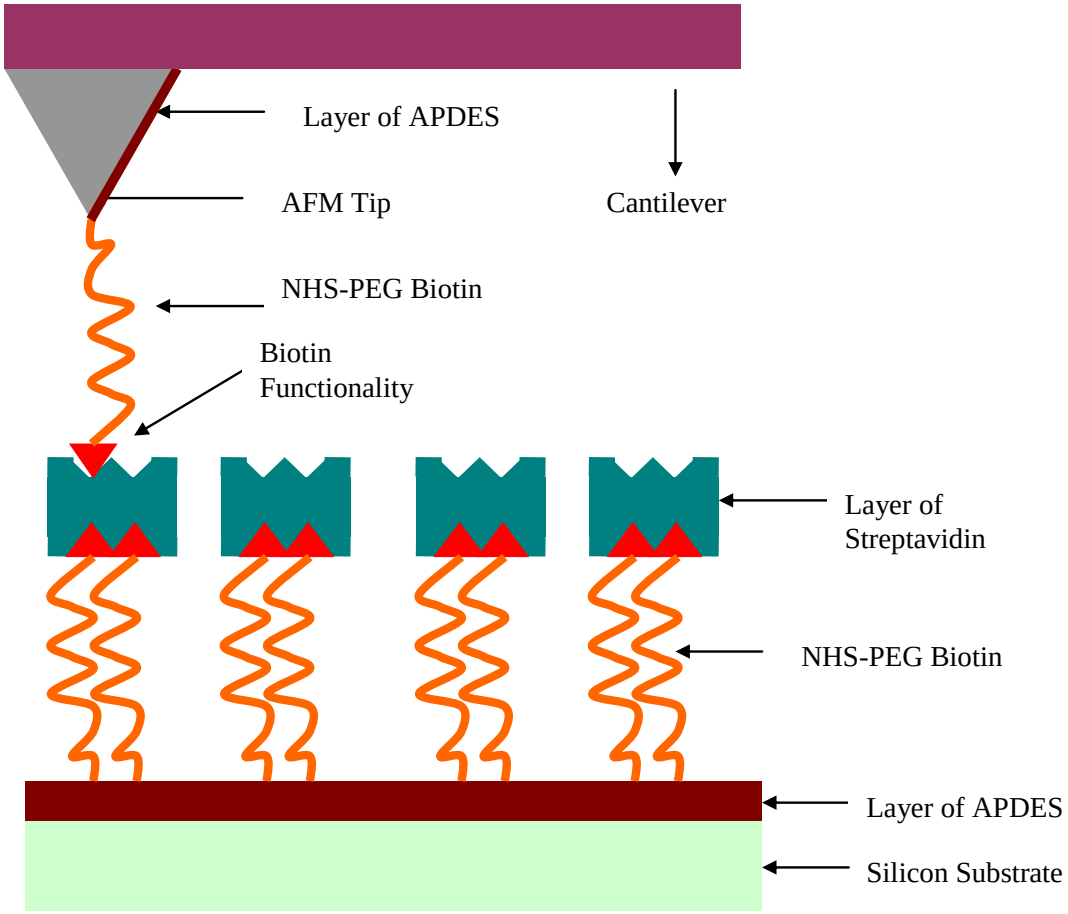

Figure 2.5: Diagrammatic representation of the streptavidin-biotin system where the AFM tip functionalised with biotinylated PEG (NHS-PEG3400-biotin) interacts with streptavidin immobilised on the silanized silicon substrate via the biotinylated PEG cross linker.

2.6 - Results

The unbinding events due to the streptavidin-biotin complexes were observed in the retract traces of the AFM force measurements. The unbinding force was taken as a measure of the ligand-receptor biotin-strept(avidin). To avoid damaging to the functionalised tip, the maximum tip-surface contact force was manually maintained at a maximum of 500pN using the MFP-1D, and automatically maintained at 500pN when using the Picoforce instrument. AFM measurements with the Picoforce were found to be more convenient in this regard. It

allowed fixing of the desired contact force value in the beginning of the experiment, which was not possible with MFP-1D. As shown in Figure 2.6 several hundred unbinding force curves were collected after performing thousands of approach-retract cycles at each retract speed. In these experiments adhesion events due to single specific, non-specific, multiple interactions were observed, in addition to force curves having no adhesion events. To reduce the percentage of non-specific adhesion events, the AFM tip and the sample surface were prepared with a paucity of reactive sites, as small amount of ligand (biotin)-receptor (streptavidin) was used for their immobilization on the tip and the surface respectively. This was done to ensure that the vast majority of specific interactions recorded are due to single rather than multiple interactions.

The specific interactions due to single interactions occurred with rupture lengths (50nm-62nm) less or approximately twice the length of PEG linker. The length of PEG was estimated as described in the literature [62], as follows: the number of ethylene glycol monomeric repeats was first calculated from the molecular weight of PEG linker (3400 Daltons) by dividing the molecular weight of single ethylene glycol monomeric unit (approximately 62 Daltons). The calculated value obtained was multiplied by the estimated total bond length of the ethylene glycol monomeric unit. Therefore the total length of the two biotinylated-PEG linkers was approximately 60nm. Specific measurements of biomolecular interactions were characterised by a specific arc shape curve corresponding to the non-linear extension of the PEG cross linker of not more than twice the length of the biotinylated PEG linker (60nm). Adhesion events devoid of an arc shape and non-linear extension of cross linker were considered to be non-specific adhesion events. Nonspecific adhesion events also occurred with a zero rupture length. Examples of specific, non-specific, multiple and no adhesion force-displacement curves for the streptavidin– biotin system are shown in Figure 2.6 (a), (b), (c), (d). To ensure that adhesion was mediated by a

single adhesion event (single streptavidin-biotin interaction), the force exerted on the cantilever during approach was regulated so that approximately 10% (one in ten) of the trials resulted in an adhesion event.

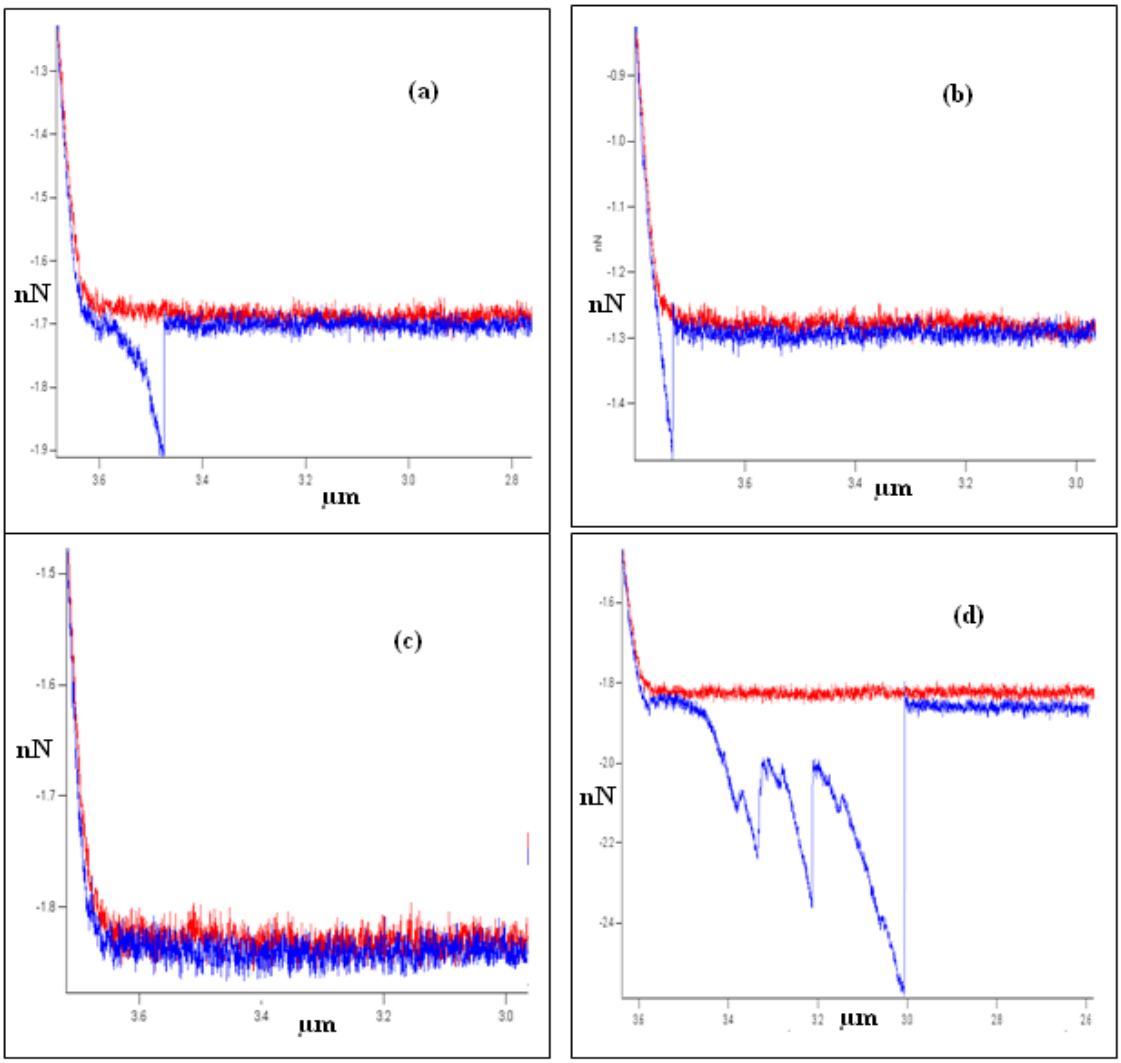

Figure 2.6: (a) Specific, (b) non-specific, (c) no adhesion (d) multiple force displacement curves of the interaction between a biotinylated PEG-functionalized tip and the silicon surface functionalised with streptavidin. The measurement recorded the force on the AFM cantilever on approach and retraction of the cantilever from the substrate immobilised with streptavidin. Red and blue lines/curves show the approach and retract traces of AFM cantilever towards and away from the substrate surface respectively.

The specificity of the interaction was confirmed at the end of experiments by adding free streptavidin to the solution which resulted in a decrease in the number of force traces where specific adhesion forces were observed. This was confirmed after observing no specific adhesion in more than 95% of the force traces, when approximately 1000 force curves were recorded. Thousands of the force measurements could be recorded in each experiment confirming that the rupture had not occurred elsewhere in the system and that observed interaction events were due to streptavidin-biotin interactions. The retract traces of the force measurement were found sometimes to exhibit several transitions in force, due to the sequential unbinding of multiple strept(avidin)-biotin complexes as shown in Figure-2.6(d).

Unbinding forces were measured at a range of cantilever retraction velocities. The unbinding force of the molecular attachment established between the AFM cantilever (transducer) and the functionalised surface is calculated by the maximum extension Δx, of the AFM cantilever when it retracts from the surface using the equation below.

$$f = k_s \Delta x \qquad (2.3)$$

where k_s is system spring constant.

The loading rate used in the force measurements is given by the product of spring constant of the system and the cantilever retraction speed.

$$r_f = k_s V_c \qquad (2.4)$$

where (r_f) is loading rate, (V_c) is cantilever retract velocity [23].

For the calculation of loading rate, the stiffness of the system (k_s) was to be calculated. The system spring constant in turn depends on the spring constant of the PEG cross-linker (k_{peg}) and the spring constant of the cantilever (k_c) and the relationship is given by the following equation:

$$\frac{1}{k_s} = \frac{1}{k_{peg}} + \frac{1}{k_c} \qquad (2.5.1)$$

In this experiment biotinylated PEG polymers were used on both the tip and the surface (one attached to AFM cantilever and the other one as a cross linker between amino (NH_2-) reactive groups of APDES on the surface and streptavidin. Therefore spring constants of two biotinylated PEG polymers were taken into account in our experiments in order to calculate the effective spring constant of the system. In order to double the contour length one has to double the fractional extension to achieve the same force. So the x/l ratio is the same. The stiffness of the double length polymer $k_{peg(series)}$ is 1/2 that of the single length one k_{peg}.

$$\frac{1}{k_{peg}} = \frac{k_B T}{b}\left(\frac{1}{2l}\right)\left(1-\frac{x}{l}\right)^3 + \frac{1}{l} \qquad (2.5.2)$$

$$\frac{1}{k_{peg\,(series)}} = \frac{k_B T}{b}\left(\frac{1}{4l}\right)\left(1-\frac{2x}{l}\right)^3 + \frac{1}{2l} = \frac{1}{2}k_{peg} \qquad (2.5.3)$$

where l is contour length and b is persistence length of PEG.

The effective spring constant of two biotinylated PEG polymers each with same spring constant (k_{peg}) in series is given by the equations below:

$$\frac{1}{k_{peg\,(series)}} = \frac{1}{2} k_{peg} \qquad (2.5.4)$$

This resulted in the modification of the system spring constant equation-(2.5.1) into a new equation given below:

$$\frac{1}{k_s} = \frac{1}{\frac{1}{2} k_{peg\,(series)}} + \frac{1}{k_c} \qquad (2.5.5)$$

$$\frac{1}{k_s} = \frac{2}{k_{peg\,(series)}} + \frac{1}{k_c} \qquad (2.5.6)$$

It is difficult to measure k_s directly because of an incomplete knowledge of the properties of the molecular linkages k_{peg}. In order to estimate the value of k_{peg}, we therefore measured the extension of the PEG linker at a particular rupture force. The worm-like chain (WLC) model can be used to describe the extension of the PEG linker [63]. This model gives a general empirical description of the force-extension behaviour of a polymer and is parameterised by two variables: the contour length (l_c) – the total length of the polymer when fully extended, and the persistence length (b) – a measure of the stiffness of the polymer.

$$F(x) = \frac{k_B T}{b} \left(\frac{1}{4} \left(1 - \frac{x}{l_c} \right)^{-2} - \frac{1}{4} + \frac{x}{l_c} \right) \qquad (2.6)$$

F(x) is the force required to hold the ends of a polymer at a distance *x* from each other. The contour length (l_c) ~30 nm and persistence length (b) = 0.4 nm for the PEG chain used here.

The spring constant of the PEG is therefore given by the following equation:

$$k_{peg} = \frac{\partial F(x)}{\partial x} = \frac{k_B T}{b}\left(\frac{1}{2l_c}\left(1-\frac{x}{l_c}\right)^{-3} + \frac{1}{l_c}\right) \qquad (2.7)$$

The estimated stiffness of the PEG was in the range of 11pN/nm to 35pN/nm. In this experiment the calculated system spring constants were in the range of 7pN/nm to 19pN/nm. This was used to calculate the loading rate (eq.2) and the range of loading rates used, calculated to be between 10.60pN/s and 80.6pN/s. In all the AFM measurements change in the loading rate was achieved either by changing the AFM cantilever or cantilever retraction velocity or both. The observed unbinding force increases with increasing loading rate. The mode *(f*)* of the unbinding forces of the single streptavidin-biotin complex at each loading rate was determined from a force histogram of greater than 150 measurements by plotting all the adhesion values in F_{Dist} as shown in Figure 2.7 (a), (b), (c), and (d).

F_{Dist} is a method {developed by Prof. Phil Williams, Nottingham} which assumes that the force measured has been subject to some error and determines the mode of discretely sampled adhesion forces by determining a cumulative distribution as the sum of Gaussians of specific width. F_{Dist} calculates the modal rupture force *(f*)* for each set of adhesion values with standard deviation (s.d). The s.d, is the standard deviation between the mode of cumulative distributions and predicted distributions for a single molecule.

The cantilever noise is expected in the force measurements due to temperature fluctuations as cantilever is always in a state of oscillation. This force noise is given by the equation:

$$ForceNoise = k_c\left(\frac{k_B}{k_c}\right)^{\frac{1}{2}} \qquad (2.8)$$

where k_BT = 4.11pN.nm. The noise level in this experiment was around 10pN.

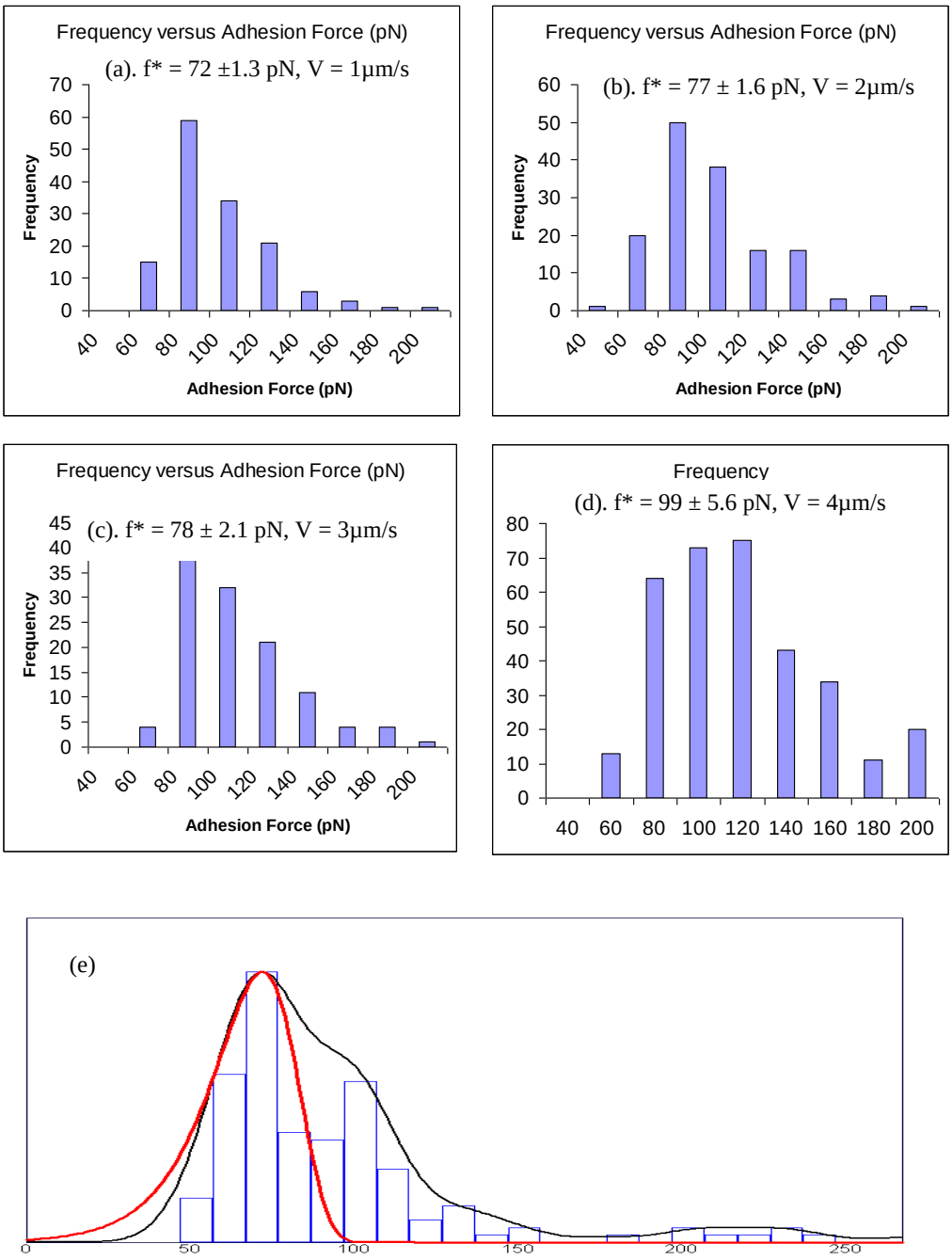

Figure 2.7: (a), (b), (c), (d) respectively represent the frequency distributions of all the individual adhesion values obtained at retraction speeds of 1µm/s, 2µm/s, 3µm/s and 4µm/s. However the modal rupture (f) force with standard deviation for each set of adhesion values was obtained after plotting them in F_{Dist}. (e) Represents the histogram of all the individual adhesion values at a retract velocity of 2µm/s after plotting them in F_{Dist} to obtain the mode (f*). Here f* represents the mode with standard deviation recorded at each retract speed. Black line represents the cumulative distribution of all the Gaussians. Its slope represents the force scale (f_β) and red line calculates the predicted mode of all the distributions by using the force scale (f_β).*

Modal rupture force *(f*)* values of streptavidin-biotin complex were plotted against a range of loading rates to obtain the DFS as shown in Figure 2.8.

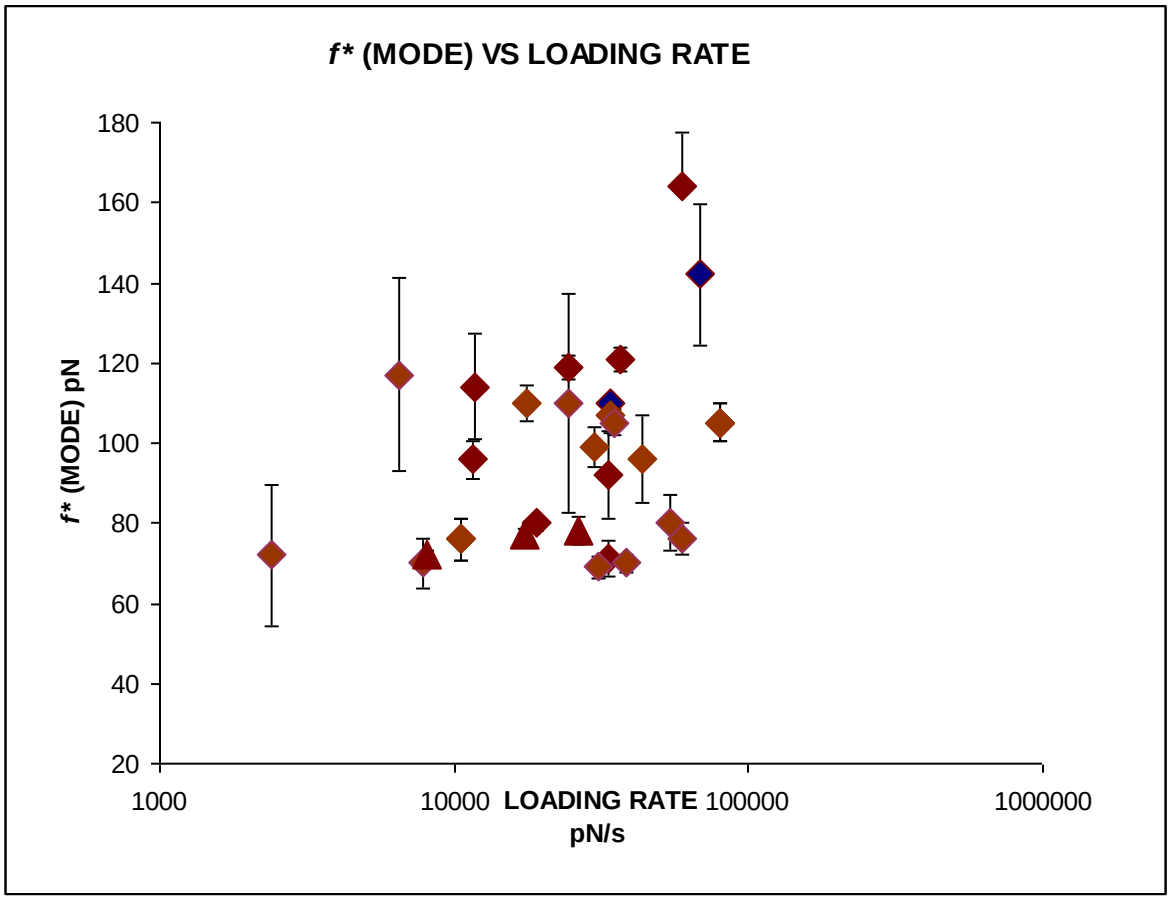

Figure 2.8: Semi-logarithmic plot of modal rupture forces of streptavidin-biotin interactions against range of loading rates at room temperature showing scattered data. Different symbols represent data collected in each experiment.

2.7 - Discussion

Figure 2.8 showed the dynamic response of streptavidin-biotin unbinding force measurements to a range of loading rates recorded at room temperature. All the data points presented look scattered and no obvious trend showing the behaviour of modal rupture force against loading rate is observed. Therefore, in order to compare our data with previous studies on streptavidin-biotin unbinding force measurements, all the data was first

compressed to a line corresponding to the previously reported behaviour of this complex to force (as shown in Figure 2.9)[19].

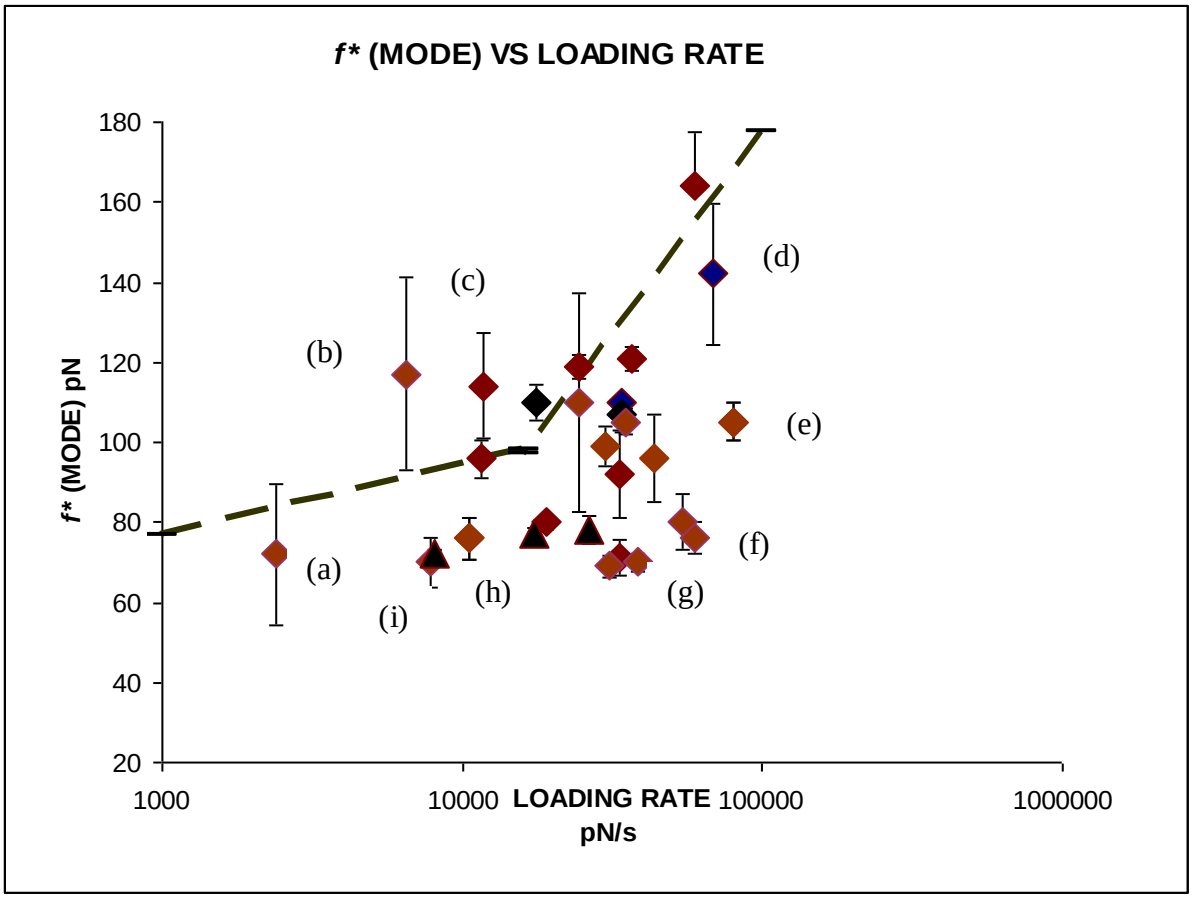

Figure 2.9: Semi-logarithmic plot of modal rupture forces of streptavidin-biotin interactions against range of loading rates at room temperature showing comparison with predicted fitted data (previous studies). Black dotted lines show behaviour predicted by previous DFS studies of this interaction [19]. Different symbols represent force data collected in each experiment. Slopes and thermal off-rate values for the first and second regimes of bond strength were (f_β = 7.7 pN, v = 0.006/s) and (f_β = 44pN, v = 40/s) *respectively.*

Many of the data points can be seen close to the expected behaviour shown by dotted lines in previous DFS studies [19]. However, there are some data points which don't fit to the line the ones with large error bars [(a), (b), (c), (d)] and the ones [(e),(f),(g),(h),(i)] with small error bars which lie too far from the predicted regimes of bond strength. Such "outliers" may arise from wrong estimation of the system spring constant and the Inverse Optical Lever Sensitivity (INVOLS) as described in section 2.5. The variation in rupture forces

above and below the predicted regime of bond strength could be also due to system errors because of different cantilevers used in the whole range of experiments. In addition the large error bars in data points could be simply because of multiple interactions due to large contact force which occurred in some early experiments. However, the data points with small error bars differ by only a few Pico-Newton forces from the predicted values of bond strength, possibly due to small error in spring constant calibration and the INVOLS. Therefore, the data points with large error bars obscure the general trend within the data. To investigate their impact, these points were eliminated. The elimination of these data points modifies our data into a more refined data, presented in Figure 2.10.

Figure 2.10 shows two regimes of bond strength and it is very much evident that the modal rupture force of streptavidin-biotin complex increases with increasing loading rates and showed an initial gradual increase, followed by a more rapid increase with increasing loading rates. This is an observation consistent with previous studies [19].

The dynamic response of the bond to sustain less load and large load at lower and higher loading rates respectively has been attributed to the difference in the activation energy between inner and outer energy barriers [55]. The two linear regimes of bond strength map the location of the energy barriers to dissociation.

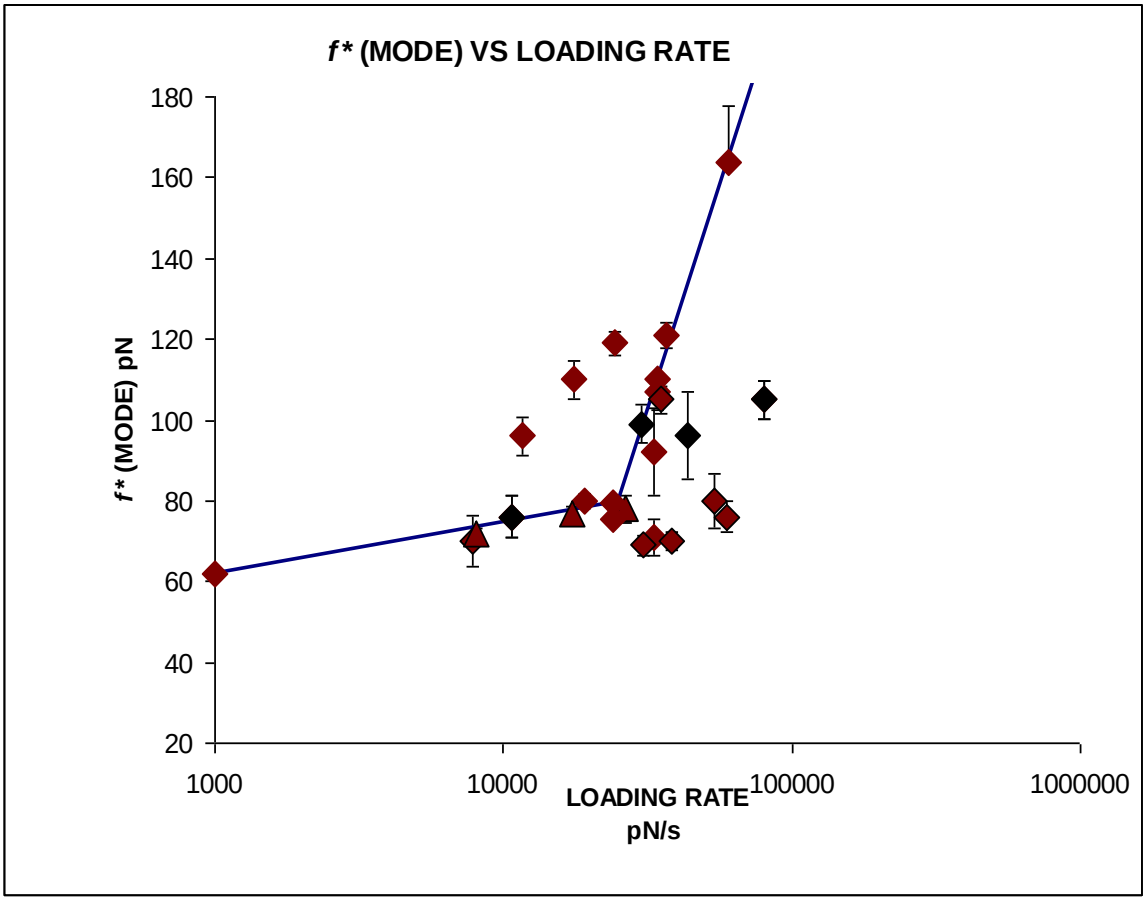

Figure 2.10: Semi-logarithmic plot of modal rupture forces of streptavidin-biotin interaction against range of loading rates at room temperature showing modified fitted data. Solid black lines are fits based on theory to the refined data. Different symbols represent force data collected in each experiment. Slopes and thermal off-rate values for the first and second regimes of bond strength calculated from the fit were (f_β = 5.5 pN, ν = 0.0024/s) and (f_β = 97pN, ν = 113.8/s) respectively.

Therefore, our data confirms that the streptavidin-biotin complex overcomes two transition states before its final dissociation as discussed in the beginning. This observation is also in agreement with previous studies [55]. Moreover, the calculated slope and thermal off-rate for the first regime of bond strength were almost similar to the values previously reported for first regime of bond strength. However, the slope and thermal off-rate values for the second regime of bond strength were larger than the previously reported values as shown in Figure 2.9. This is probably due to the reason, that we investigated the strength of strept(avidin)-biotin bonds using a narrow range instead of loading rates differing by orders

of magnitude. That is also why the number of data points corresponding to the second regime of bond strength is less when compared to the data fitted to the first regime of bond strength.

It is important to take into account possible modifications of the compliance of the ligand–receptor system due to the experimental protocol because the primary source of error in this analysis comes from the uncertainty of the spring constant value of the whole system including the cross-linkers. Therefore, in order to understand the relation between the rupture forces measured by AFM and the real non-covalent bonds in the studied bio-complexes, more systematic investigations of ligand-receptor interactions on model systems are necessary.

2.8 - Conclusions

The dynamic force spectroscopic measurements of streptavidin-biotin interactions were found to increase with increasing loading rate with an initial gradual increase, followed by a more rapid increase with increasing loading rates. The resultant spectrum of rupture forces showed two regimes of loading rates, revealing the presence of two transition barriers in the unbinding process. These findings are consistent with that previously reported for dynamic force studies of the streptavidin-biotin complex [19], [55].

The experimental insight of the dynamic force measurements of streptavidin-biotin complex at the room temperature has provided the baseline for studying the effect of temperature on these measurements described in Chapter 3.

CHAPTER -3:

EFFECT OF TEMPERATURE ON DYNAMIC FORCE SPECTROSCOPIC MEASUREMENTS OF STREPTAVIDIN-BIOTIN INTERACTIONS

Chapter–3: Effect of Temperature on Dynamic Force Spectroscopic Measurements of Streptavidin-Biotin interactions

3.1 - Introduction

As described in Chapter 1, the probing of weak non-covalent interactions at the molecular level is important as these forces govern the interfacial structure and function of many biological processes. Since these bonds are very weak and have limited lifetimes, they dissociate easily under applied force, making it possible to investigate the energy landscape of a bond of interest [55]. To study the chemical energy landscape of an interaction, and the barriers present along the dissociation pathway, DFS has been widely employed by experimentalists to study the effect of force on the dissociation process as discussed in Chapter 2. Several experiments have been reported to probe the unbinding kinetics of single ligand-receptor molecules such as strept(avidin)-biotin [19], DNA-oligonucleotides [35] , protein unfolding [31], RNA dissociation [59] etc. In all these experiments, it has been found that the modal rupture force (unbinding force) of any particular single ligand-receptor bond depends on the loading rate (force applied per unit time on the bond/or the force with which the bond is loaded). It also has been found that the external mechanical force lowers the activation energy of the complex and diminishes energy barriers present along the dissociation pathway, so reducing the life-time of the bond and promoting its dissociation [19,35].

Applied force is not the only factor which influences the unbinding force of single ligand-receptor molecules. The unbinding forces will also be influenced by temperature. It has been reported that the free energy of the solvation is increased when the temperature of a protein system is raised in accordance with the following relation $\Delta G = \Delta H - T\Delta S$ [65], where ΔH and ΔS are respectively the changes in the enthalpy and entropy of the ligand-receptor system. The temperature induced denaturation transforms a protein (eg. streptavidin) from

an ordered structure to a disordered state in which hydrophobic amino-acids stacked inside the protein core come in to direct contact with the surrounding aqueous medium.

This gives water molecules the opportunity to surround the exposed hydrophobic amino acids. As a consequence of which, ordered structures are produced with relatively lesser enthalpy and entropy than the native protein moiety. Each ordered structure is associated with high specific heat capacity, and therefore energy is required to denature a protein. The specific heat capacity during temperature induced denaturation is generally assumed to be positive [66]. Therefore, the difference in the enthalpies of the native and the denatured protein increases. This same effect is observed in the entropy difference between native and denatured states. The locally ordered structures melt at a particular temperature known as critical temperature. At the critical temperature ΔH and $T\Delta S$ are equal and cancel each others effect, therefore rendering ΔG to be zero. This promotes the transition from the native state to the denatured state. Furthermore, an increase in temperature reduces the binding capability of the proteins such as streptavidin to hold their ligands (eg. biotin), because of the denaturation of the binding sites of the protein [3].

At present only a very few researchers have investigated the effect of temperature on the unbinding kinetics of single bio-molecular bonds such as between complementary DNA strands [67]. Studies are therefore required to explore the effect of temperature on the modal rupture forces of single ligand-receptor bonds. Here the effect of temperature on streptavidin-biotin unbinding force measurements is investigated. Firstly the unbinding forces obtained from more than 120 force measurements of streptavidin–biotin interactions at three different temperatures (25ºC, 35ºC and 45ºC) using a single retract speed (1µm/s) were investigated followed by an equal number of unbinding force measurements at 35ºC using a retraction speed of 2µm/s for comparative analysis.

3.2 - Aims

The main objective of this experiment was to investigate the effect of temperature on single-molecule force measurements. Here it was to explore whether single-molecule force measurements and the number of different kinds of adhesion events observed (single, multiple, non-specific) could be influenced by varying temperature at a single retract speed or at a range of retract speeds of the AFM cantilever. The streptavidin-biotin system was used as a model to provide a direct comparison with previously studied streptavidin-biotin force measurements at room temperature.

3.3 - Materials and Methods

Apart from the AFM liquid heater cell (LHC), all the materials and methods used in this series of experiments are as described in the experimental section of Chapter 2. The LHC was employed to regulate the temperature of the liquid medium (PBS) in which force measurements were carried out. In order to mount the sample on to the magnetic sample holder of the picoforce scanner (PFS), the top of the PFS was covered with a thin layer of Parafilm to prevent the entry of liquid into the piezo scanner.

3.4 - Functionalisation of AFM Cantilevers and Silicon Chips

The sample preparation and attachment chemistries were the same as described in Chapter 2.

3.5 - AFM Force Measurements

Force traces at a fixed retract velocity were captured using AFM cantilevers functionalised with biotinylated PEG that interacted with the surface coated with streptavidin. Each AFM cantilever was calibrated using the thermal fluctuation method as stated in Chapter 2. Measured spring constants of the cantilevers were close to their nominal values and were in the range of 27pN/nm to 28pN/nm. The sensitivity of each AFM cantilever was measured

from the slope of the contact curve recorded in a liquid medium on the streptavidin coated silicon surface.

The rate with which streptavidin-biotin bonds were loaded in the force measurements was controlled by the cantilever retraction velocity from the surface of the substrate and the effective spring constant of the system (k_s). Loading rate and system spring constants were calculated as discussed in Chapter 2. The calculated system spring constants did not vary significantly and were in the range of 4pN/nm to 8pN/nm. The estimated stiffness values of PEG in this experiment were in the range of 8pN/nm to 13pN/nm. The loading rates used in this experiment were in between 4pN/s -18pN/s and were calculated as stated in Chapter 2.

Several hundred streptavidin-biotin force curves with rupture events were collected to help confirm that the adhesion events were specific and provided strong evidence that the employed tip/sample chemistry had worked. Force measurements were recorded at a temperature of 25ºC, 35ºC and 45ºC at a retract speed of 1µm/s. At each temperature the apparatus was allowed to equilibrate for 10-15 minutes before recording force measurements.

Force measurements were also recorded at a retract speed of 2µm/s when the temperature of the system was 35ºC for comparative analysis i.e; to investigate whether an increase in retract speed at this temperature influenced the unbinding force. The force at which the AFM probe contacted the surface was fixed and kept to a minimum (500pN) to reduce possible damage to the tip/surface chemistry.

3.6 - Results

In each set of force measurements rupture events were observed and the strength of streptavidin-biotin interaction was measured from the retract traces of the AFM cantilever. As stated in Chapter 2, interacting surfaces were prepared with a low density of reactive sites in order to minimise the number of observed multiple interactions and to ensure that most of the observed interactions were due to single molecular pairs and were specific in nature.

Single specific, non-specific, multiple and no adhesion events were reported in each set of force measurements at each temperature. The proportion of single specific, non-specific, multiple and no adhesion events in each set of force measurement varied with the rise in temperature. It was observed that the number of multiple interaction events increased with increasing temperature. The proportion of multiple interaction events in the force measurements recorded at 25ºC, 35ºC and 45ºC at a speed of 1µm/s were in the approximate ratio of 1:2:3. It was also observed, that with an increase in temperature the number of adhesion events increased from 1 out of 10 at 25ºC to 2 out of 10 when the temperature of the medium was 45ºC. Figure 3.1 shows examples of the different kinds of adhesion events observed.

All the force traces which appeared with a single specific adhesion event recorded at each temperature were individually analyzed to calculate the unbinding force of each rupture event. All the unbinding force values were accumulated to produce force distribution histograms and F_{Dist} was employed to obtain the mode *(f*)* of the individual unbinding force values as shown in Figure 3.2.

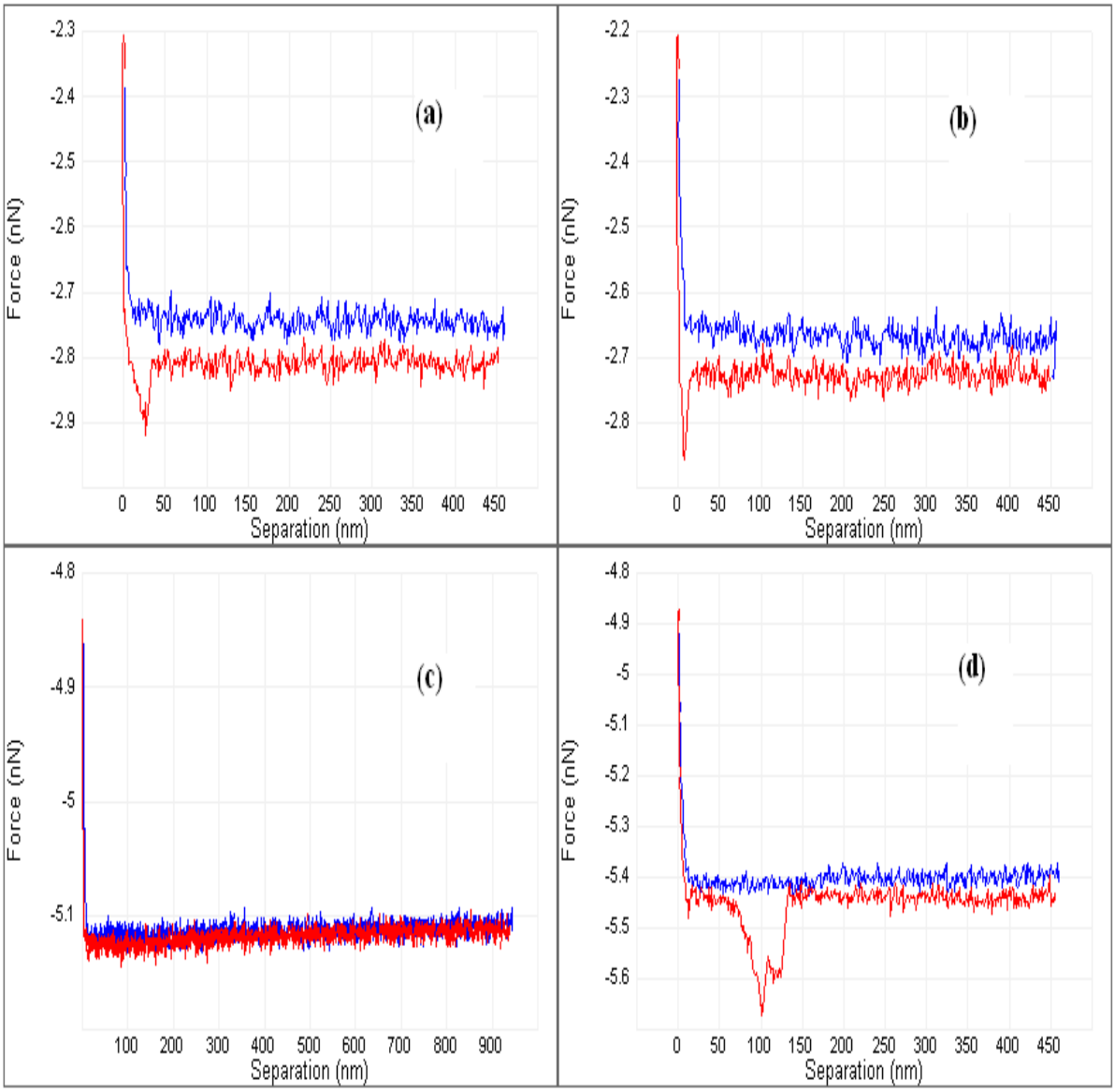

Figure 3.1: Examples of (a) single specific, (b) non-specific, (c) no adhesion and (d) multiple adhesion events when an AFM cantilever decorated with biotinylated PEG interacts with surface of the substrate functionalised with streptavidin at 45℃. Blue and red lines respectively show approach and retract traces of AFM tip, to and away from the surface.

A plot of the unbinding forces against temperature shows that the modal rupture force decreases at first markedly with an increase in the temperature and then less so. This can be seen in Figure 3.3, when temperature rises from 25 ºC to 35ºC, the decrease in modal rupture force is 24pN, in contrast to 3pN when temperature rises from 35ºC to 45ºC. With an increase in the retraction speed from 1µm/sec to 2µm/sec at 35ºC the data in Figures 3.4

demonstrates that the modal rupture force of the streptavidin-biotin complex increased from 48pN to 52pN. Although this is a small increase in force, due to the relatively small increase in speed, it does suggest an effect of retract speed on modal force as would be expected.

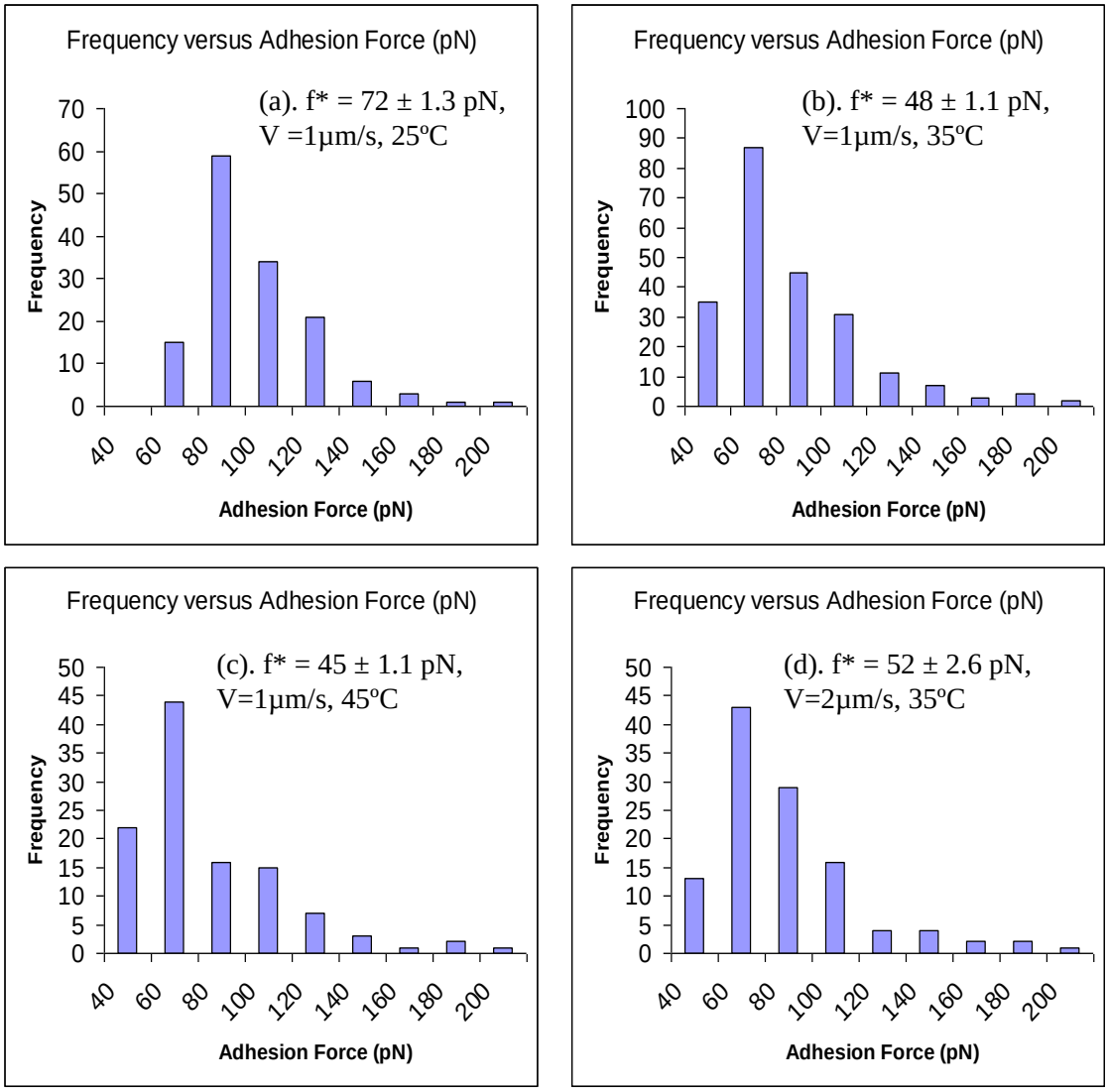

Figure 3.2: Histograms of the unbinding forces compiled from more than 120 unbinding force measurements of streptavidin–biotin interactions at three different temperatures: (a) 25ºC, (b) 35ºC and (c) 45ºC using a single retract speed (1µm/s). Here f represents the mode with standard deviation recorded at each temperature. It clearly shows that the modal rupture force shifts downward with the rise in temperature. (d) Shows the probability distribution of unbinding forces recorded at 35ºC using a retract speed of 2µm/s.*

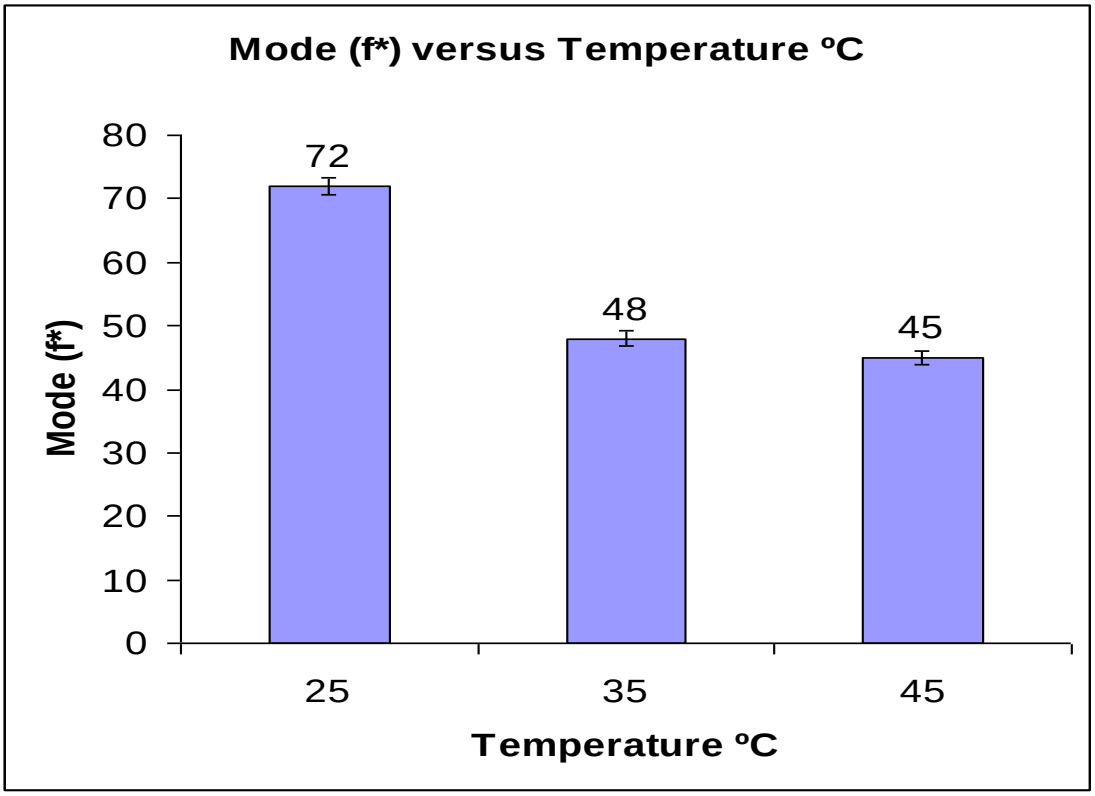

Figure 3.3: A plot of modal rupture force against temperature at a retract speed of 1µm/s. Blue bars clearly show that with the rise in temperature, the modal rupture force decreases. The modal rupture forces recorded with standard deviations at 25ºC, 35ºC and 45ºC were 72 ± (1.3) pN, 48 ± (1.1) pN, and 45 ± (1.1)pN respectively.

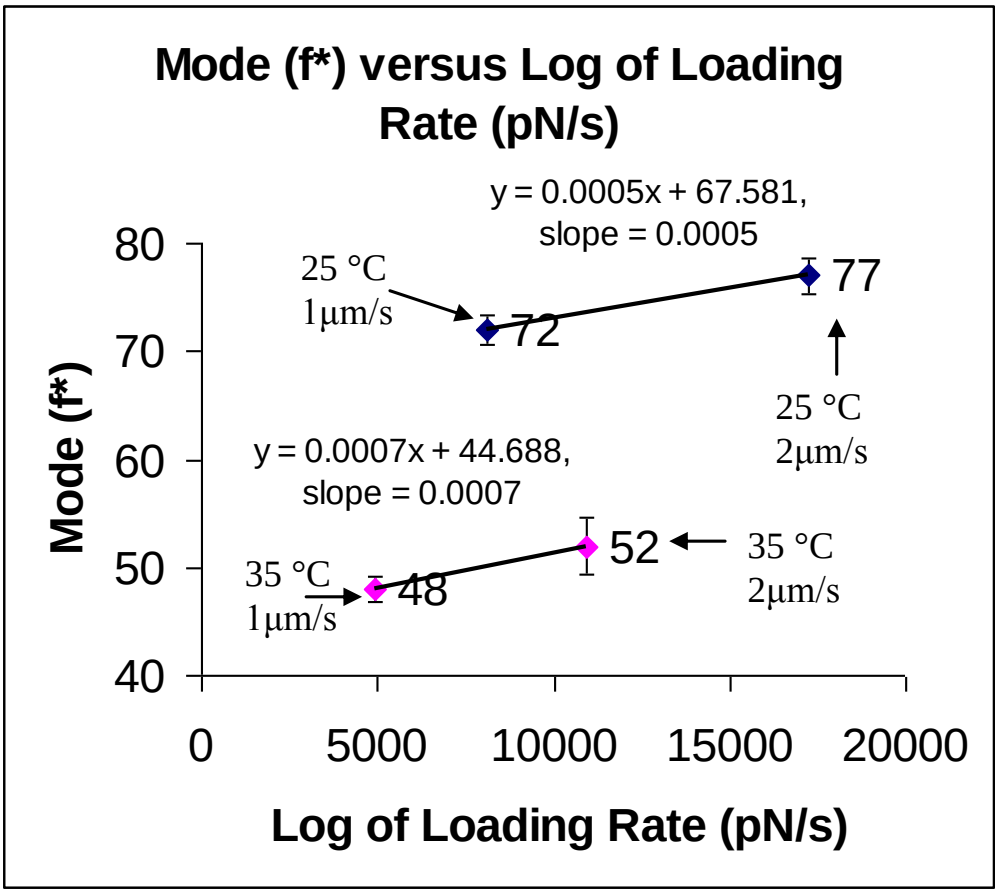

Figure 3.4: (a) Semi-logarithmic plot of modal rupture force against loading rate at two different temperatures. Blue and pink squares represent modal rupture forces recorded at 25ºC and 35ºC respectively. The calculated slopes of the rupture forces (72pN and 77pN) recorded at 25ºC are less than the slopes of the rupture forces (45pN and 48pN) recorded at 35ºC indicating different values of (x_β) at each temperature. The modal rupture forces recorded with standard deviations at 25ºC were around [72 ± (1.3)pN, (1µm/s)], [77 ± (1.6)pN (2µm/s)] and at 35ºC were [48 ± (1.1)pN, (1µm/s)], [52 ± (2.6)pN, (2µm/s)].

3.7 - Discussion

The data in Figure 3.3 illustrate the impact of temperature on streptavidin-biotin unbinding force measurements at a single retract speed. It has been reported by several researchers that two or more energy barriers exist in the energy landscape of the streptavidin-biotin complex along the dissociation path way. When a ligand-receptor bond is formed, it has a tendency to

break. In terms of the behaviour under load the link between the strength of the single specific linkage established (ie. between streptavidin and biotin upon interaction) and the energy gradient (dE/d*x*) is that the established linkage breaks only when an applied external load exceeds the bond energy to the effective bond distance (*x*) [64].

A ligand receptor interaction is in fact a macromolecular bond, where numerous types of atomic scale interactions together constitute the energy landscape. The energy of each different kind of atomic scale interaction individually contributes to the internal energy of the energy landscape. Therefore, the different types of atomic interactions lead to the formation of different kinds of barriers within the energy landscape. The entropy of the system is increased by the thermal energy gained from the surroundings and the interacting liquid medium. Therefore, a ligand receptor bond under no applied force can dissociate spontaneously (entropy driven), implying no strength in the bond [55]. When there is no external mechanical force applied on the ligand receptor system, diffusion of molecular states constituting the energy landscape is not directional. However, when an external mechanical force is applied this guides the diffusion of the different atomic scale interactions in the direction of applied force, which reduces the bond lifetime and therefore decreases the strength of the linkage (ligand-receptor bond).

The effect of force in reducing bond lifetime can be explained by considering the thermal energy increase (k_BT) of a system, when the external mechanical force makes the diffusion of different types of atomic interactions directional. This thermal energy increase provides the driving force (F) for the escape from the bound state to the excited state.

$$F = -\exp\left(\frac{E_b}{x_\beta}\right) \tag{3.1}$$

Since $E_b = f.x_\beta$ (3.2)

The thermal force scale gives us a measure of the transition state, when thermal activation of the complex diminishes the energy barrier. [23]

i.e; $f_\beta = \frac{k_B T}{x_\beta}$ (3.3)

Since thermal energy $(k_B T)$, at room temperature is approximately 4.11pN.nm, x_β can reach to around 1nm.

The rate of unbinding (thermal off-rate) increases exponentially with applied force

$$k_{off} = \frac{1}{t_D} \exp\left[\frac{f}{f_\beta}\right] \quad (3.4)$$

where f is the applied force [43].

Therefore, unbinding force depends on the type of force measurement performed and on the details of the functional relationship between bond lifetime, the applied rate of loading and temperature. Since there are many reaction paths present in the energy landscape of a bond the shape of the energy landscape can also become modified when the temperature of the system is increased [64].

In the context of the presented results, the decrease in modal rupture force with the rise in temperature may therefore be explained on the basis of a thermal energy increase of the system which not only lowers the internal energy of the energy barriers present in the energy landscape, but may also select a different unbinding pathway which requires less energy to overcome the barrier present.

Moreover in increasing the temperature, the contribution of entropy to the dissociation process will also be increased which results in a decrease in the effective barrier energy [55,66]. From the expression of the thermal force scale as stated above (equation 3.3), a linear increase in the force scale (and hence rupture force) would also be produced by an increase in temperature, assuming that the dissociation pathway (x_β) remains unchanged. However, such a linear increase is overwhelmed by the exponential impact of temperature on (equation 3.4) thermal off-rate, and thus their combined effect will lead to a decrease in the rupture force observed.

This explanation is consistent with the observed decrease in the modal rupture force with increasing temperature but cannot as yet reveal why for the first 10ºC rise (25ºC-35ºC) in temperature causes a larger drop in force 24 ± (0.2)pN than the next 10ºC (35ºC-45ºC) which is 3 ± (0)pN. It may possibly due to decrease in the heat capacity of the system at higher temperatures. As already discussed temperature may also influence dissociation process, by selecting an alternative pathway [3]. To see if this is likely we can estimate the slope (f_β) from the measurements recorded at two different temperatures (25ºC and 35ºC) using retraction speeds of 1µm/s and 2µm/s. For the comparison of the forces recorded at the same rate but two different temperatures, it can be seen in Figure 3.4 that the slope of the unbinding forces recorded at 25ºC is less than that recorded at 35ºC using the same retract speeds. From the calculated slopes, it suggests that the temperature influences the

dissociation pathway and hence may provide the most likely reason for the more dramatic drop in unbinding force on the initial increase in temperature. Different slopes would indicate a different dissociation pathway has been selected at a higher temperature.

It is important to note however, that other factors that may have a role in these measurements, such as the mechanical properties of the cantilever, stiffness of the PEG polymers etc which could all be influenced by temperature. These factors remain beyond the scope of this work but are believed within the narrow range of temperatures studied not to play a major role in the data.

3.8 - Conclusions

A novel study of the effect of temperature on the unbinding forces observed for streptavidin-biotin has been presented. The unbinding force of the streptavidin-biotin interaction has been found to decrease non- linearly with an increase in temperature. This has been shown to be consistent with the accepted models for forced dissociation of receptor-ligand pairs [66]. The decrease in the unbinding force is due to the increase in the thermal energy of the system as well as a possible shift to a different dissociation pathway.

Chapter–4:Dendron based immobilization for Dynamic Force Spectroscopic Measurements of DNA Oligonucleotides Hybridisation: The Effect of Temperature

4.1 - Introduction

Screening of bio-molecules with ultrasensitive force measurement techniques has attracted the interest of researchers over the years. As mentioned in Chapters 1 and 2, a number of studies have been undertaken to explore the unbinding kinetics of single molecular ligand-receptor pairs. Various experimental techniques, such as AFM, OT, and the BFP, based on applying and measuring pico-Newton forces between single molecules have been employed and have contributed to a better understanding of the mechanics of single-molecular ligand-receptor interactions.

The measurement of force provides a detailed insight into the binding-energy landscapes of single-molecular ligand receptor pairs, besides exploring their structure and function. In addition, such studies confirm that bio-molecular processes are governed by pico-Newton forces. However, as already discussed in Chapter 3 such measurements can be affected by various factors such as probe sensitivity, method of bio-molecular surface attachment, surface chemistry and topography, instrumental design, and experimental factors such as drift and temperature. In particular, future bio-molecular screening applications based on force measurements will require excellent methods of immobilization to create surfaces with high uniformity and functionality. To this end a new and novel class of polymers called dendrimers has attracted the focus of researchers for their excellent bio-molecular immobilization properties. The general idea of the dendrimers and their properties is given in the following text.

4.1.1 – Dendrimers

Dendrimers were first discovered in the early 1980's by Donald Tomalia and co- workers [66]. These are well defined, hyper branched synthetic polymeric macromolecules composed of multiple monodisperse macromolecules. Each individual identical fragment (monodisperse polymeric section of a dendrimer with multiple terminal functional groups) emanating from the central core of a dendrimer is termed a dendron. A dendron has three distinct regions; a core, an interior and a periphery. The core is the focal point of a dendron, the interior are the branches and the periphery corresponds to the surface functional groups. Dendrimer is derived from a Greek word "dendron" (tree). Figure 4.1 shows a schematic of a first, second and third generations of a dendrimer molecule.

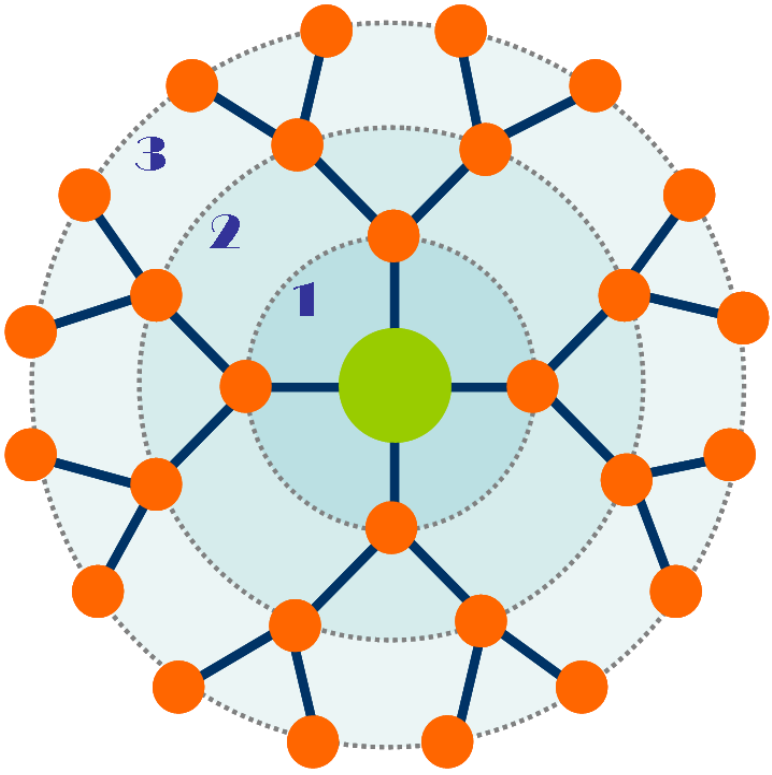

Figure 4.1: Representation of first, second and third generations of a dendrimer. The green dot represents the core, the blue lines represent branches and the orange dots represent the branch points, each new generation has twice the number of branch points compared to its previous generation (*Adapted from* [86]).

Dendrimers are synthesised by repetitive branching sequences, extending radially out from a central core, where each complete step makes a branch point. The number of branch points increases as we move away from the central core toward the periphery of the dendrimer. Each branch point corresponds to the dendrimer generation.

Dendrimer synthesis can be divergent or convergent. In convergent synthesis, the dendrimer is constructed in a sequential manner, starting from the terminal groups and progressing radially inwards towards the multifunctional central core. Each branched polymeric arm extending radially inwards from the periphery to the central core is called a dendron. However, in divergent synthesis dendrimer grows radially outwards from the central multifunctional core molecule, which reacts with monomeric molecules containing two or more than two functional groups, resulting in first generation dendrimer. The terminal functional group reacts with other monomeric molecules, and results in other generations (1, 2 and so on). The divergent method can be used to synthesise high generation dendrimers with ease, which is not possible in convergent synthesis because of problems associated with steric hindrance between the dendrons and the core molecules.

Different chemistries have been employed for the preparation of dendrimers and dendrons, such as PAMAM (poly(amidoamines)) [68], poly(amines) [69], and Organophosphorus dendrimers [70]. However the most widely used with distinct chemical structures include the poly(amidoamine)s (PAMAM) (see Figure 4.2).

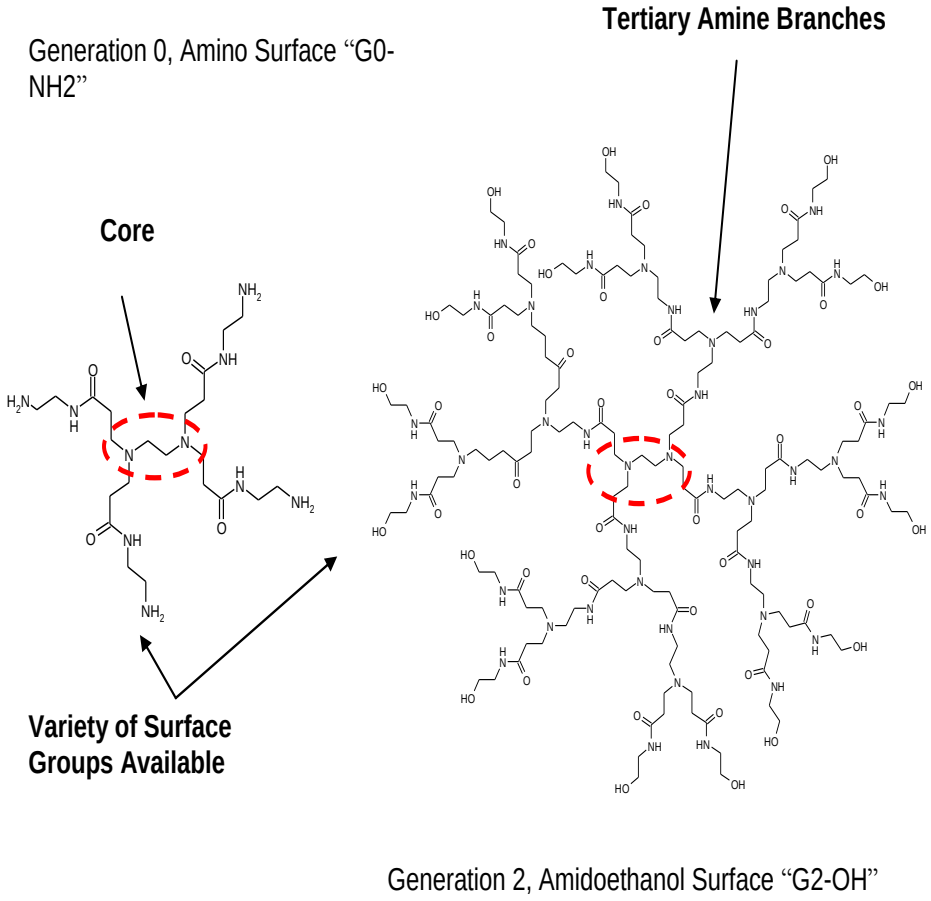

Figure 4.2: Chemical structure of PAMAM Dendrimer (*Adapted from* [68]).

Dendrimers have several unique characteristics. They are:

(1) Highly symmetrical and three dimensional in structure.

(2) Nanometre sized in dimension, which bestows them with higher degree of solubility and low viscosity.

(3) Multi-valent (presence of multiple functional groups), which is the most exploited property of dendrimers. One of the important properties of dendrimers is that their terminal functional groups do not squeeze with the generation increase, and therefore, they are ideal candidates for drug delivery. Moreover, their solubility can be regulated by the nature of terminal functional groups. For instance hydrophobic end groups of a dendrimer with a

hydrophilic core will increase solubility in oil where as hydrophilic end groups of a dendrimer with hydrophobic core will increase its solubility in water.

(4) Distinct in their molecular structure, in that the core and the surface can be considered separate and exploited to encapsulate and expel molecules which are chemically incompatible with the exterior environment. This property can be used for encapsulating drugs etc.

(5) Easy to tune, through changes in chemical synthesis, in terms of shape, size, surface/interior chemistry, flexibility, and topology. The dendrimers are so versatile that they can be synthesised to the same dimensions as biological molecules [71].

All the properties of dendrimers and dendrons are not, however known, but the above described novel properties have made them ideal candidates for many biomedical and industrial applications, including as within therapeutic agents in drug delivery [72,73], for biomedical imaging [74], as in-vitro diagnostics [72,75], as scaffolds for tissue repair [76], and for bio-molecular immobilization [77]. For example, PAMAM dendrimers have been exploited as anti-bacterial targetted carriers for sulphamethaxzole [78]. PAMAM dendrimers in gene delivery have shown lower toxicity and higher efficiency than conventional transfection agents [79]. It has also been reported that the dendrimers also increase the solubility of drugs; the solubility of anticancer drug cisplatin increases 10 fold when conjugated with a dendrimer [72]. High functional-group densities and low solution-viscosities make them ideal for repairing corneal wounds [76]. Dendrimers have also been used as carriers for magnetic resonance imaging contrast reagents [74].

These are only a few of the main applications of the dendrimers and dendrons, but the most important in the context of this Chapter is their use in bio-molecular immobilization for single molecule force spectroscopic measurements. It has been reported that both

dendrimers and dendrons provide highly refined and reproducible architectures for bio-molecular immobilization [47]. To have a surface with intended characteristics (e.g. the optimum density of the surface functional groups, sufficient spacing between the immobilized molecules for unhindered interactions etc.) is very important for the single molecule investigation. Most of the presently employed bio-molecular attachment methods, such as the silanization approach [80], and via alkyl thiol [81], self assembled monolayers (SAM)s, are inadequate for the investigation of single-molecular receptor bonds, because they typically lead to steric hindrance, nonspecific attachments and the formation of multiple adhesion events [82]. Although mixed SAMs can provide a control of the density of functional groups, their random distribution can make SAMs inconvenient for the immobilization process. Moreover, they typically lead to the formation of aggregates.

Appropriate control of the spacing between the immobilized molecules is very important in enhancing the interaction on the surface. This has made researchers develop new immobilization approaches with high specificity and enhanced functionality, such as with the dendron immobilization approach. This approach provides less steric hindrance, due to the ample spacing between the immobilized molecules (mesospacing = 3nm), and low non-specific attachments and an optimum density of surface functional groups. A comparative outlook of an APDES (3-aminopropylmethyldiethoxysilane) modified surface which has a high density of amine functional groups, and the dendron modified substrate for DNA microarray fabrication is shown in Figure 4.3.

A number of single molecule force measurement studies using the dendron approach for the bio-molecule surface immobilization have been performed. It has been reported that the specificity of the streptavidin-biotin interactions increased considerably when a dendrimer monolayer was used for the immobilization of biotin on surface. It was found that an

increase in specificity/binding was comparatively more than when biotin were immobilised on SAM modified surfaces. Figure 4.4 shows the dendron for the immobilization of biotin [83].

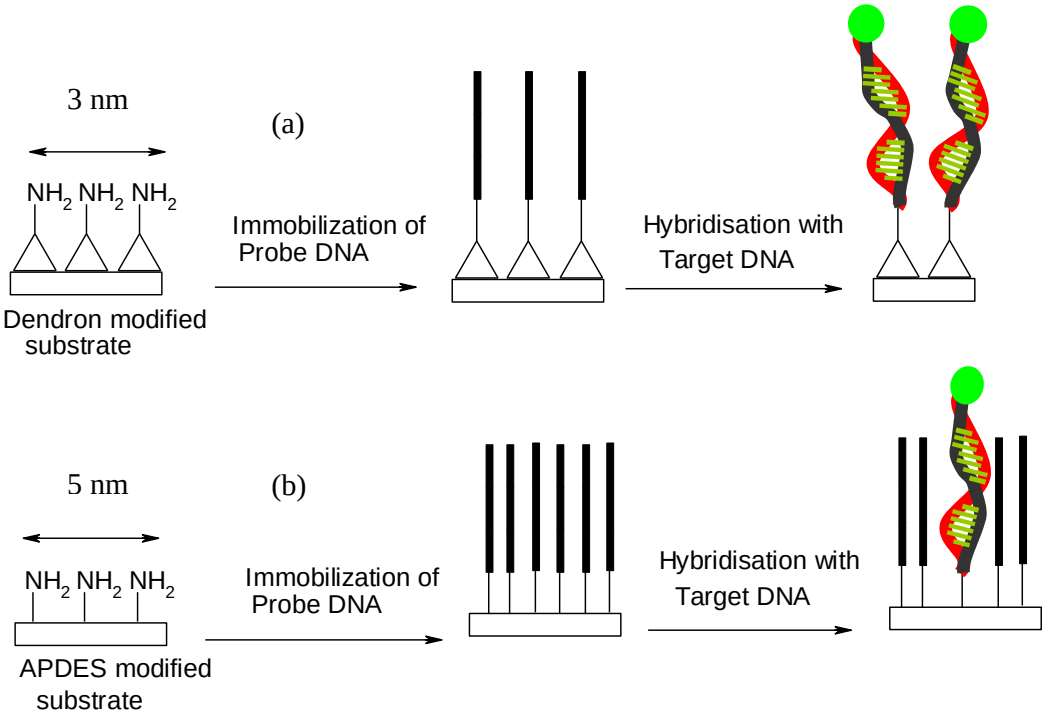

Figure 4.3: Schematic overview of DNA hybridization events on (a) a Dendron-modified substrate and (b) on an APDES-modified substrate (*Adapted from* [87]).

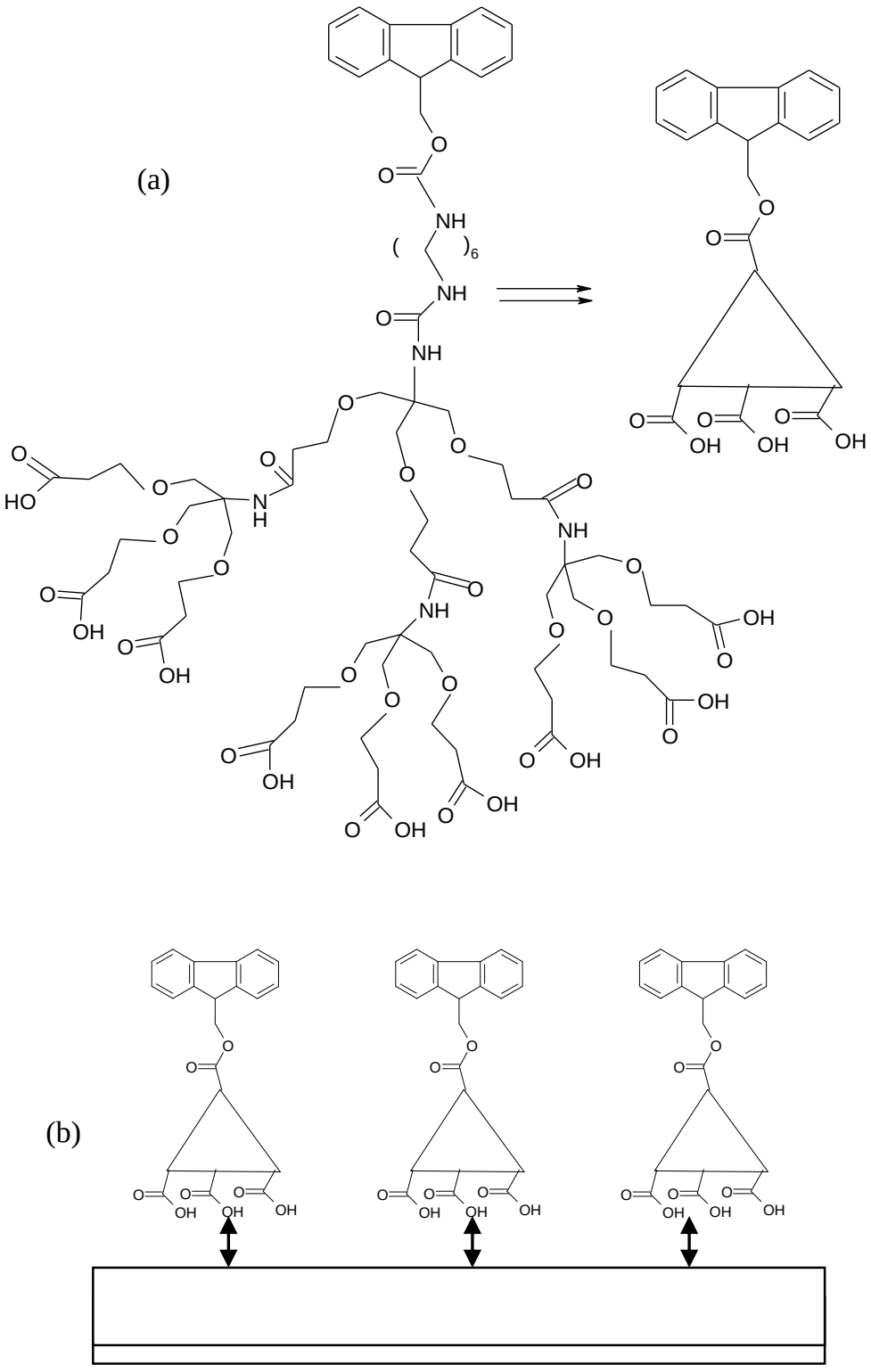

Figure 4.4: (a) Molecular structure of the dendrimer employed for the immobilization of biotin. (b) Biotinylated dendrimer monolayer (*Adapted from* [83]).

Dendrons have been also found to improve the selectivity of hybridisation. The mesospacing (3.2nm) generated by the cone shaped dendron has been observed to provide sufficient space for the incoming strand of DNA to interact with target DNA, and was found to improve the selectivity so that it was almost equal to that observed in the solution phase (Figure 4.5.) The ability of dendron-DNA microarrays to discriminate the single nucleotide variations has also been reported [47].

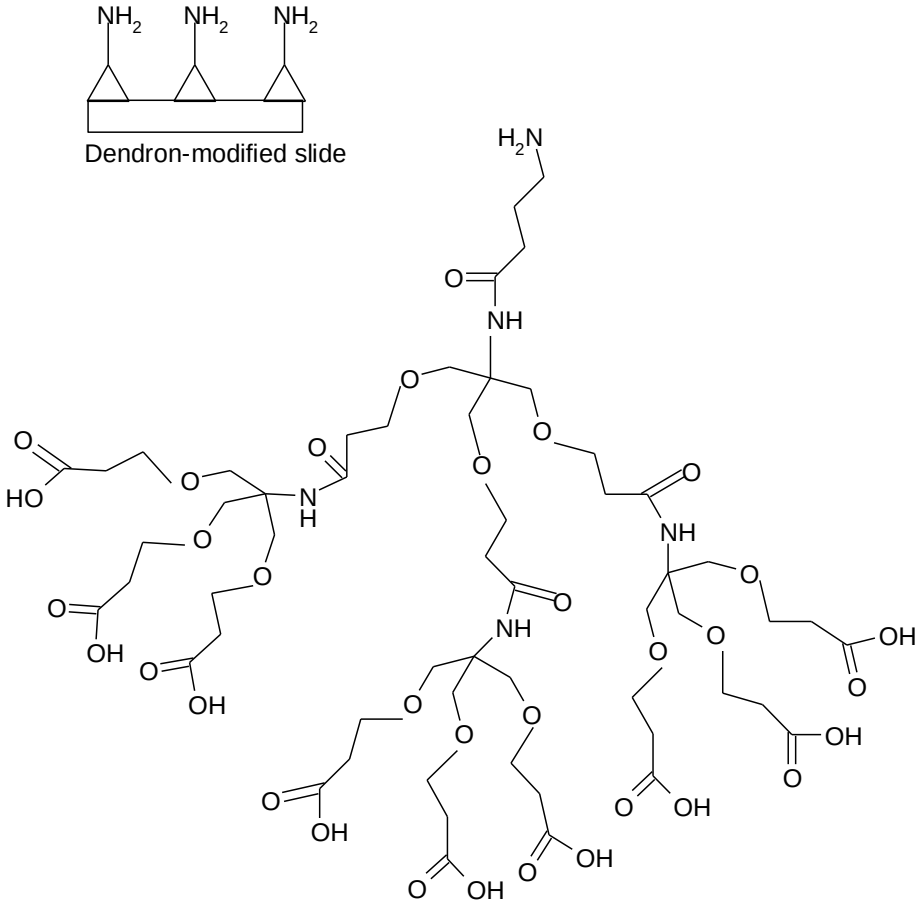

Figure 4.5: The dendron molecule employed for the detection of single nucleotide variations of DNA microarrays (*Adapted from* [47]).

Researchers have attributed the efficient performance of dendron-DNA microarrays and the enhanced specificity of streptavidin-biotin interactions on dendron modified surfaces to the mesospacing provided not only between the immobilised molecules but also between immobilized capture probes and target molecules. In turn, this results, in a reduction of steric hindrance, especially in the case of dynamic force spectroscopic studies performed on dendron modified complementary DNA oligonucleotides [47]. For a proper understanding of DNA force spectroscopic measurements immobilised on dendron modified surfaces, it is very important to also have a basic knowledge of the DNA structure.

4.1.2. - Structure of DNA

The double helical structure of DNA proposed by Watson and Crick (in 1953) comprises two complementary anti-parallel polynucleotide strands twisted around each other. There are ten base pairs in each turn and each base pair is placed at a distance of 0.34nm after the previous one (Figure 1.3). The width of the DNA duplex is 2 nm. Each spiral strand is composed of a sugar phosphate backbone with attached bases. The two strands are held together by hydrogen bonds between complementary base pairs; Adenine (A) pairs with Thymine (T) by two hydrogen bonds and Guanine (G) pairs with Cytosine (C) by three hydrogen bonds. The high stability of DNA structure stems from the hydrogen bonding between its complementary base pairs [84].

4.1.3. - Measurements of DNA hybridization on Dendron functionalized surfaces

DNA force spectroscopic measurements between the complementary nucleotides immobilized on dendron {9-anthrylmethyl-N-({[tris9{[2-[({tris-[(2-carboxyethoxy) methylpropylcarbamate)} modified surfaces showed some unique properties, such as the ability to observe attractive jump in events in more than 80% of the force-measurements

recorded [47]. Moreover, the rupture forces of the complementary DNA oligonucleotides (20mer, 30mer, 40mer and 50mer) at a range of cantilever retraction speeds were found to increase linearly with the number of complementary base pairs at room temperature as shown in Figure 4.6.

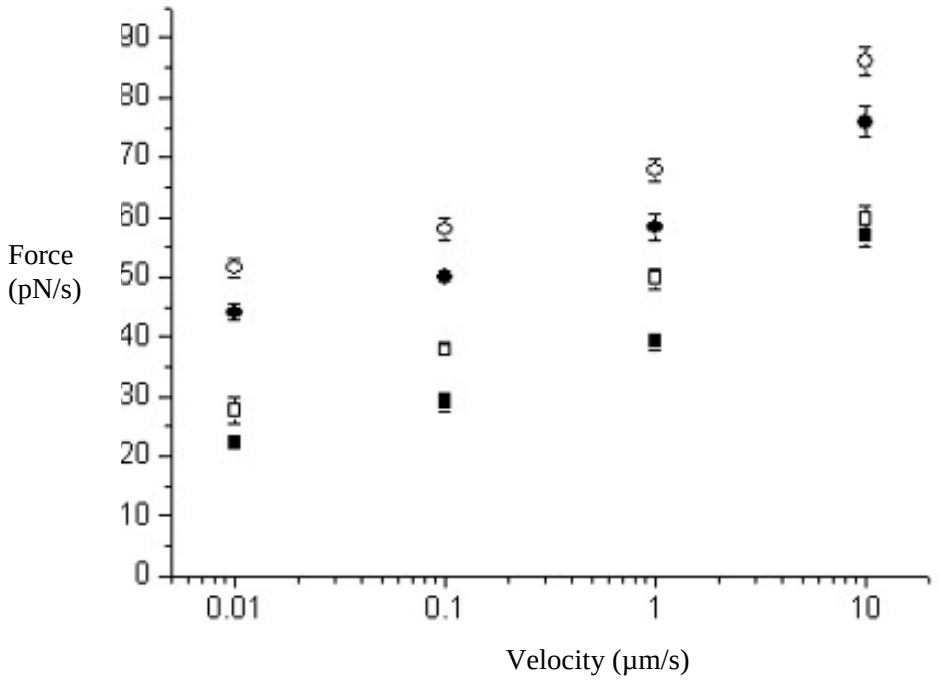

Figure 4.6: Dependence of the unbinding forces of complementary DNA oligonucleotides at a range of cantilever velocities. Filled square 20mer, open square 30mer, filled circle 40mer, open circle 50mer [47].

It was found that the unbinding forces for each complementary oligonucleotide increased linearly with an increasing in the speed of the force measurement, which was explained on the basis of an entropic steric model. According to this model, the two complementary oligonucleotide strands (each negatively charged) form a negatively charged steric entropic barrier above the underlying surfaces. The complementary oilgonucleotide strands when bought close to each other exert a repulsive force on each other, but when they are close enough to contact each other, the negatively charged repulsive steric entropic barrier collapses and hybridisation takes place. The length of the barrier destroyed upon

hybridisation is equal to the length of the each interacting complementary oligonucleotide or equal to the length of the duplex formed upon hybridisation [47].

The unbinding kinetics of oligonucleotides as a function of loading rate has been investigated several times [49,85], but the effect of temperature on the dynamic force spectroscopic studies of oligonucleotide dissociation has been rarely studied. It was observed that the dissociation force of the oligonucleotides decreases with an increase in temperature. The temperature increase was proposed to reduce the unbinding force of the complementary oligonucleotide strands due to a decrease in the height of the effective barrier energy. Moreover conformational changes, enthalpic and entropic contributions were proposed to be other prominent factors which could play a significant role in aiding thermal energy to conquer the energy barrier quickly [49,85].

As already highlighted in Chapter 3, very little has been investigated with regards the unbinding forces of the ligand-receptor interactions as a function of temperature. Therefore, here an attempt was made to study the unbinding forces of complementary oligonucleotides as function of temperature.

4.2 – Aims

It has been reported that dendron surfaces functionalized with complementary DNA oligonucleotides experience attractive jump in events in force measurements recorded between them. Moreover, the detection of single base pair mismatches was also reported [47]. The binding/unbinding kinetics of complementary DNA oligonucleotides can potentially be influenced by several factors such as temperature, drift, underlying chemistry, and instrumental errors. The effect of the factors other than temperature on the force-spectroscopic measurements of single molecules is far less important than the effect of

temperature. Therefore, the main objective of this experiment was to investigate the effect of temperature on the unbinding forces of complementary DNA oligonucleotides. In this experiment, the effect of dendron immobilization approach on the unbinding force measurements of complementary oligonucleotides at three different temperatures was investigated. The dendron employed for the immobilization of complementary oligonucleotides was same as that used by Jung and co workers [47].

4.3. - Materials and Methods.

4.3.1. - Materials

The samples for this experiment were provided as a kind gift from Prof. Joon Woon Park (Pohang University of Science and Technology, POSTECH). The main materials used in their preparation of the samples [47] (as per their sample preparation protocol),were the dendron(9-anthrylmethyl-N-({[tris9{[2-[({tris-[(2-carboxyethoxy)methyl propylcarbamate), the silane coupling agent N-(3-(-triethoxysilyl)propyl-o-ployethyleneoxide urethane (TPU), fused silica plates, silicon wafers (dopant phosphorus); De-ionised water (18Mcm) and Pirhana solution. All the chemicals used for the preparation of samples were of the reagent grade from Sigma-Aldrich.

4.3.2. - AFM Cantilevers

Dendron modified AFM (MLCT-AUNM, Veeco) cantilevers of nominal spring constant 10pN/nm were functionalised with the 30mer oligonucleotide sequence (5'-H_2N-CTTCGTTCCAGGGCGTGTCCATAGCAGC-3').

4.3.3. - Silicon Subsatrates

Dendron modified silicon surfaces were functionalised with the 30mer oligonucleotide sequence (5'-H_2N-CCATCGTGGTTGCTCCTAG-3').

4.3.4. - AFM Force Measurements

The force measurements were performed using a multimode AFM with Nanoscope V controller and Picoforce system (Veeco). Spring constants of the employed cantilevers were calibrated using the thermal fluctuation method [33], as stated in Chapter 2. The calculated values were between 12-14pN/nm. Sensitivities of the AFM cantilevers were measured from the slope of the contact curve recorded in a liquid medium on the dendron modified silicon surface functionalised with oligonucleotides. The calculated sensitivity of the cantilevers used was around 57pN/nm to 59pN/nm. The contact force was fixed to round about 300-500pN at the start of the experiment. The dendron modified AFM tip was allowed to interact with dendron modified silicon surface using approach/retract speed of 1µm/s (Figure 4.7).

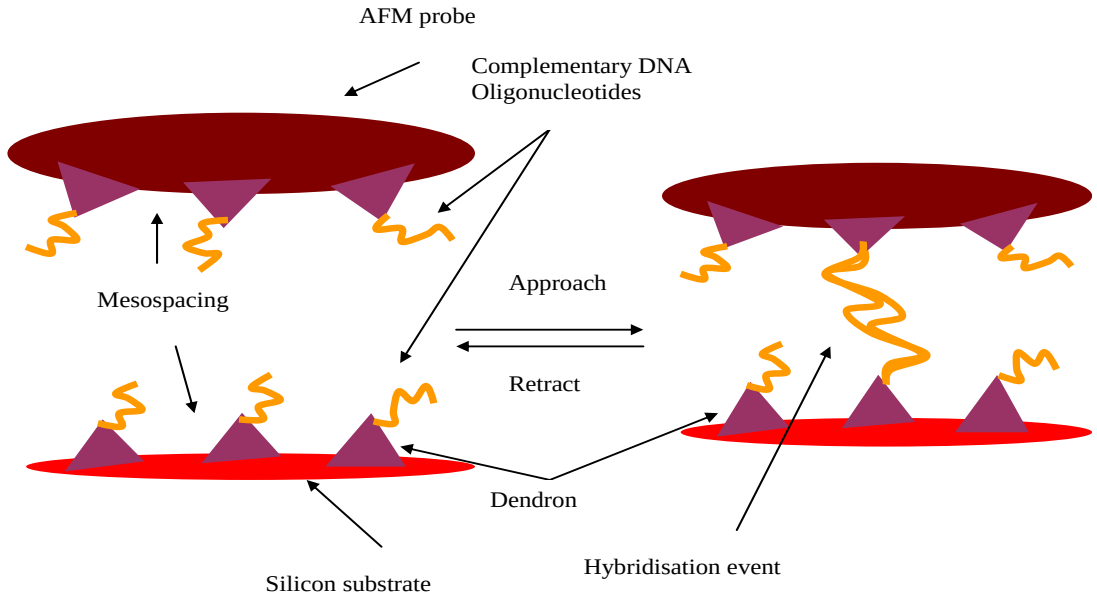

Figure 4.7: Diagrammatic representation of the dendron modified AFM probe and silicon substrate surfaces immobilised with complementary DNA oligonucleotides. The figure clearly shows mesospacing provided by the cone shaped dendron. An event of hybridisation between complementary DNA oligonucleotides can occur as the probe DNA is unhindered.

The DNA oligonucleotides (30mer) were covalently attached to silicon surfaces and silicon nitride AFM cantilevers via their 5' termini using a modification of a dendron based surface immobilization method as described earlier [47]. No PEG linkers were used in this

experiment and the elastic properties of the dendrons were not known. Therefore, the best approximation possible for the effective spring constant of the system was to assume that it was equal to the stiffness of the cantilever (k_c). All the force measurements were carried out in PBS buffer (pH 7.4). The force measurements were carried at four different temperatures (26 ºC, 35 ºC, 45 ºC, 55 ºC). Several hundred force curves were recorded at each temperature using different AFM cantilevers and samples to achieve reproducibility and fidelity in our measurements.

4.4. - Results

Once the AFM probe and the substrate surface functionalised with the complementary DNA oligonucleotides were allowed to interact, force curves were observed. Several hundred force curves with unbinding events and some with attractive jump in forces were collected. Unlike the previous study, attractive jumps in the unbinding force traces were rarely seen. Although the precise reason for this is not known, it may be reflective of the presence of volatile siloxane contaminants on the AFM tips and surfaces (originating from the Gel Pack box in which they were transported to us). However, the modal rupture force at a speed of 1µm/s was found to be 52pN, identical to that reported in the JACS paper [47], therefore providing evidence that attachment chemistry had to some extent survived transport from Korea. More than 150 force measurements were recorded at a temperature of 25ºC, 35ºC, 45ºC, 55ºC, at a velocity of 1µm/s. At each temperature the apparatus was allowed to equilibrate for 10-15 minutes before recording force measurements.

Force traces collected at each temperature showed unbinding events between the complementary DNA oligonucleotides. As discussed in Chapter 2, single specific, non-specific, multiple and no adhesion events were also reported here in each set of force measurements at each temperature (see Figure 4.8). However, the effect of temperature on

the number of different kinds of adhesion events showed a different scenario. The percentage of force curves with multiple adhesion events at all the three temperatures was higher than that reported previously [47], again possibly due to the presence of siloxane contamination. However, no such effect was observed in the number of single specific and non-specific adhesion events.

The percentage of the force traces with single specific adhesion events recorded at each temperature was near 80% as reported in the literature. This suggested that the temperature did not influence the number of single specific adhesion events.

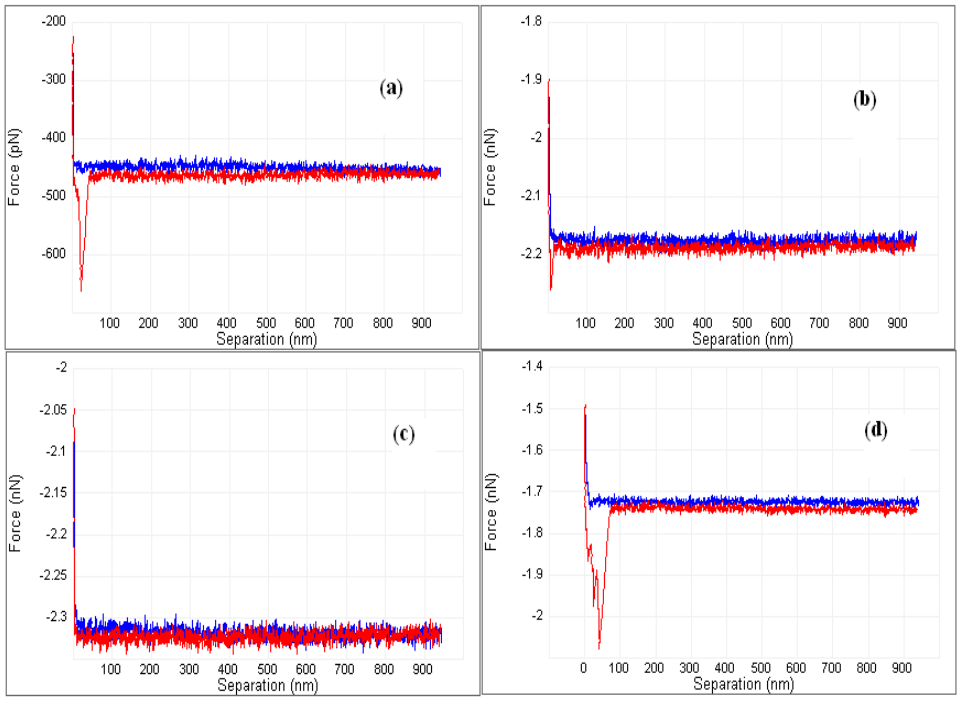

Figure 4.8: Examples of (a) single specific, (b) non-specific, (c) no adhesion and (d) multiple adhesion events observed when dendron modified surfaces of an AFM cantilever and silicon substrate functionalised with complementary oligonucleotides (30mer) were allowed to interact with each other. The blue and red lines respectively show approach and retract traces of AFM tip, to and away from the surface.

Force curves with single-specific adhesion events, recorded at each temperature were individually analyzed to calculate the modal rupture force for each unbinding event as

discussed in Chapters 2 and 3. All the rupture force values were collected to produce force distribution histograms and F_{Dist} was employed to obtain the mode *(f*)* of the individual unbinding force values at each temperature. Figure 4.9 shows the distributions for complementary oligo-nucleotides at a speed of 1µm/s.

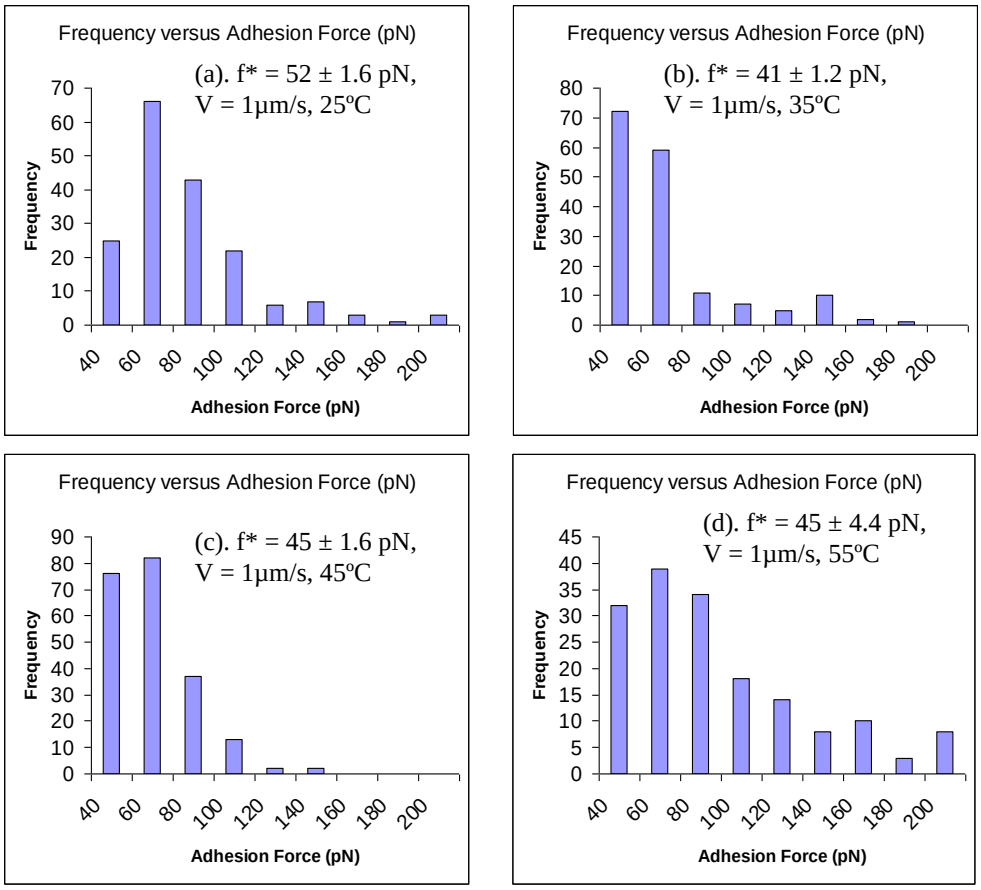

Figure 4.9: Histograms of the unbinding forces compiled from more than 150 unbinding force measurements of complementary DNA oligo-nucleotide interactions at four different temperatures (a) 25ºC, (b) 35ºC, (c) 45ºC and 55 ºC using a single retract speed (1µm/s).

Figure 4.10 shows the modal rupture force *(f*)* of the complementary oligonucleotides (30mer) at a speed of 1µm/s at room temperature is 52pN. When temperature rises from 25 ºC to 35ºC, the decrease in modal rupture force is 9pN, then increases by 4pN when temperature is increased from 35ºC-45ºC. From 45ºC-55ºC, mode remains unchanged. The effect of the temperature on the strength of the interaction between complementary DNA

oligonucleotides is therefore different from that observed in case of streptavidin-biotin complex (Chapter 3). Like the streptavidin-biotin complex however, the modal rupture forces of hybridised DNA duplex (30mer) are reduced at temperatures higher than 25ºC.

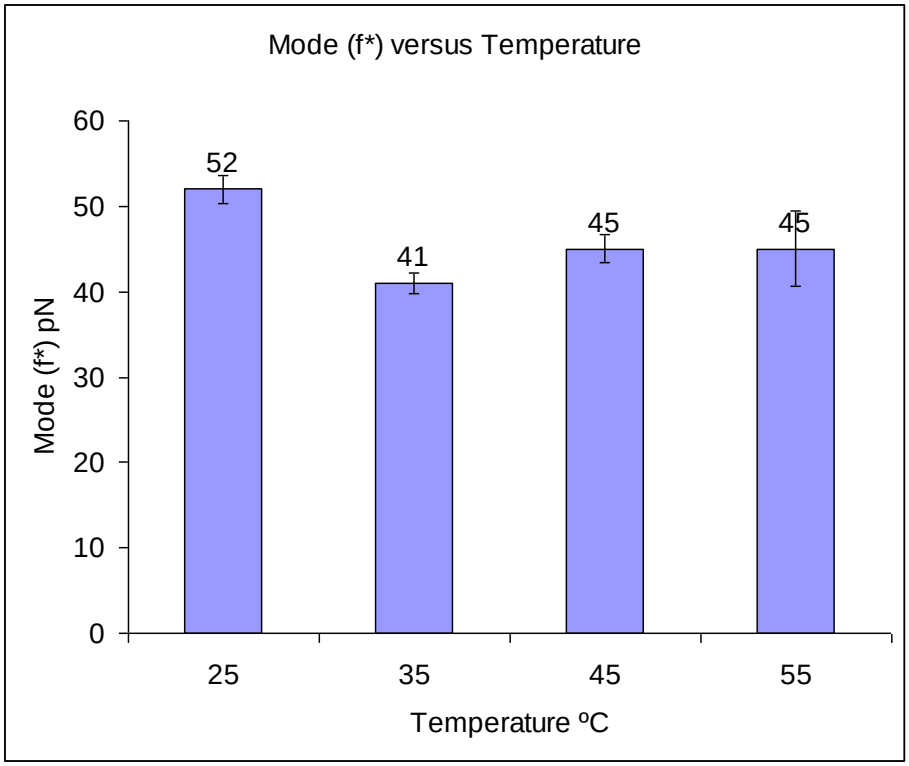

Figure 4.10: A plot of modal rupture force against temperature at a retract speed of 1µm/s. The modal rupture forces recorded with standard deviations at 25ºC, 35ºC, 45ºC and 55ºC were 52 ± (1.6) pN, 41± (1.2) pN, 45 ± (1.6) pN and 45 ± (4.4) pN respectively. Each error bar corresponds to standard deviation recorded for each value of mode at that temperature. Blue bars represent the modal force at each temperature.

4.5-Discussion

Figure 4.10 reflects that the modal rupture force for the complementary oligonucleotides (30mer) recorded in these experiments at room temperature (at a speed of 1µm/s) was identical to that reported in previous studies (see Figure 4.6) [47]. Molecular unbinding events were observed in all the recorded force traces at each temperature. However, the ability to observe many attractive jump in events in approach traces was inconsistent with

previous studies. At each temperature, the number of attractive jump in the rupture force traces was poor when compared to previous studies. As already discussed this was probably due to contamination of the AFM tips and surfaces. The increase in the number of multiple adhesion events observed with a rise in temperature is likely also to be reflective of such contamination. The negligible number of force traces with non-specific adhesion, 80% of the force traces with adhesion events, and the identical modal rupture force for the 30mer DNA duplex at a speed of 1µm/s, however confirmed that the surfaces were behaving in a manner that was consistent with previous studies.

To explain the effect of temperature on the unbinding forces between the complementary oligonucleotide strands, it is essential to understand the forced unbinding behaviour of complementary oligonucleotide strands. It has been reported by researchers that in this experimental set up DNA oligonucleotide strands act to form a negatively charged entropic steric barrier above the underlying substrates [47]. Therefore, when an AFM cantilever and the silicon substrate functionalised with dendrons and complementary DNA oligonucleotides are allowed to interact with each other, their hybridisation is hindered by this steric barrier. According to this steric barrier model proposed by Jung *et al*. (2007), when the load is applied the two surfaces are brought close enough to each other, the barrier (repulsive barrier) collapses and the two complementary oligonucleotide strands hybridise to form a duplex, causing the underlying surfaces to attract and collapse together. The length of the barrier destroyed upon hybridisation would then be equal to the length of the each complementary strand of DNA/length of the duplex. Once the duplex is formed, like all other ligand receptor bonds, it has a tendency to break, and the intimate relationship exists between the strength of the duplex formed and the rate at which it is broken.

The decrease in the unbinding force of the DNA oligonucleotides with an increase in temperature may be well explained on the basis of decrease in the effective bond length and an increase in thermal energy of the system [66]. When the external mechanical force is applied in the form of loading rate, the different states within the energy landscape are diffused in the direction of applied force as stated in Chapter 2. This results in an increase in the thermal energy of the system and hence thermal dissociation of the complex takes place. Each complementary base pair in the hybridised duplex acts as an individual energy barrier, and therefore the internal energy of all the 30 complementary base pairs collectively build the binding energy landscape of the hybridised DNA duplex [66]. An increase in temperature will increase the quantity (k_BT). The increasing temperature will also increase the entropy of the system, and may change the three dimensional conformation of the individual energy barriers within the binding energy landscape, thus affecting the dissociation path way (x_β) along the length of DNA duplex.

In previous studies, the decrease in unbinding force of the duplex with temperature has been explained by a decrease in the effective bond length, the energy barrier for dissociation per base pair) when temperature approaches the melting temperature T_m [66]. T_m is the temperature at which DNA dissociates in solution, into single strands due to the breakage of hydrogen bonds between the complementary base pairs. Due to the rise in temperature, at higher temperatures some of the hydrogen bonds between complementary bases pairs in series will already be in a dissociated state, before the external load is applied. Thus, the average fraction of bonded base pairs in hybridised DNA duplex decreases with increase in temperature. Consequently the shortening of the effective bond length (due to reduction in the number of those complementary base pairs which are normally held together by hydrogen bonds within the hybridised duplex) decreases the length of the cumulative energy barrier to dissociation. The decrease in the effective bond length (the fraction of bonded

base pairs in the strand) will however, also increase the thermal force scale [35]. The drop in the unbinding force for a 30mer oligonucleotide from 25ºC to 35ºC at a loading rate of 14pN/s observed in these studies is similar to that reported for 12mer oligonucleotide at the same temperature and loading rate. This is an observation consistent with previous studies [23,66], and proves the validity of our experiment.

However it should also be noted that the increasing temperature will also increase the entropy of the system, and may change the selected pathway along the dissociation energy landscape. The height of the individual energy barriers for each base pair may also change with an increase in temperature. As already discussed in Chapter 3, the thermal force scale (f_β) will experience a linear increase with temperature, but this will be marked by increases in the thermal off rate, which observe an exponential increase, and thus their combined effect leads to decrease in the observed rupture force. These factors, together with the rise in the modal rupture force for the next 10ºC (from 35ºC to 45ºC) and the lack of change in the modal rupture force when temperature was increased from 45ºC to 55ºC, warrant thorough investigation in future studies.

4.6 – Conclusions

The modal rupture force of the complementary oligonucleotides (30mer) at room temperature was found to be identical to that reported in previous studies [47]. This confirms the validity of our experiment. However, the unbinding forces were found to change non-linearly with an increase in temperature, although in general they were lower than that observed at room temperature. In previous studies the temperature increase has been attributed to a decrease in the average fraction of bonded base pairs in a hybridised DNA duplex which therefore, reduces the length of the energy barrier [23, 66]. The

observed drop in the unbinding force at 35ºC using a loading rate of 14pN/s is consistent with these studies [66].

The temperature rise also increases the thermal energy (k_BT) of the system, which reduces the internal energy of the binding energy landscape and may also change the three dimensional conformation of the duplex. Moreover, the enthalpy and entropic contributions help the thermal energy to reach the top of the barrier quickly [66].The cumulative effect of all these factors help in reducing the unbinding force of the complementary oligonucleotides. An increase in temperature may also influence the other parameters such as physics of the cantilever, underlying chemistry, which in turn may affect the unbinding forces. Such factors require further investigation.

Chapter -5 Summary

The work presented has explored the application of single molecule force spectroscopic measurement experiments to streptavidin-biotin and a novel dendron immobilized oligonucleotide system. The effect of temperature on the unbinding forces of single molecules, immobilized via conventional (silanization) and the dendron approach has been studied.

Streptavidin-biotin represented an excellent model system due to the high affinity and specificity of its interaction. An investigation of the dependence of the unbinding forces of strept(avidin)-biotin complex on the loading rate, and a direct comparison with DFS results obtained in previous studies was carried out. The data obtained was consistent with previous work showing an increase in unbinding force with loading rate [19]. Moreover, the spectrum of the unbinding forces showed two regimes of strength, revealing that the streptavidin-biotin complex overcomes two energy barriers during its dissociation process. This is again an observation consistent with previous studies [19]. Similarly, the modal rupture force of the complementary oligonucleotides (30mer) at room temperature was identical to that reported in previous studies [47].

As well as the fundamental effect of loading rate, several experimental factors can influence single–molecule force measurement such as instrument drift, the nanomechanical properties of the cantilevers, noise, underlying chemistry, and temperature. The impact of the first three factors on single molecule force measurement is predominantly external and can be reduced by appropriate changes in instrumental design and careful handling of the experiment. However, the other factors such as underlying chemistry and temperature highly influence single molecule force measurements and demand more focused attention. The presently employed surface attachment methods such as silanization and SAMs are not

considered as efficient attachment methods for single molecule force spectroscopic measurement methods, because they lead to steric hindrance, non-specific attachments and an uncontrolled density of the surface functional groups. Recently, a dendron immobilization approach has been found to provide sufficient mesospacing (spacing between the immobilized molecules/probe molecules), an optimum density of surface functional groups and fewer non specific attachments. This makes it convenient for bio-molecular immobilization [47]. Keeping this in view, the above described benefits of dendron immobilization approach, an attempt was made in this work to investigate the effect of temperature on the unbinding kinetics of dendron immobilized complementary oligonucleotides interaction. Besides providing a direct comparison with previously studied DNA oligonucleotide hybridisation events at room temperature this work is amongst the first to explore the effect of temperature.

The unbinding forces of both streptavidin-biotin interactions and the rupture forces of complementary oligonucleotide hybridisation events decreased non-linearly with an increase in temperature. The decrease in the modal rupture force for the first 10ºC was found to be more prominent in both the studied systems. The decrease in the unbinding forces of the streptavidin-biotin complex is probably due to an increase in the thermal energy of the system which not only tilts the energy landscape in the direction of applied force, but also increases the thermal force scale and exponentially reduces the thermal off-rate. The cumulative effect of these changes reduces the unbinding force of the streptavidin-biotin complex. Similar reasons can explain the unbinding kinetics of complementary oligonucleotides (30mer) at room temperature. However the decrease in the unbinding force of complementary oligonucleotides (30mer) is also due to a reduction in the average fraction of bonded base pairs in the direction of applied force, as a consequence of which the length of the energy barrier is reduced. The decrease in the effective bond length (fraction of

bonded base pairs in the strand) increases the thermal force scale and thermal off-rate. The observed decrease in the unbinding force at 35ºC using a loading rate of 14pN/s is consistent with previous studies [23] [66].

It should be noted that the increase in temperature may also affect the cantilever and the stiffness of the polymers (PEG polymers in case of streptavidin-biotin interactions), (oligonucleotides and dendrons in case of DNA) which could also influence the unbinding force. This remains a topic for future research.

All this experimental work helped me to develop a fundamental insight into the single – molecule force spectroscopic measurements. Starting off with the streptavidin-biotin model system was excellent, because before starting this project, there was very little I knew about the basic fundamentals of single-molecule force spectroscopic measurements and the instruments which are usually employed to investigate the unbinding kinetics of single-molecule interactions. The reasons for choosing the streptavidin-biotin model system were that it is the most widely studied ligand-receptor system. Moreover, there is plenty of literature available about the streptavidin-biotin system, which made it easier for me to have some theoretical knowledge about this system.

Whilst the objectives of this work have been met, in the future a more comprehensive experimental investigation is required to fully understand the temperature dependent unbinding kinetics of single-molecule ligand receptor interactions and the role of the underlying immobilization chemistry. Here the temperature dependent unbinding kinetics of single-molecule interactions has been investigated using only two loading rates and a limited temperature range. This in the future should therefore be expanded to encompass a greater range of data. For example several orders of loading rate could be employed to

investigate in more detail the impact of the underlying dendron chemistry and the effect of a range of temperatures on single molecule force interactions. A greater range of loading rates could be achieved through the use of greater range of force measurement speeds, and also other force measurement techniques such as the BFP [17].

Very little work within the current literature has investigated the temperature dependence of forced unbinding kinetics of single molecules. This attempted work, together with the proposed future work would help to clarify the impact of temperature on single-molecule interactions, which in turn would be helpful in understanding the effect of temperature on fundamental bio-molecular recognition and folding processes (protein and nucleic acids) in a greater detail. Therefore, this in the long term would be highly beneficial in understanding underlying mechanisms of ligand-receptor interactions, which within our body underlie many biological processes and form the basis for pharmacological intervention of human diseases in medicine.

Acknowledgements

I would like to thank my supervisors Prof. Clive Roberts and Dr Stephanie Allen, who both are not only masters in their respective areas but wonderful and generous human beings. I must also pay thanks to Head of School, Prof. Saul Tendler for providing me with the opportunity to study within the School of Pharmacy.

I would also like to thank Prof. Phil Williams whose valuable guidance helped me a great deal in assimilating the theoretical aspects of force spectroscopy. I am also very much grateful to Prof. Xinyong Chen for his valuable training, in addition to Dr. Matthew Batchelor and Sede Alodehou, who also played their role in supporting me in the beginning of my studies. A special thanks to everyone in the LBSA for their help and cooperation in my learning process.

Infinite thanks to Almighty God, who came to my rescue in the form of my mentors/supervisors. Finally, I would to dedicate this thesis to my mother Mrs. Misra Bano and my eternal mentor Respected Gulzar Sahib. Without my mother, I could have done nothing in my life. I salute my lovely mother for her mighty contribution.

References

[1] J. Wong, A. Chilkoti, and V.T. Moy, (1999) Direct force measurements of strept(avidin)-biotin, *Biomolecular Engineering*, 16:45-55.

[2] Marzena de Odrowąz, Piramowicz, P. Czuba, M.Targosz, K. Burda, and M. Szymoński, (2006) Dynamic force measurements of avidin-biotin and streptavidin-biotin interactions using AFM, *Acta Biochemica Polonica*, 53:93-100.

[3] J.K. Myers, and C.N. Pace, (1996) Hydrogen bonding stabilizes globular proteins, *Biophysical Journal*, 71:2033-2039.

[4] McDonald, and J. Thornton, (1994) Satisfying hydrogen bonding potential in proteins, Journal of Molecular Biology, 238:777-793.

[5] www.geocities.com/athens/thebes/5118/bitn/br_cl.htm (October. 2009-03-29).

[6] G. Karp, (2007) Cell and Molecular Biology, 5th ed, *John Wiley and Sons, Inc*.

[7] Dirk Zahn, (2004) How does water boil? *Physical Review Letters*, 93:227801

[8] T. Suzuki, (2008) The hydration of glucose:the local configurations in sugar–water hydrogen bonds, *Physical Chemistry, Chemical Physics and Biophysical Chemistry*, 10:96-105.

[9] T. Kortemme, A.V. Morozov, and D. Baker, (2003) Orientation-dependent Hydrogen Bonding Potential Improves Prediction of Specificity and Structure for Proteins and Protein–Protein Complexes, *Journal of Molecular Biology*, 326:1239-1259.

[10] T. Boland, and B.D. Ratner, (1995) Direct measurement of hydrogen bonding in DNA nucleotide bases by atomic force microscopy, *Proceedings of the National Academy of Sciences*, 92: 5297-5301.

[11] J.M. Berg, J.L. Tymoczko, L. Stryer, (2002) Biochemistry, 5ed. *W.H. Freeman and Company.*

[12] G. Hummer, S. Garde, E. Angel, E. M. Paulatis, and L.R. Pratt, (1998) The pressure dependence of hydrophobic interactions is consistent with the observed pressure denaturation of proteins, *Proceedings of the National Academy of Sciences,* 95:1552-1555.

[13] B. Alberts, A. Johnson, J. Lewis, M. Raff, K. Roberts, P. Walter, (2002) Molecular Biology of The Cell, 4ed. *Garland Science*.

[14] http://ibchem.com/IB/ibfiles/bonding/bon_img/induced-dipole.gif (October. 2008-10-24)

[15] F.J. David, Tees, T. John, Woodward, D. A. Hammer, (2001) Reliability theory of receptor-ligand interaction, *Journal of Chemical Physics*, 114:17-18.

[16] R. Zahradník, and F. Achenbach, (2004).Theoretical approaches to interactions between biomolecules: Legends and approximations to reality, *International Journal of Qunatum Chemsitry*, 35:167-180.

[17] E. Evans, (1999) Looking inside molecular bonds at biological interfaces with DFS, *Biophysical Chemistry*, 82:83-97.

[18] J. Zlatanova, S.M. Lindsay, S. H. Leuba, (2000) Single molecule force spectroscopy in biology using the atomic force microscope, *Progress in Biophysics and Molecular Biology*, 74:37-61.

[19] R. Merkel, P. Nassoy, A. Leung, K. Ritchie and E. Evans, (1999) Energy Landscapes of receptor-ligand bonds explored with dynamic force spectroscopy, *Nature*, 397: 51-53.

[20] M.S.Z. Kellermayer, S.B. Smith, H.L. Granzier, C. Bustamante, (1997) Folding-unfolding transitions in single titin molecules characterized with laser tweezers, *Science*, 276:1112–1116.

[21] G. Charvin, T.R. Strick, D. Bensimon, and V. Croquette, (2005) Tracking topoisomerase activity at the single-molecule level, *Annual Review Biophysics and Biomoleular Structure,* 34:201–219.

[22] H.O. Willemsen, M.E. Margot, S.A. Cambi, J. Greve, B.G. De Grooth, C. G. Figdor, (2000) Biomolecular Interactions Measured by Atomic Force Microscopy, *Biophysical Journal,* 79:3267-3281.

[23] R. Mckendry, J.Y. Zhang, Y. Arntz, T. Strunz, M. Hegner, H.P. Lang, M.K. Baller, U. Baller, E. Meyer, H.J. Guntherodt, C. Gerber, (2002) Multiple label-free biodetection and quantitative DNA-binding assays on a nanomechanical cantilever array, *Proceedings of the National Academy of Sciences,* 99:9783-9788.

[24] Tsukasaki K. Kitamura, K. Shimizu, A.H. Iwane, Y. Takai, and T. Yanagida, (2007) Role of multiple bonds between the Single Cell Adhesion Molecules, Nectin and Cadherin: Revealed by High Sensitive Force Measurements, *Journal of MolecularBiology,* 367:996-1006.

[25] H. Clausan Schuman, M. Seitz, R. Krautbauer, and H.E Gaub, (2000) Force spectroscopy with single molecules, *Current Opinion in Chemical biology,* 4:524-530.

[26] K.C. Neuman, and A. Naggy, (2008) Single-molecule force spectroscopy: optical tweezers, magnetic tweezers and atomic force microscopy, Nature Methods, 5:491-505.

[27] E.A. Abbondanzieri, W.J. Greenleaf, J.W. Shaevitz, R. Landick, and S.M. Block, (2005) Direct observation of base-pair stepping by RNA polymerase, *Nature,* 438:460–465.

[28] R.J. Davenport, G. J. Wuite, L.R. Bustamante C, (2000), Single-Molecule Study of Transcriptional Pausing and Arrest by E. coli RNA Polymerase, *Science,* 287:2497-2500.

[29] A.F. Oberhauser, P.K. Hansma, M. Carrion-Vazquez, and J.M. Fernandez, (2000) Stepwise unfolding of titin under force-clamp atomic force microscopy, *Proceedings of the National Academy of Science*, 98:468-472

[30] M. Rief, F. Oesterhelt, B. Heymann, H.E. Gaub, (1997) Single molecule force spectroscopy of on polysaccharides by atomic force microscopy, *Science*, 276:1295-1297.

[31] M. Rief, M. Gautel, A. Schemmel, H.E. Gaub, (1998) The mechanical stability of immunoglobulin and fibronectin III domains in the muscle protein titin measured by atomic force microscopy, *Biophysical Journal*, 75:3008-3014.

[32] S. Allen, X. Chen, J. Davies, M.C. Davies, A.C. Dawkes, J.C. Edwards, C.J. Roberts, J. Sefton, S.J.B. Tendler, and P.M. Williams, (1997) Detection of antigen-antibody events with atomic force microscope, *Biochemistry*, 36:7457-7463.

[33] R. Levy, and M. Maaloum, (2002) Measuring the spring constants of atomic force microscope cantilevers, *Nanotechnology*, 13:33-37.

[34] J.E. Sader, I. Larson, P. Mulvaney, and L.R. White, (1995) *Review of Scientific Instruements*, 66-3789-3798.

[35] G.U. Lee, D.A. Kidwell and R.J. Colton, (1994) Sensing discrete streptavidin-biotin interactions with atomic force microscopy, *Langmuir*, 10:354–357.

[36] T.J. Ignacio, and C. Bustamanate, (2002) The effect of force on thermodynamics of kinetics of single molecule reactions, *Biophysical Chemistry*, 101:513-533.

[37] V.T. Moy, E. L. Florin, and H.E. Gaub, (1994) Intermolecular forces and energies between ligands and receptors, *Science*, 266:257–259.

[38] S.S. Wong, E. Joselevich, A.T. Woolley, C.L. Cheung, C.M. Lieber, (1998) Covalently functionalised nanotubes as nanometre-sized probes in chemistry and biology, *Nature*, 394:52-55.

[39] M.C. Williams, and L. Rouzina, (2002) Force spectroscopy of single DNA and RNA molecules, *Current Opinion in Structural Biology*, 12:330-336.

[40] B.V. Mario, L.I. Pietrasanta, J.B. Thompson, A. Chand, I.C. Gebeshuber, J.H. Kindt, M. Richter, H.G. Hansma, and P.K. Hansma, (2000) Probing protein-protein interactions in real time, *Nature Structural Biology*, 7:644-647.

[41] A.M. Mark, A . Noy, (2005) Researchers unveil reliable new approach to cancer drug delivery, *News Release.*

[42] G.U. Lee, L.A. Chrisey, R.J. Colton, (1994) Direct measurement of forces between complementary strands of DNA, *Science,* 266:771-773.

[43] A. Noy, D.V. Vezenow, J.F. Kayyem, T.J. Meade, C.M. Lieber, (1997) Stretching and breaking duplex DNA by chemical microscopy, *Chemical Biology*, 4:143-146.

[44] Q. Du, O. Larsson, H. Swerdlow, and Z. Liang, (2005) DNA immobilization: Silanized Nucleic acids and Nanoprinting, *Topics in Current Chemistry*, 261:45-61.

[45] R.F. DeBono, G. D. Loucks, D.D. Manna, and U.J. Krull, (1996) Self-assembly of short and long-chain n-alkyl thiols onto gold surfaces: A real-time study using surface plasmon resonance techniques, *Canadian Journal of Chemistry*, 74:677-688.

[46] S.J. Oh, S.J. Cho, C.O. Kim, J.W. Park, (2002) Characteristics of DNA Microarrays Fabricated on Various Aminosilane Layers, *Langmuir*, 18:1764-1769.

[47] Y.J. Jung, B.J. Hong, W. Zhang, J. B.S. Tendler, P.M. Willimas, S. Allen, J.W. Park, (2007) Dendron Arrays for the Force-Based Detection of DNA Hybridisation Events, *Journal of American Chemical Society*, 129:9349-9355

[48] E. Evans, and K. Ritchie, (1997) Dynamic strength of molecular adhesion bonds, *Biophysical Journal*, 72:1541–1555.

[49] T. Strunz, K. Oroszlan, R. Shafer, H.J. Gundtherodt, (1999) Dynamic force spectroscopy of single DNA molecules, *Proceedings of the National Academy of Science,* 96:11277-11282.

[50] R. Kraubtbauer, M. Rief, and H.E. Gaub, (2003) Unzipping DNA Oligomers, *Nanoletters*, 3:493-496.

[51] G.Q. Binnig, C. F. Rohrer, (1986) Atomic Force Microscope, *Physics Review Letters*, 56:930-933.

[52] A. Ashkin, J.M. Dziedzic, T. Yamane, (1987) Optical trapping and manipulation of single cells using infrared laser beams, *Nature,* 330:769-771.

[53] Z. Guttenberg, A.R. Bausch, B. Hu, R. Bruinsma, L. Morader, E. Sackman, (2000) Measuring ligand-receptor unbinding forces with *magnetic* beads: molecular average, *Langmuir,* 16: 8984-8993.

[54] E. Evans, K. Ritchie, and R. Merkel, (1995) Sensitive force technique to probe molecular adhesion and structural linkages at biological interfaces, *Biophysical Journal,* 68:2580–2587.

[55] E. Evans, (2001) Probing the Relation between Force –lifetime and chemistry in single molecular bonds, *Annual Review Biophysics and Biomoleular Structure,*30:105-128.

[56] C. Yuan, A. Chen, P. Kolb, and V.T. Moy, (2000) Energy Landscape of Streptavidin-Biotin Complexes Measured by Atomic Force Microscopy, *Biochemistry*, 39:10219-10223.

[57] S. J. Koch, and M.D. Wang, (2003) Dynamic force spectroscopy of protein-DNA interactions by unzipping DNA, *Physical Review Letters*, 91:28103.

[58] N.H. Green, P.M. Williams, O. Wahab, M. C. Daves, C.J. Roberts, S.J.B. Tendler, and S. Allen, (2004) Single molecule investigations of RNA Dissociation, *Biophysical Journal*, 86:3811-3821.

[59] A. Chilkoti, T. Boland, B.D. Ratner, P.S. Stayton, (1995) The relationship between ligand-binding thermodynamics and protein-ligand interaction forces measured by atomic force microscopy, *Biophysical Journal*, 69:2125-2130.

[60] W.A. Hendrickson, A. Pähler, J.L. Smith, Y.Satow, E.A. Merritt, and R.P. Phizackerley, (1989) Crystal structure of core streptavidin determined from multiwavelength anomalous diffraction of synchrotron radiation, *Proceedings of the National Academy of Sciences*, 86:2190-2194.

[61] B.A. Katz, (1997) Binding of biotin to streptavidin stabilizes inter subunit salt bridges between Asp61 and His87 at low pH, *Journal of Molecular Biology*, 274:776-800.

[62] P. Hinterdorfer, F. Kienberger, A. Raab, H.J. Gruber, W. Baumgartner, G. Kada, C. Riener, S. Wielert-Badt, C. Borken, and H. Schindler, (2000) Poly(ethylene glycol): An ideal spacer for molecular recognition force microscopy/spectroscopy, *Single Molecules*, 1:99-103

[63] C. Bouchiat, M.D. Wang, J.F. Allemand, T.Strick, S.M. Block, and V. Croquette, (1999) Estimating the Persistence length of a Worm-Like Chain Molecule from Force-Extension Measurements, *Biophysical Journal*, 76:409-413.

[64] F.S. Lee, and W.R. Bauer, (1985) Temperature dependence of the gel electrophoretic mobility of superhelical DNA, *Nucleic Acids Research*, 13:1665-1682.

[65] M.C. Williams, J.R. Wenner, I. Rouzina, and V.A. Bloomfield, (2001) Entropy and heat capacity of DNA melting from temperature dependence of single molecule stretching, *Biophysics Journal*, 80:1932-1939.

[66] I. Schumakovitch, W. Grange, T. Strunz, P. Bertoncini, H.J. Guntherodt and M. Hegner, (2002) Temperature Dependence of Unbinding Forces between Complementary DNA strands, *Biophysical Journal*, 82:517-521.

[67] A.S. Chauhan, S. Svenson, L. Reyna, D. Tomalia, (2007) *Material Matters*, 2:24-26

[68] A. Deborah, P.A. Wade, Torres, A.T. Sheryl, (1999) Spectrochemical investigations in dendritic media: evaluation of nitromethane as a selective fluorescence quenching agentin aqueous carboxylate-terminated polyamidoamine (PAMAM) dendrimers, *Analytica Chimica Acta*, 39:17-31.

[69] J. Issberner, M. Bohme, S. Grimme, M. Nieger, W. Paulus, F. Vogtle, (1996) Poly(amine/imine) dendrimers bearing planar chiral terminal groups-synthesis and chiroptical properties, *Tetrahedron Asymmetry*, 7:2223-2232.

[70] A.M. Caminade, J.P. Majoral, (2005) Phosphorus dendrimers possessing metallic groups in their internal structure (core or branches): Synthesis and Properties, *Coordination Chemistry Reviews*, 249:1917-1926.

[71] C. Gorman, (2008) Dendrimers: Polymerisation and Properties, *Encyclopedia of Materials, Science and Technology*, 2042-2052.

[72] J.B. Wolinsky, and M.W. Grinstaff, (2008) Therapeutic and diagnostic applications of dendrimers for cancer treatment, *Advanced Drug Delivery Reviews*, 60:1037-1055.

[73] Y. Cheng, and T. Xu, (2007) The effect of dendrimers on the pharmacokinetic behaviors of non-covalently attached drugs, *European Journal of Medicinal Chemistry*, 43: 2291-2297.

[74] H. Kobayashi, and M.W. Brechbiel, (2003) Dendrimer-based macromolecular MRI contrast agents: characteristics and application, *Molecular Imaging*, 2:1-10.

[75] D.A. Tomalia, (2007) Dendrimers: key properties of importance to nanomedicine. *Nanomedicine: Nanotechnology, Biology and Medicine*, 3:338-342.

[76] X. Duan, and H. Sheardown, (2006) Dendrimer cross linked collagen as a corneal tissue engineering scaffold: Mechanical properties and corneal epithelial cell interactions, *Biomaterials*, 27: 4608-4617.

[77] T. Böcking, L.S. Elicia, Wong, M. James, J.A. Watson, C.L. Brown, T. C. Chilcott, K.D. Barrow, G.L. HansCoster, (2006) Immobilization of dendrimers on Si-C linked carboxylic acid-terminated monolayers on silicon (111), *Thin Solid Films*, 515:1857-1863.

[78] M. Ma, Y. Cheng, Z. Xu, P. Xu, H. Qu, Y. Fang, T. Xu, L. Wen, (2007) Evaluation of polyamidoamine (PAMAM) dendrimers as drug carriers of anti-bacterial drugs using sulfamethoxazole (SMZ) as a model drug, *European Journal of Medicinal Chemistry*, 42:93-98.

[79] L. Balogh, S.S. Nigavekar, B.M. Nair, W. Lesniak, C. Zhang, L.Y. Sung, Muhammed, S.T. Kariapper, A. El-Jawahri, M. Llanes, B. Bolton, F. Mamou, W. Tan, A. Hutson, L. Minc, M.K. Khan, (2007) Significant effect of size on the in vivo bio-distribution of gold composite nanodevices in mouse tumor models, *Nanomedicine: Nanotechnology, Biology and Medicine*, 3:281-296.

[80] M. Joshi, R. Pinto, V. R. Ra., S. Mukherji, (2007) Silanization and antibody immobilization on SU-8, *Applied Surface Science*, 253:3127–3132.

[81] Y.C. Liu, C.M. Wang, and K. P. Hsiung, (2001) Comparison of Different Protein Immobilization Methods on Quartz Crystal Microbalance Surface in Flow Injection Immunoassay, *Analytical Biochemistry*, 299:130-135.

[82] T. Tanii, T. Hosaka, T. Miyake, G.J. Zhang, T. Zako, T. Funatsu, and I. Ohdomari, (2004) Preferential immobilization of biomolecules on silicon microstructure array by means of electron beam lithography on organosilane self-assembled monolayer resist, *Applied Surface Science,* 234:102-106.

[83] Y.S. Choi, C.W. Yoon, H.D. Lee, M. Park, and J.W. Park, (2004) Efficient protein-ligand interaction by guaranteeing mesospacing between immobilized biotins, *Chemical Communications*, 1316-1317.

[84] B. Heddi, N. Foloppe, C. Oguey, B. Hartmann, (2008) Importance of Accurate DNA Structures in Solution: The Jun-Fos Model, *Journal of Molecular Biology*, 382:956-970.

[85] C. Bustamante, S.B. Smith, J. Liphardt, D. Smith, (2000) Single-molecule studies of DNA mechanics, *Curent Opinion in Structural Biol*ogy, 10:279–85.

[86] http://eddejong.eu/wp-content/dendrimer.png

[87] B. J. Hong, S. J. Oh, T. O. Youn, S.H. Kwon, and J. W, Park, (2005) Nanoscale-Controlled Spacing Provides DNA Microarrays with the SNP Discrimination Efficiency in Solution Phase, *Langmuir*, 21:4257-4261.